PERINEURONAL NETS IN HIPPOCAMPAL AREA CA2: REGULATION BY ACTIVITY AND DISEASE

Kelly Elizabeth Carstens

A dissertation submitted to the faculty at the University of North Carolina at Chapel Hill in particial fulfillment of the requirements for the degree of Doctor of Philosophy in the Department of Neurobiology

Chapel Hill
2018

Approved by:

Serena Dudek

Benjamin Philpot

Richard Weinberg

Patricia Maness

Garret Stuber

ABSTRACT

Kelly Elizabeth Carstens: Perineuronal nets in hippocampal area CA2:
Regulation by activity and disease
(Under the direction of Serena Dudek)

Perineuronal nets (PNNs) first appear in the brain during early postnatal development and increase until they are fully expressed in adulthood, often tracking the end of critical windows of synaptic plasticity[1, 2]. The experience-dependent development of PNNs in the brain is thought to function as a molecular brake on plasticity during the closure of these critical windows [3, 4]. PNNs are typically associated with inhibitory neurons throughout the brain; however, I characterized a dense localization of PNNs surrounding a population of excitatory pyramidal neurons in hippocampal area CA2. I found that PNNs in CA2 function to restrict plasticity at CA2 synapses in mice 14-18 days old (P14-18). I also identified a novel window of plasticity in area CA2, P8-11, an age prior to the maturation of PNNs in CA2.

PNNs are reportedly altered in several neurodevelopmental disorders such as temporal lobe epilepsy (TLE) and Rett syndrome. I found that PNNs are precociously increased and develop prematurely in a Rett mouse model. Moreover, PNNs appear to be at least one mechanism restricting plasticity prematurely in CA2 of the Rett model mouse. Finally, because PNNs are regulated by pathological activity, I characterized PNNs in a TLE mouse model. PNNs were attenuated in CA2 by age P45, but were unchanged at younger ages after the onset of seizures (P21). To further examine how activity regulates PNNs in CA2, we chemogenetically increased or decreased CA2 activity for five days and found that PNNs are inversely regulated

by activity in CA2. Overall, these findings reveal a critical function for PNNs in restricting plasticity in CA2 and identify a novel window of plasticity in the hippocampus that may be critical for understanding the severe hippocampal-dependent learning deficits associated with many neurodevelopmental disorders.

I dedicate this work to my mother. Thank you for believing in me, always. I couldn't have achieved this without you.

ACKNOWLEDGMENTS

The Dudek laboratory has provided me plentiful resources over the past five years in which to pursue my lifelong interest in studying learning and memory on a molecular and electrophysiological level. Dr. Dudek always granted me the independence to follow questions that peaked my curiosity and guided me in identifying key knowledge gaps in the field. My experience in the Dudek lab has built my confidence as a researcher; having provided me with many opportunities to present and discuss my research findings, both in formal and casual settings. I thank Dr. Dudek for fostering this constructive and fun training environment. Most importantly, I thank her for training me as a researcher, challenging me to critically think, involving me in peer reviewing, working closely with me during the writing process, introducing me to her widespread network of colleagues, and allowing me to present my work in numerous prestigious conferences.

I also had incredible support from members of the Dudek lab, many of whom are both mentors and friends. I had extensive support in troubleshooting during experiments and received incredibly valuable training on *in vivo* viral techniques from Dr. Georgia Alexander. I also want to thank Dr. Alexander in particular for sharing her expertise in epilepsy and her tireless support scientifically and emotional during grant writing. I am grateful for the diverse background of members in the Dudek lab, who always provide me with excellent feedback during lab meetings. I also appreciate all the birthday celebrations, especially sharing my birthday lunch with Dr. Mark Bear, my scientific ‘grandfather’. Finally, I want to thank the members of the core facilities

at the NIEHS, specifically the imaging, viral vector, sequencing and biostatistics cores, for their support with data acquisition and analysis.

My thesis committee has been consistently supportive, providing me with valuable feedback on my research and helping me identify relevant experiments in the field. Thank you Drs. Benjamin Philpot, Richard Weinberg, Patricia Maness and Garett Stuber for serving on my committee. Dr. Philpot was specifically integral in my electrophysiology training, allowing me to freely work under his senior graduate students and postdocs during my first year at UNC. The skills that I learned during that time were foundational to my success in studying synaptic plasticity. I also appreciate Dr. Weinberg and his lab members for training me in electron microscopy techniques from start to finish. The breadth of expertise on my committee has been an asset in my studies, especially for experiments related to neurodevelopmental disorders.

Finally, I again thank Dr. Serena Dudek for graciously sharing her expertise, indispensable guidance, and always being available for guidance. I acknowledge the funding provided through the NIH at the NIHES (Z01 ES100221) and a grant from the Rett Syndrome Foundation (#3006). I was also supported by the NIH T32 training grant through the UNC Neurobiology curriculum. Finally, and most importantly, I thank my family, my friend family and especially my mom for their constant support. I wouldn't have gotten here without each of you.

PREFACE

Several figures in this thesis were done in collaboration with other researchers. For example, Chapter 2 consists of work from my first publication, in which I worked with Dr. Lucas Pozzo-Miller and his graduate student Mary Phillips at University of Alabama to more closely examine the types of synapses found imbedded in CA2 extracellular matrix (Fig 2). This figure also contains electron micrograph images that were collected by Susan Burette, a technician in Dr. Weinberg's lab at UNC. The paper was published previous to this dissertation with the following citation:

> Carstens KE, Philips ML, Pozzo-Miller L, Weinberg R, Dudek S. Perineuronal nets suppress plasticity of excitatory synapses on CA2 pyramidal neurons. J Neurosci. 2016. Jun 8;36(23):6312-20.

Permission to include the manuscript in its entirety in a PhD dissertation was retained from The Journal of Neuroscience as explained at: http://www.jneurosci.org/content/general-information#policies

Chapter 3 represents work that has been done primarily by myself, with the help of a previous lab member Daniel Lustberg and current lab technician Emma Shaughnessy. This paper is in preparation for submission. Chapter 4 represents unpublished research that was conducted predominantly by myself in the past two years with the help of Dr. Georgia Alexander, and Dr. Shannon Farris on the DREADD experiment and on the MECS, respectively. I thank the viral

vector at the NIEHS, especially Dr. Bernd Gloss, Dr. Negin Martin, and Patricia Lamb, for their technical assistance with the design, generation, and packaging of the AAV encoding ChABC. I acknowledge Georgia Alexander for her immense help with the following experiments: measuring *in* vivo electrophysiology data in the TLE mouse model, conducting the Gq/ Gi DREADD experiments (infusing the animals with virus and administering CNO), and training me in viral infusion surgeries. I thank Daniel Lustberg for his extensive support with animal perfusions and immunohistochemistry and the NIEHS Fluorescence Microscopy and Imaging Center and the animal care staff for their support.

TABLE OF CONTENTS

LIST OF TABLES

LIST OF FIGURES

LIST OF ABBREVIATIONS

A disintegrin and metalloproteinase (ADAMs)

Action potential (AP)

Adeno-associated virus (AAV)

AMPA receptor (AMPAR)

Bacterial artificial chromosome (BAC)

Bienenstock, Cooper, and Munro (BCM)

Brain derived neurotrophic factor (BDNF)

Calcium/ calmodulin-dependent protein kinase II (CaMKII)

Central nervous system (CNS).

Chondroitin sulfate proteoglycans (CSPGs)

Chondroitinase (ChABC)

Clozapine N-oxide (CNO)

Cornu Ammonis (CA)

Delta-opioid receptor (DOR)

Dentate gyrus (DG)

Designer Receptors Exclusively Activated by Designer Drugs (DREADDs)

Differential interference contrast (DIC)

Entorhinal cortex (EC)

Excitatory postsynaptic currents (EPSC)

Extracellular matrix (ECM)

Fibroblast growth factor 2 (FGF-2)

GABA (γ-aminobutyric acid)

Glutamate receptor 1 protein (GluR1)

Glycosaminoglycan sugars (GAGs)

Hyaluronan synthase (HAS)

In situ hybridization (ISH)

Input-timing dependent plasticity (ITDP)

Local field potential (LFP)

Long-term depression (LTD)

Long-term potentiation (LTP)

L-type voltage voltage-dependent calcium channels (LVDCC)

Lynx1 (Ly6/ neurotixin1)

Matrix metalloproteinase (MMP)

Maximal electroconvulsive shock (MECS)

Monocular deprivation (MD)

NMDA receptor (NMDAR)

N-methyl-D-aspartate (NMDA)

Ocular dominance plasticity (OD)

Orthodenticle homeobox 2 (OTX2)

Paired-pulse facilitation (PPF)

Paraventricular nucleus (PVN)

Parvalbumin (PV)

Pentylenetetrazole (PTZ)

Perineuronal nets (PNNs)

Plasma membrane calcium ATPase (PMCA)

Postnatal day (PN)

Postsynaptic current (PSC)

Primary visual cortex (V1)

Protein kinase A (PKA)

Purkinje cell protein 4 (PCP4)

Regulator of G-protein signaling 14 (RGS14)

Schaffer collaterals (SC)

Sharp wave ripple (SWR)

Stratum oriens (SO)

Stratum pyramidale (SP)

Stratum radiatum (SR)

Striatal-enriched protein tyrosine phosphatase (STEP)

Supramammillary nucleus (SuM)

Temporal lobe epilepsy (TLE)

Tissue-type plasminogen activator (tPA)

Vesicular glutamate transporter (VGLUT1)

α-amino-3-hydroxy-5-methyl-4-isoaxazole propionic acid (AMPA)

CHAPTER I- INTRODUCTION

Synaptic plasticity

The cellular basis of learning and memory has long been attributed to long-lasting changes in synaptic function. The most well-characterized example of such synaptic plasticity is long-term potentiation and depression (LTP or LTD respectively) of excitatory synaptic transmission. LTP is the persistent strengthening of excitatory currents in the postsynaptic cell in response to a high frequency electrical stimulation or a postsynaptic depolarization paired with a lower frequency stimulation. This phenomenon was initially theorized by Donald Hebb, who proposed that persistent neuronal activity can strengthen neighboring cells via "some growth process or metabolic change"- now referred to at Hebbian plasticity [5]. It wasn't until about 20 years later when an electrophysiological readout of plasticity was first characterized in the rabbit hippocampus [6, 7]. Many mechanisms have since been proposed to explain LTP, many of which require the postsynaptic calcium and ionotropic glutamatergic receptors NMDA (*N*-methyl-D-aspartate) and AMPA (α-amino-3-hydroxy-5-methyl-4-isoaxazole propionic acid). Regulation of synaptic plasticity is integral for refining circuit development and learning, especially during critical windows of plasticity in the developing brain, such as ocular dominance plasticity in the visual system.

Synaptic plasticity is thought to play a critical role in both the activity-dependent refinement of neuronal circuits during development [8] and in learning in the mature brain [9]. Early studies of experience-dependent plasticity in development revealed that plasticity is more robust

in immature sensory cortical regions compared to adult [10-13]. For example, LTP is readily inducible in layer IV somatosensory neurons (by stimulation of thalamic inputs) in young rat slices (P3-7) but resistant in older slices (P8-14) [14]. Likewise, the ability to induce LTD is also downregulated with age [15, 16]. This age-restriction of thalamocortical plasticity was found in several other brain regions, such as visual and auditory cortices, at different age windows. However, most investigators presumed initially that the restriction of plasticity in the adult was permanent in these areas. We now understand there to be many factors regulating cortical plasticity in the mature brain, eg. neuromodulators such as acetylcholine [17]. Overall, significant progress has been made in identifying the molecular switches that occur during critical windows of plasticity, however the precise mechanisms underlying plasticity in distinct regions of the developing brain versus the mature brain remain unclear.

Critical period plasticity: a brief overview

The concept of critical periods in brain development has been an area of study for decades [18, 19]. A critical period, or sensitive window, in behavior and neural development refers to a window in postnatal development when experience is required for normal development and is vulnerable to abnormal experience. For example, early studies of sensitive windows of learning identified chick imprinting as an experience-dependent behavior in early postnatal development [20, 21]. Similarly, experience of trauma or stress during early childhood development has profound effects on cognitive and neural circuit development [22-26]. Another way to study how experience can change brain circuitry is the development of sensory systems. For example, the development of vision and underlying visual system circuitry is dependent on activity from the eye [27]. Normal maturation of visual cortical circuits requires normal visual experience during

postnatal life [19, 28]. This form of experience-dependent learning is by far the most well-studied and is known as 'the critical period'. The study of the visual system during sensitive versus non-sensitive stages of development has provided insight into the onset, duration and closure of the sensitivity, and the underlying mechanisms regulating these different stages of plasticity.

The critical period was first characterized at the neuronal level more than 50 years ago by Hubel and Wiesel while recording activity of primary visual cortex (V1) neurons in response to visual stimuli [25]. They discovered that visual deprivation of one eye by lid suture (monocular deprivation; MD) causes a shift favoring responses to stimulation of the open eye. Referred to as ocular dominance plasticity (OD) [19, 25, 29], this shift was found to occur only during a temporary developmental window when synapses are highly sensitive to disruptions of activity; upon structural and physiological maturity, synapses become much less sensitive to such manipulation [1]. This period of heightened sensitivity to MD lasts between 4-5 week of age in cats [19], up to 4- 5 weeks in rodents [30], and during the first year of life in human [31]. During the critical period, long-term changes in visual input, like MD, cause a shift in neural response, or a strengthening and weakening of synapses of visual cortical neurons. To explain this adaption of cortical neurons, a theory was proposed by Bienenstock, Cooper, and Munro (BCM) theory [32]. They provide a mathematic framework for how synapse strength is altered by the length and degree of activity changes during the critical period.

In OD plasticity, visually depriving one eye with an eye-lid suture shifts the responses of visual cortical neurons to the open eye and deprived eye responses eventually cease to respond [19, 29, 33]. Three distinct processes occur during OD shift toward deprived-eye; a rapid weakening of the deprived-eye cortical responses via LTD, a strengthening of open eye responses via LTP, and a delayed threshold shift from depression to potentiation after long-term deprivation, also known

as ‘modification threshold’ [35, 36]. These data demonstrate a bidirectional threshold shift between LTD and LTP [36]. Importantly, the depression of cortical responses of the deprived-eye requires weak sensory input (retinal activity) because ablation of retinal activity, eg. via intravitreal injection of tetrodotoxin, is sufficient to prevent the depression of cortical response [19, 34, 37]. OD is rapidly shifted when MD occurs around 4 weeks old and is detectable within 1 day of darkness [34]. Also, a brief re-exposure to light can rapidly reverse these effects [35, 38, 39]. This critical period is observed in other species [40-42].

The shift in OD in visual cortex after MD is necessarily assessed at the functional level. However, activity-dependent plasticity of the component structures has also been observed. For example, MD of kittens during the critical period caused dramatic anatomical changes in the visual system, such as reduced horizontal connections [43], decreased thalamic afferents to the deprived eye [33, 44], and shrinkage of the geniculate neurons themselves [19, 25, 45]. Dendritic spines also become pruned on V1 pyramidal neurons of the deprived eye, while thalamic axons from the open eye progressively expand [44, 46-48]. These structural changes are absent and spines are more stable during adulthood [49]. Although the mechanisms underlying the loss of dendritic spines associated with MD during the critical period are unknown, the changes have been linked to the regulation of the extracellular matrix, perhaps by release of tissue-type plasminogen activator (tPA), during the critical period but not in adulthood [46, 47]. Long-term studies following dendritic spines *in vivo* corroborate these findings, showing that spines extend and retract over hours during early development, while the majority are stable for days/ months (~96%) in adulthood [50-52, 53]. However, whether and how LTD-like mechanisms trigger this plasticity during critical periods is still unknown.

Many cellular mechanisms have been reported to mediate this form of plasticity. For example, experience-dependent molecular changes in NMDA subunit expression and subsequent modification of NMDAR function are thought to regulate changes in synaptic strength [39, 54-56] and AMAPR trafficking [57-60]. Moreover, synaptic scaling has been proposed as a mechanism of activity-dependent synaptic changes [46, 47, 61, 62]. The depression of synaptic strength in response to deprivation has also been explained by enhanced intracortical inhibition and described as a long-term potentiation of inhibition [63, 64]. More recent studies have focused on molecular factors such as calcium-regulating enzymes (eg. calcium/ calmodulin-dependent protein kinase II (CaMKII)), molecular breaks (eg. the extracellular matrix (ECM) or prototoxins such as Lynx1 (Ly6/ neurotixin1)) and molecular triggers (eg. Otx2 or BDNF (orthodenticle homeobox 2 homeoprotein) (brain-derived neurotrophic factor)) [65-68]. Much effort has been directed toward understanding the mechanisms underlying this and other critical periods that have since been identified in other brain regions and across species [69, 70].

Taken together, the onset, duration and closure of critical period plasticity are regulated by numerous physiological and molecular factors throughout postnatal development. The focus of this thesis is on the role of the extracellular matrix in regulating synaptic plasticity in the hippocampus during early postnatal development. In principle, the characteristics of synaptic plasticity observed in the visual critical period should resemble those of synapses in the hippocampus [32, 71, 72]. However, a critical period in the hippocampus has yet to be defined, as synaptic plasticity, particularly LTP, in the hippocampus persists into adulthood. A few studies, though, have implicated the hippocampus in modulating a sensitive window for fear learning in early postnatal development [73-75].

Hippocampal Plasticity during Development

The anatomical regions of the hippocampus are fully distinguishable by the first postnatal week of life in rodent [76]. While anatomy is not necessarily a readout of functional maturity, it can still be a useful indicator [77]. Early studies found that LTP at CA3-CA1 synapses emerges in the second postnatal week in the rodent and in the third week in DG [78-80]. Moreover, excitatory neurotransmission in the hippocampus matures around P14 in the rodent [81], while inhibitory transmission develops around P9 in CA1/ P5 in CA3, and matures by P14-18 [82-85]. More recently, Yasuda and colleagues show CA1 LTP is indeed inducible in the neonatal rodent (<P9) and report that the underlying mechanisms regulating immature versus mature plasticity are distinct [86, 87]. CAMKII is well-known to play a critical role in downstream signaling of LTP induction at adult CA1 synapses. They show that immature LTP induction does not require CaMKII (P7-9 hippocampal slices), but instead requires cyclic AMP-dependent protein kinase A (PKA) [87, 88]. Other explanations for the developmental changes in hippocampal plasticity have been proposed [89, 90].

The development of mature LTP in CA1 has been linked to the unsilencing of silent synapses during early postnatal development. Silent synapses are those that show NMDA receptor (NMDAR) but no AMPA receptor (AMPAR) response. In rodent hippocampal CA1 neurons, the conversion of AMPA-silent synapses to AMPA-signaling synapses occurs around P12 when there is a developmental decline in the number of AMPA-silent synapses [86, 91-93]. Several other mechanisms have been identified at this developmental switch: an increase in multivesicular release at CA3-CA1 synapses, increase in AMPAR signaling (increase in open probability/ single-channel conductance), and a change in the expression of AMPAR scaffolding proteins eg. SAP-102 to PSD-95 [94-96]. Also, there is a shift in AMPAR and NMDAR subunit

composition during the second and third postnatal weeks which reflects distinct LTP mechanisms regulating plasticity during development [97].

AMPAR/ NMDAR subunit composition in development

The glutamatergic NMDAR is a heterotetramer made up of two obligatory NR1 subunits and two variable NR2 subunits. NR2B composition switches from predominantly NR2B to NR2A in the cortex during development. This switch is activity-dependent (delayed by sensory deprivation experiments) and the timing appears to parallel critical periods of plasticity, eg. NR2A is expressed between P3-10 in the somatosensory cortex and between P12-30 in the visual cortex in rodent [98, 99]. The subunit switch alters NMDA-mediated excitatory postsynaptic currents (EPSC) kinetics. NMDARs that are dominant in NR2B subunit have a prolonged ESPC, while NR2A-dominant have a truncated EPSC decay [99]. The change in EPSC efficacy is proposed to underlie critical periods of plasticity [38, 39, 54, 55 14]; however, the timing of visual critical period plasticity is surprisingly unaffected by the loss of NR2A subunit [30]. Also, AMPAR GluR1 subunit is critically involved in mature LTP [100], while GluR2/4 subunits seem critical to early NMDAR and PKA-dependent LTP [101].

GABA transmission: excitatory to inhibitory

Lastly, the effects of inhibitory neurotransmission on synaptic activity notably switches during early postnatal development. GABA (γ-aminobutyric acid) is typically thought of as the primary inhibitory neurotransmitter in the adult brain that inhibits neuronal firing by either hyperpolarizing the membrane potential or by shunting excitatory input. However, early in development, GABA transmission is excitatory in that GABA signaling causes a large depolarizing postsynaptic potentials/ increase in intracellular calcium, and can trigger action

potentials [102]. In the hippocampus, the developmental GABA switch from excitatory to inhibitory occurs around between P7 and P13 in rodent [103, 104]. The switch indicates a change in the electrochemical gradient of chloride ions. In the adult brain, the reversal potential for GABA currents is very negative but more depolarized in the developing brain due to a higher intracellular chloride concentration at younger ages. This difference is attributed to a developmental increase in the K+-coupled Cl- transporter, which increases the rate of Cl- extrusion and a shift of E_{GABA} to a more negative potential [105, 106].

Taken together, many molecular and structural changes occur during critical windows in the brain that influence the regulation and function of plasticity throughout development. It has been hypothesized that early LTP may be important for the formation and refinement of synaptic contacts (by stabilizing single release site connections) and mature LTP might reflect activity-dependent functions within a network of connections.

A role for PNNs in limiting functional plasticity

The extracellular matrix (ECM) is emerging as a key player in regulating plasticity throughout development in the central nervous system (CNS). Recent discoveries in the field have led to an evolved theory called the 'tetrapartite synapse' that considers the pre and postsynaptic cell, astrocytes and the ECM in synaptic signaling [107]. Perineuronal nets (PNNs) are a specialized form of the extracellular matrix localized around predominantly inhibitory neurons in the CNS. In the hippocampus, the matrix predominantly localizes around GABAergic interneurons, specifically those that are positive for parvalbumin (PV). However, we sought to characterize an unstudied concentration of PNNs surrounding a dense population of excitatory neurons in area CA2 [108-112]. PNNs first appear in early postnatal development, increase in

expression with age and are regulated by experience [1, 113, 114]. The maturation of PNNs interestingly tracks the closure of critical windows of synaptic plasticity and therefore were hypothesized to play a role in dampening synaptic plasticity [115]. Early studies discovered that PNN maturation requires normal experience during postnatal development in several brain regions including motor [116], visual [113, 117, 118] and somatosensory [114] systems. Furthermore, similar experiments performed in the adult mouse appeared to have little effect on PNN expression [114]. These findings demonstrate that the formation of PNNs is dependent on neuronal activity in the developing brain, but is resistant to similar manipulations in adulthood.

The composition of the extracellular space in the CNS differs from other tissues. Non-CNS ECM contains fibrous proteins such as collagen/ elastic and adhesive glycoproteins such as laminin/ fibronectin, whereas CNS ECM contains much less fibrous proteins and more glycosaminoglycan sugars (GAGs) [119, 120]. The specialized CNS ECM, PNNs were first described in the 1890's by both Camillo Golgi and Santiago Ramón y Cajal but it was not until the advent of more advanced histology and biochemical assays in the 1980's that their composition was characterized [121]. PNNs are composed of a complicated meshwork of molecular components that are organized into a scaffold around the 'backbone' polysaccharide hyaluronan. The majority of PNNs components are negatively charged proteoglycans known as chondroitin sulfate proteoglycans (CSPGs), bound to core proteins and a non-sulfated GAGs, tenascin-R [122-125]. It is believed that the PNN matrix is predominantly anchored to the cell membrane via hyaluronan docking to the hyalaronan synthase (HAS) receptor [126, 127].

PNN components are typically synthesized by the cell they encompass. Briefly, the transcripts for the PNN core protein are trafficked from the nucleus to the rough endoplasmic reticulum where the protein is synthesized and transferred to the Golgi apparatus where the

protein is glycosylated (process by which carbohydrate chains are attached to the protein) and/or sulfated (process by which a sulfate group is added to the proteoglycan) [125]. The molecules are then packaged into secretary vesicles and transported to the cell surface where they are released from the cytoplasm into the extracellular space. The synthesis of the CSPG can be stimulated by transforming growth factor B (TGFβ), and inhibitors of TGFβ are sufficient to suppress expression of several CSPGs [128, 129].

Mechanisms of PNNs regulating synaptic plasticity in development

The underlying mechanism(s) by which PNNs regulate plasticity are unclear. During development, the ECM is more permissive. The ECM is predominantly composed of hyaluronan during early development, which is a linear, non-branching GAG and thus allows for a soluble and spacious extracellular environment for axonal migration and motility [126, 130-133]. As the brain matures, hyaluronan becomes bound to more complex GAGs and CSPGs such that the ECM ultimately becomes insoluble and structural plasticity is restricted. PNN mechanisms have been studied in both the context of structural and functional plasticity. After the early finding that dark-rearing cats delayed the development of PNNs, many groups worked to characterize the mechanisms behind experience-dependent maturation of PNNs in many other brains and across species [117].

In 2002, Pizzorusso and colleagues demonstrated a direct association between PNNs in the visual cortex and the closure of critical period plasticity [134]. Moreover, several PNN-component knockout mouse models have implicated PNNs in regulating LTP and LTD at excitatory glutamatergic synapses in the hippocampus [135-138]. Synaptic plasticity is generally thought to be induced by activity-dependent elevations in calcium in the postsynaptic cell, which ultimately triggers calcium-dependent intracellular signaling cascades that are required for the

induction of synaptic plasticity. PNN components might play a role in elevating postsynaptic calcium via several mechanisms, which are not mutually exclusive. PNNs may regulate AMPA receptor lateral motility between extrasynaptic sites and the active zone of the postsynaptic density. When PNNs are densely localized at the synapse, they may be acting as a physical barrier preventing trafficking of the AMPAR to the active zone [139, 140]. In another theory, CSPGs carry a strong negative charge therefore PNNs may be acting as an ionic buffer of calcium or other cations that are associated with the induction/ maintenance of plasticity [140-142]. For example, calcium diffusion is increased in rat hippocampal slices after degradation of PNNs with the enzyme chondroitinase (ChABC) [142]. Cell-surface integrin proteins have also been implicated as a mechanism by which PNNs regulate plasticity [67, 143]. β1 integrin signaling triggers NDMA receptor phosphorylation in CA1 neurons and increases the amplitude of NMDA receptor currents [144]. Also, postnatal deletion of β1 protein impairs LTP in CA1 [145]. Evidence of a direct interaction between a PNN component and cell surface integrins is lacking, however the PNN-degrading enzyme matrix metalloproteinase (MMP) directly binds and regulates several integrins, which could be an alternative PNN-associated signaling mechanisms regulating plasticity [146].

L-type voltage voltage-dependent calcium channels (LVDCC) have also been implicated in ECM-mediated plasticity in the hippocampus. LVDCCs contribute to the influx of postsynaptic calcium after high-frequency stimulations and thus support LTP induction [147]. LVDCC-dependent LTP cannot be induced in tenascin-C deficient mice in CA1 but can be partially rescued by pharmacological potentiation of LVDCC's [136]. Blocking LVDCC activation in a hippocampal culture system downregulates PNN expression [148]. Furthermore, PNN degradation in an acute hippocampal slice reduced LVDCC calcium currents and abolished the

LVDCC-component of CA1 LTP. Exogenous bath perfusion of hyaluronan was able to rescue LVDCC currents and LTP, strongly linking PNNs and LVDCC in regulating LTP [149]. However, evidence of a direct interaction between ECM molecules and LVDCCs is lacking and may suggest that several ECM molecules may be acting in a signaling complex [150].

Finally, PNNs may limit plasticity by sequestering molecular factors that regulate plasticity. For example, Otx2 homeoprotein co-localizes with PNN+ PV neurons throughout the cortex, interacts with tenascin-R, and was found to trigger the onset of the visual critical period [151] [152]. Infusion of Otx2 into the visual cortex during the critical period accelerated PNN development and functional onset of the critical period, while Otx2 infusion in adulthood degraded PNNs around PV neurons and reopened critical period plasticity [66, 152]. PNNs also sequester growth-promoting or chemorepulsive proteins. For example, the chemorepulsive protein sema3a is strongly associated with PNNs in the adult rodent brain during postnatal development and its signaling receptors (PlexinA1/4) localize to the cell membrane of PNN+ neurons [153]. ChABC treatment *in vivo* abolishes sema3a staining. Moreover CSPG-4 interacts with FGF-2 (fibroblast growth factor 2) and acts as a co-receptor to present FGF to its signaling receptor, a receptor tyrosine kinase, which ultimately leads to cell migration/ proliferation signaling [154]. Interestingly, the only direct binding interactions between PNNs and a cell surface receptors (not including hyaluronan and its enzyme HAS) is with the receptor protein tyrosine phosphatase sigma (RPTP-sigma), which is a signaling inhibitor of neural regeneration [155]. Taken together, PNNs appear to act either directly or indirectly to signal multiple guidance cues, such as chemorepulsion, and provides a likely mechanism by which PNNs restrict plasticity in the adult brain.

Disentangling the effects of PNN degradation in the brain

PNNs are endogenously degraded in the brain via extracellular proteolysis. This process is thought to be critical for synaptic remodeling and plasticity [156]. The known ECM-degrading enzymes in the brain are MMPs (matrix metalloproteases), ADAMs (a disintegrin and metalloproteinase), and tPA. MMP-9 is the most well-characterized protease and is heavily implicated in activity-dependent structural and functional changes at the synapse. For example, MMP-9 is increased in response to neuronal activity by both aberrant increases in activity or by learning and memory tasks [157, 158]. MMP-9 is also required for late-phase long-term potentiation in CA1 [159]. A possible mechanism by which MMP-9 may be acting to regulate plasticity is signaling through β1 integrin, as previously mentioned [160]. Blocking β integrin signaling inhibited MMP-9-induced LTP in CA1 [161]. Several PNN-degrading proteases are well known to upregulate after brain insults, such as stroke or seizure, as well as in neurological disorders such as Alzheimer's [162-165]. In reference to critical period plasticity, a recent study showed that light reintroduction after dark exposure in adulthood increased MMP-9 and degraded PNNs in the visual cortex [166]. Because dark exposure in adults reactivates critical period plasticity, the loss of PNNs may be a critical mechanism by which the adult brain shifts to a juvenile state [167].

One study compared the effects of ChABC degradation of PNNs versus a mouse knockout of the PNN component tenascin-R. Both ChABC *in vitro* and tenascin-R KO was sufficient to attenuate CA1 LTP [137]. Interestingly, the authors also found that LTD in CA1 was impaired by ChABC in acute hippocampal slices, but not in the tenascin-R KO. Conversely, short-term plasticity was unaffected by ChABC but increased in the tenascin-R KO mouse. The CA1 LTP deficit is also apparent in other PNN-component KO's; for example, a brevican knockout mouse showed impaired LTP but no impairment in excitatory or inhibitory synaptic

transmission, as well as no learning and memory deficits [168]. Lastly, LTP was minimally impaired in a neurocan KO mouse, suggesting that neurocan either plays a more subtle role in regulating plasticity or is redundant with other CSPGs [169].

Degradation of PNNs *in vivo* with ChABC in the mouse amygdala abolished LTP at thalamo-amygdalar inputs in slice and impaired LTP of inhibitory neurons, which reflects loss of plasticity at glutamatergic inputs onto feedforward interneurons [170]. However, ChABC treatment of mouse hippocampal cultures increased the excitability of hippocampal interneurons (note: cultures were harvested at P1-3, developed diffuse PNNs by 5 days *in vitro*, and fully matured by 2 weeks) [148]. Degradation of PNNs with ChABC in *ex-vivo* hippocampal slices increased sharp wave ripple (SWR) (extracellular recordings of SWR frequency in CA1 SR) [171]. SWRs reflect excitatory events, typically initiated in CA3 and represents depolarization of CA1 dendrites [172]. They tend to occur during rest/ slow-wave sleep and appear to be important for learning and memory consolidation. Because PV neurons are heavily implicated in modulating SWRs, the authors suggest that loss of PNNs around PV neurons impairs glutamatergic transmission onto PV neurons (in agreeance with the amygdala study [170]), decreasing PV excitability, and ultimately increasing hippocampal excitability due to the loss of inhibition onto CA1 neurons.

In 2002, Pizzorusso and colleagues demonstrated a direct association between PNNs in the visual cortex and the closure of critical period plasticity. They found that degradation of PNNs *in vivo* with the enzyme chondroitinase (ChABC) in the adult visual cortex ‘re-opens’ the critical period and reinstatement of ocular dominance plasticity [134]. Similarly, CSPG development in the amygdala coincides with the developmental switch in fear memory regulation and have been implicated in the maintenance of fear memory in adulthood. Fear memory is more readily extinguished in young rats (P17) versus adult and it was recently found

that PNN degradation in the adult basolateral amygdala reopens a critical window for fear learning such that fear memories are more readily erased [173] [170]. These data suggest that PNNs may function to maintain erasure-resistant fear memories and loss of PNNs may render memories more susceptible to erasure by extinction learning. Similarly, PNN removal in the adult auditory cortex prevented consolidation of fear learning to tones 24-48 hours after conditioning, but not 30 minutes after [174]. Interestingly, they also found PNNs are increased 4 hours, but not 24-hours, after fear learning, overall suggesting that PNNs appear to be critical in long-term, but not short-term, memory consolidation.

Lastly and most recently, degradation of PNNs *in vivo* in the visual cortex decreased inhibitory activity and increased gamma during a visual stimulus (recording single unit and population activity in awake, freely behaving animals) [175]. MD in adult ChABC-treated mice caused an immediate potentiation of gamma activity, which was not observed in control adults, but was seen in juvenile mice after MD. This study provides compelling evidence that the loss of PNNs reinstates a 'juvenile' plasticity environment. Performing similar experiments, this group also found that PNNs are required for retrieval of visual fear memory in the secondary visual cortex [176]. Taken together, these studies reveal a convincing role of PNNs regulating glutamatergic transmission, LTP and critical plasticity windows such as ocular dominance plasticity and fear learning.

The focus of this thesis will be on the role of the specialized extracellular matrix, perineuronal nets (PNNs), in regulating a window of plasticity in hippocampal area CA2 during early development.

Plasticity resistance in hippocampal area CA2

CA2 morphology and anatomy

Hippocampal area CA2 was first described in by Ramón y Cajal and Lorente de Nó as a small region that was distinct in cytoarchitecture and connectivity [177, 178]. The hippocampus consists of several subregions, namely the Cornu Ammonis (CA) regions and the dentate gyrus (DG). The CA regions, CA1, CA2, and CA3, are organized into a layer of pyramidal neurons with apical and basal dendrites extending into the stratum radiatum (SR) or stratum oriens (SO), respectively. The CA2 region is distinguishable from other hippocampal subregions by several features such as morphology, molecular profile, and its resistance to plasticity and injury.

CA2 neurons are morphologically distinct in that their cell somas are typically larger than CA1 neurons and their dendrites lack thorny excrescences (postsynaptic specializations associated with mossy fibers and characteristic of CA3 pyramidal neurons) [178]. Compared to the homologous and organized morphology of CA1 neurons, CA2 cells are heterogeneous based cell soma and dendritic anatomical analysis [179]. CA2 neurons predominantly receive direct inputs from CA3 Schaffer collaterals, entorhinal cortex layer II, and more recently discovered, inputs from newborn DG granule neurons, extrahippocampal inputs from the supramammillary nucleus (SuM) and the paraventricular nucleus (PVN) of the hypothalamus, among others [180, 181 182-184]. The absence of DG terminals has also been used as an anatomical identifier of CA2 neurons. Initially, the CA2/3 border was thought sit at the ending of DG axons, however many studies, across species, have since described DG inputs extending deep into CA1 [178, 185, 186]. Outside of these distinct anatomical and circuit properties, CA2 neurons also exhibit unique cell signaling pathways and respond distinctly several neuromodulators.

CA2 neurons have a higher mean firing rate than CA1 and CA3[187, 188] A chronic loss of CA2 output leads to increased excitability in the recurrent CA3 network, which was found to result in widespread hyperexcitability during exploration and high frequency CA2 discharges during rest; overall implicating CA2 as a gateway for the spread of excitatory activity in the hippocampus [189].

Plasticity (and the lack thereof) in CA2

Most research on synaptic plasticity has been focused predominantly on mossy fiber synapses from DG to CA3 and on Schaeffer collateral synapses from CA3 to CA1 [6, 190]. Researchers initially became intrigued by CA2 because, unlike neurons in other hippocampal regions that are vulnerable to damage from seizure, ischemia or traumatic insult, CA2 neurons are resistant to cell death from injury in human, as well as in rodent [191-195].

CA3 Schaffer collateral (SC) synapses on CA2 dendrites are highly resistant to the induction of LTP such that high frequency stimulation or a pairing protocol (postsynaptic depolarization during stimulation) surprisingly fails to induce plasticity in CA2 neurons as they do in CA1 [196]. Although we have yet to fully understand the mechanisms behind this resistance to plasticity, a number of CA2-specific genes and extracellular matrix components are implicated in plasticity resistance [197]. One or more of these mechanisms involve regulation of intracellular calcium levels. For example, LTP can be induced in CA2 by elevating intracellular calcium, either by blocking calcium extrusion in the postsynaptic cell using an inhibitor of the plasma membrane calcium ATPase (PMCA) or by elevating extracellular calcium to 10mM (182). Simons and colleagues also use calcium imaging to show that CA2 dendrites and spines have smaller rises in free calcium in response to action potential and have a significantly faster rate of calcium extrusion compared to neighboring CA1/3 neurons. These data, in, addition to the

enrichment of several other calcium/calmodulin-associated proteins in CA2, such as PCP4 (purkinje cell protein 4), RGS14 (regulator of G-protein signaling 14), strongly suggests that robust calcium handling properties play an important function in limiting plasticity in CA2.

RGS14 protein is also highly expressed in CA2 and is a suppressor of LTP. Mice lacking RGS14 express LTP at CA2 SR synapses and exhibit enhanced spatial and object recognition memory compared to wildtypes [198]. Mechanistically, RGS14 is likely to act as a scaffolding protein that negatively regulates ERK/MAPK activation and inhibits signal transduction by driving G-protein α subunits into their inactive state [199]. However, recent data showing that RGS14 also binds several proteins linked to calcium signaling such as calmodulin and CaMKII, suggest that RGS14 may also be important in regulating both calcium and ERK pathways [200]. RGS14 mRNA and protein are upregulated during postnatal development, with the protein first being detectable in rodent CA2 at P7 and maximally expressed in adulthood [201]. Although RGS14 has been strongly implicated in both regulating CA2 plasticity, as well as mediating several hippocampal-dependent learning tasks, RGS14 is just one of many apparently redundant molecular brakes acting to restrict plasticity in CA2.

Plasticity modulators in CA2

CA2 plasticity is also regulated by several neuropeptides. Receptors for the social neuropeptides vasopressin and oxytocin are enriched in CA2. These neuropeptides play a role in modulating social behavior, aggression, and anxiety [202]. Bath application of both agonists are able to induce a significant excitatory potentiation at CA2 SR synapses in hippocampal slices, but not at CA1 synapses [203]. This form of vasopressin-induced potentiation is dependent on NMDA receptors, calcium, and CaMKII. Vasopressin receptor 1b (Avpr1b- arginine vasopressin receptor 1b) knockout mice show decreased social aggression but no anxiety-like behaviors [204].

Although the Avpr1b$^{-/-}$ mouse is a global knockout, viral delivery of the Avpr1b receptor to dorsal CA2 neurons was sufficient to restore aggressive behavior [203]. Moreover, vasopressin is endogenously released by neurons in PVN of the hypothalamus, a known direct CA2 input. A recent study found that optogenetic excitation of PVN neurons enhanced social memory and was subsequently blocked by an Avpr1b antagonist [205], strongly implicating CA2 in social memory function. A second peptide hormone, Substance P, originating from SuM inputs, also induces a similar NMDA-dependent potentiation in CA2 [206]. Though Substance P is considered to be an important neuropeptide in nociceptive processes, SuM inputs to the hippocampus have also been linked to stress [207].

Lastly, CA2 synapses are also potentiated by the psychostimulant drug, caffeine, and other antagonists of the CA2-enriched receptor adenosine 1 (A1R) [208 209, 210]. Unlike vasopressin-induced potentiation, caffeine-induced potentiation is independent of NMDA receptors and CaMKII, but is blocked by inhibitors of adenylyl cyclase or PKA (Fig. 1). This mechanism of action was not surprising considering A1Rs are coupled to the Gi/o family of G proteins and, when activated by its agonist adenosine, normally inhibit adenylyl cyclases. Potentiation of CA2 synapses by these neuromodulators implicate CA2 in multiple behaviors such as aggression and social memory, however the link between restricted plasticity in CA2 and regulation of these behaviors is still unclear.

Plasticity of Inhibition in CA2

Several inhibitory neuron cell-types are concentrated in CA2 relative to neighboring subregions and several groups have reported strong inhibitory drive onto CA2 neurons [211-214]. Inhibitory neuron cell types, PV-, Reelin-, somatostatin-, and calbindin-positive are all more densely localized in CA2 compared to neighboring hippocampus subregions [215]. Blocking

feedforward inhibition onto CA2 increases excitatory responses of CA2 neurons, suggesting that inhibitory input may be acting as a brake on CA2 cell firing to a larger degree than CA1 [211]. Also, similar to CA1, inhibitory synapses onto CA2 pyramidal neurons in SR are highly plastic in that they undergo LTD in response to high frequency stimulation, inhibitory LTD (iLTD) [212]. This disinhibition of CA2 synapses in response to high frequency stimulation is sufficient to evoke action potential firing in CA2 [212]. Delta-opioid receptor (DOR) activation mediates this iLTD at CA2 inhibitory synapses, specifically at PV synapses, presumably by presynaptic reduction in neurotransmitter release [216]. Similarly, another type of protocol, pairing activation of entorhinal cortex (EC) and Schaffer collateral (SC) inputs on CA2 pyramidal neurons, also results in a form of input-timing dependent plasticity (ITDP) that is a DOR-dependent iLTD [217]. This ITDP/iLTD is distinct from that in CA1, which is mediated by endocannabinoid receptors on cholecystokinin-expressing interneurons [217, 218]. Thus, because excitatory synapses in CA2 SR are normally resistant to plasticity, the authors suggest that iLTD at CA2 SR may function as a mechanism to gate CA2 excitatory output, essentially serving as a way of getting potentiation of CA2 neuron function in the absence of LTP-like processes at excitatory synapses. Interestingly, a postmortem study of schizophrenic individuals reveal that non-pyramidal neurons are 40% lower in area CA2. This finding was replicated in a mouse model of 22q11.2 deletion syndrome, where it was also found that CA2 pyramidal neurons have a reduction in feedforward inhibition [218, 219] Taken together, these data suggest that inhibitory drive on CA2 neurons is different from neighboring subregions and may represent a powerful gating mechanism of CA2 neuron firing.

Function of CA2

The hippocampus is integral in many forms of learning and memory, such as episodic/ contextual memory, spatial/ temporal cognition and fear learning, among others. However,

recent interest has focused on the function of area CA2. Several studies have recently implicated CA2 in novelty detection [187, 198, 220], spatial memory [188, 221, 222], social recognition memory, and aggression [187, 223, 224, 225]. The social and aggression behaviors have been linked to the localization of several social neuropeptide receptors in CA2, eg. oxytocin and vasopressin [203, 226, 227] and the direct vasopressinergic projection from the PVN to CA2 [183, 223]. For example, mice deficient in RGS14, a protein that is enriched in CA2 and functions to restrict synaptic plasticity, also display enhanced novel object recognition memory and faster learning acquisition in the Marris water maze [198]. Moreover, mice deficient in the vasopressin receptor and oxytocin receptor (both social neuropeptide receptors high in CA2) have deficits in social recognition memory and aggression [227-229]. Interestingly, re-expression of the vasopressin receptor in dorsal CA2 neurons is sufficient to restore normal aggressive behavior [203]. Recently, Smith and colleauges found that optogenetic excitation of PVN neurons, a pathway known to directly innervate CA2, enhanced social memory and the effect was blocked by a vosopressin 1b receptor antagonist [205]. Several studies directly manipulate CA2 neuronal activity *in vivo* and find that silencing CA2 neurons impairs social recognition memory [224, 230], and similarly, excitotoxic lesion of CA2 neurons also impaired social recognition memory [225]. CA2 neurons also display place fields (a location in space where a particular neuron will fire) however, unlike CA1, CA2 neuron ensembles become progressively dissimilar over time, or temporally remap [187, 188]. The weak spatial coding exhibited by CA2 relative to CA1/3 supports a preferential role for CA2 in social, emotional, and temporal function, rather than spatial. Taken together, these data beg the question as to what is the function of a critical period in CA2.

For the most part, hippocampal synaptic plasticity, particularly LTP, is maintained throughout adulthood, and this may be one reason synaptic plasticity in the hippocampus is

thought to underlie formation of several types of memory [231]. However, evidence suggests that some critical periods related to hippocampal function do exist. For example, adult rodents and humans are generally unable to recall memories of their early childhood (referred to as infantile amnesia), and the ability to maintain long-term declarative-like memory improves with age [232]. One specific form of hippocampal-dependent memory that is developmentally regulated is contextual fear learning [73, 233-237]. The age of functional onset of fear learning appears to be around P21-P28 in rats, generally after plasticity has matured in CA1 [73, 84]. Although the exact mechanisms regulating the window for fear learning is unknown, a leading explanation for infantile amnesia pertains to hippocampal neurogenesis; the developmental decline in hippocampal neurogenesis corresponds with the ability to form stable long-term memories (humans, nonhuman primates, and rodents) [238-241]. Another explanation might be the postnatal development of molecular brakes on plasticity, eg. the development of PNNs in CA2, the focus of this thesis. These studies are integral to our understanding of the mechanisms underlying fear learning and how human childhood trauma has detrimental effects on adult mental health. Ultimately, these studies may reveal critical therapeutic windows of intervention in the hippocampus that could intervene in the widespread psychological effects of early life trauma.

Dissertation Aims

This thesis seeks to answer outstanding questions regarding the characterization and activity-dependent regulation of perineuronal nets (PNNs) in hippocampal area CA2.

Chapter 1: CA2 PNNs are described using fluorescent and electron microscopy to characterize composition and anatomical localization around the cell soma and synapses in

pyramidal and SR regions. The cellular origin of PNN synthesis in area CA2 is identified using fluorescent *in situ* hybridization. PNN postnatal development is tracked and tested for experience-dependent modulation using an environmental enrichment paradigm. Lastly, the functional role of PNNs are tested using electrophysiological techniques in mouse hippocampal slices where PNNs are degraded and CA2 intrinsic, synaptic and plasticity properties are measured.

Chapter 2: I characterized the development and function of PNNs in a mouse model Rett Syndrome, a PNN-associated neurodevelopmental disorder. Using a mouse knockout of MeCP2, I quantified the premature development and aberrant increase of PNNs in CA2 compared to control mice, and investigated the functional effects of premature PNN development on CA2 plasticity in slices from young animals. Finally, to study the cell-autonomous effects on PNN development, I deleted to Rett gene, MeCP2 (methyl-CpG binding protein 2) from CA2 pyramidal neurons and quantified changes of PNNs in the hippocampus.

Chapter 3: Finally, PNNs have been strongly implicated in temporal lobe epilepsy (TLE). Here I aimed to quantify PNN development in a mouse model of TLE. These Kv1.1 knockout mice present with seizure activity starting at P21 and sustain recurrent spontaneous seizures into adulthood. This mouse also allows for the study of aberrant activity during adolescence, a developmental time point when PNNs are differently regulated by activity [242, 243]. To better study the effects of PNN regulation *in vivo,* I also describe the creation of a viral vector system designed to conditionally target the degradation of PNNs in CA2 with the enzyme ChABC, with the long-term goal of studying the function of CA2 PNNs in behavior.

CHAPTER II - PERINEURONAL NETS SUPPRESS PLASTICITY AT EXCITATORY SYNAPSES ON CA2 PYRAMIDAL NEURONS[1]

Overview

Long-term potentiation of excitatory synapses on pyramidal neurons in the stratum radiatum rarely occurs in hippocampal area CA2. Here, we present evidence that perineuronal nets (PNNs), a specialized extracellular matrix typically localized around inhibitory neurons, also surround mouse CA2 pyramidal neurons and envelop their excitatory synapses. CA2 pyramidal neurons express mRNA transcripts for the major PNN component aggrecan, identifying these neurons as a novel source for PNNs in the hippocampus. We also found that disruption of PNNs allows synaptic potentiation of normally plasticity-resistant excitatory CA2 synapses; thus, PNNs play a role in restricting synaptic plasticity in area CA2. Finally, we found that postnatal development of PNNs on CA2 pyramidal neurons is modified by early-life enrichment, suggesting that the development of circuits containing CA2 excitatory synapses are sensitive to manipulations of the rearing environment.

[1] This chapter previously appeared as an article in the Journal of Neuroscience. The orginal citation is as follows: Carstens, K.E., M.L. Phillips, and L. Pozzo-Miller, *Perineuronal Nets Suppress Plasticity of Excitatory Synapses on CA2 Pyramidal Neurons.* 2016. **36**(23): p. 6312-20.

Introduction

Although components of the extracellular matrix (ECM) have been implicated in promoting synaptic plasticity, perineuronal nets (PNNs), a specialized form of ECM typically found around inhibitory neurons, are thought to inhibit plasticity [67]. We previously identified hippocampal area CA2 as a region where synaptic plasticity is limited, even relatively early in postnatal development [196]. Unlike PNNs in other brain regions, PNNs in area CA2 appear to be near excitatory synapses of pyramidal neurons [108, 109, 244], leading us to wonder whether PNNs are related to pyramidal neurons in some way.

PNNs first appear in the brain around postnatal day (PN) 14 in the mouse, and gradually increase until they are fully expressed in adulthood, often tracking the end of critical windows of synaptic plasticity [1, 2]. Interestingly, the onset of PNN expression requires normal early experience in several brain regions, including motor, visual, and somatosensory systems, and similar manipulations performed in adulthood were without effect [113, 114, 116-118]. Because PNN deposition is experience-dependent and increases during postnatal development, these structures have been hypothesized to function in dampening synaptic plasticity during the closure of critical periods. For example, Pizzorusso et al. (2002) demonstrated an association between the presence and absence of PNNs in the visual cortex and the closure and reopening of ocular dominance plasticity, strongly supporting a role for PNNs in limiting experience-dependent plasticity [134]. Because PNNs associated with pyramidal (i.e., presumed excitatory) neurons are rare in cortical structures [245], the role of this matrix in limiting plasticity is widely thought to be due to their association with nonpyramidal (i.e., presumed inhibitory) neurons, specifically parvalbumin (PV)-positive interneurons.

The structural and physiological effects of removing PNNs enzymatically have been well studied in inhibitory neurons. Degradation of PNNs around inhibitory neurons in culture (mainly PV-positive interneurons) with the bacterial enzyme chondroitinase (ChABC) increases interneuron excitability without affecting the number or distribution of perisomatic GABAergic presynaptic terminals [148], suggesting that PNNs function to regulate inhibitory neuron activity. Interestingly, manipulation of neuronal activity seems to modulate the development of PNNs both in culture and *in vivo*. For example, blocking neuronal activity in culture decreases PNNs around inhibitory neurons. Similarly, decreasing activity via dark rearing delays and attenuates PNN development around inhibitory neurons in the visual cortex [134].

Hippocampal area CA2, positioned between areas CA3 and CA1, has recently been appreciated as an important module of the hippocampus that is molecularly distinct from its neighboring areas [197, 246]. CA2 neurons receive excitatory synapses from the dentate gyrus, entorhinal cortex, and area CA3, and it is these synapses from CA3 in CA2 stratum radiatum (SR) that are highly resistant to plasticity [184, 196, 211]. Although we have yet to fully understand the mechanism(s) behind this resistance to synaptic plasticity, several genes highly expressed in area CA2 are implicated in this lack of plasticity [198, 209, 247, 248]. Based on these observations and previous studies implicating PNNs in restricting plasticity, we investigated whether PNNs around pyramidal neurons in area CA2 play a role in restricting synaptic plasticity of CA2 excitatory synapses and are modified by early-life experience.

Materials and Methods

Animals

Animals in all experiments were housed under a 12:12 light/dark cycle with access to food and water *ad libitum*. All procedures were approved by National Institute of Environmental Health Sciences, University of Alabama at Birmingham, and University of North Carolina Animal Care and Use Committees and were in accordance with the National Institutes of Health guidelines for care and use of animals.

Immunohistochemistry

Mouse lines expressing enhanced green fluorescent protein (EGFP) were used to label hippocampal CA2 pyramidal neurons (Gene Expression Nervous System Atlas, Amigo2-EGFP; Tg(Amigo2-EGFP)LW244Gsat/Mmcd) and GABAergic interneurons (Riken BioResource Center, Gad67-GFP; Cg-Gad1<tm1.1Tama>). Adult male mice were deeply anesthetized with Fatal-Plus and perfused with cold PBS, followed by 4% paraformaldehyde in PBS, pH 7.4. Brains were removed and postfixed overnight at 4°C and submerged in 30% sucrose. Forty-micrometer-thick sections were cut on a sliding microtome, blocked in 5% normal goat serum and incubated in biotin-conjugated *Wisteria floribunda* agglutinin (WFA) lectin (1:1000; Sigma-Aldrich L1516) or antibodies anti-aggrecan (1:500; Millipore AB1031) or anti-neurocan (1:200; R&D Systems AF5800) overnight at 4°C. Sections were washed three times in PBS and incubated in secondary antibody at 1:500 for 40 min at room temperature: streptavidin Alexa-568 (Invitrogen), goat anti-rabbit H+L A568 (Invitrogen), or goat anti-chicken H+L (Invitrogen). Alternatively, the biotin-conjugated WFA lectin was amplified with the Vectastain Elite ABC kit (Vector Laboratories PK-6100) and reacted with 3,3′-diaminobenzidine (DAB) substrate kit (Vector Laboratories SK-4100). Sections were mounted with Vectashield antifade mounting

medium with DAPI (Vector Laboratories). Images were acquired on a Zeiss laser scanning confocal (LSM510 NLO) or a Zeiss light microscope using controlled camera settings.

Immunohistochemistry and confocal microscopy of excitatory synapses on dendritic spines

Adult male mice of the thy1-GFP line M (7–20 months; [249]) were anesthetized with a mixture of ketamine and xylazine, and perfused as described above. Thirty-micrometer-thick coronal sections of the brain at the level of the dorsal hippocampus were made with a vibratome, and immunohistochemistry was performed on free-floating sections at room temperature. Sections were blocked and permeabilized by incubation in 10% goat serum albumin, 2% bovine serum albumin, and 0.4% Triton-X in PBS for 1 h. Sections were incubated with biotin-WFA (1:100) and primary antibodies diluted in 5% goat serum albumin, 2% bovine serum albumin, and 0.1% Triton-X in PBS for approximately 48 hours. Primary antibodies used were guinea pig anti-VGLUT1 (1:1000; EMD Millipore AB5905) and rabbit anti-GFP (1:2000; Abcam 290). After washing three times for 5 min in PBS, sections were incubated for 4 h in Streptavidin-594 (1:1000; Life Technologies) and fluorescently labeled secondary antibodies (anti-rabbit Alexa-488, 1:500; Jackson ImmunoResearch; anti-guinea pig Alexa-647, 1:500; Jackson ImmunoResearch). Sections were washed three times for 5 min in PBS, incubated with DAPI (300 nm) for 5 min, and washed with PBS for 5 min before mounting with Vectashield antifade mounting media (Vector Laboratories). Sections were imaged in a laser-scanning confocal microscope (Zeiss Spectral LSM510-META) equipped with a multiline argon laser (458, 477, 488, and 514 nm) and two HeNe lasers (543 and 633 nm) using an oil-immersion 100× objective (1.4 numerical aperture). Image stacks through the *z* plane were acquired at 0.1 μm, and displayed as maximum-intensity projections in ImageJ software (National Institutes of Health).

Electron Microscopy

Adult mice (Charles River) were perfused with 4% paraformaldehyde (0.1 m phosphate buffer, pH 7.2) and 0.1% glutaraldehyde for 10 min. Brains were postfixed at 4°C overnight and 50-μm-thick coronal sections were cut on a vibrating microtome. Sections were stained for PNNs following a pre-embedding immunohistochemistry protocol and preincubated in 1% $NaBH_4$, 3% hydrogen peroxide, and 10% normal goat serum before overnight incubation in biotinylated WFA 8 μg/ml (Sigma-Aldrich L1516). Staining was amplified with a Vectastain Elite ABC kit (Vector Laboratories), developed with Ni-DAB and incubated in 1% osmium tetroxide, then in 1% uranyl acetate. Then sections were embedded in epoxy resin. Hippocampal pieces were cut from heat-polymerized wafers, glued to a plastic block, cut at 60 nm with an ultramicrotome, collected on copper grids, and stained with uranyl acetate and Sato's lead. Electron micrographs were imaged on a Philips Tecnai microscope at 80 kV.

Electrophysiology

Mice (Charles River Laboratories), age PN 14–18 of either sex, were deeply anesthetized with Fatal-Plus, decapitated, and their brains submerged into oxygenated ice-cold sucrose-substituted artificial CSF (ACSF), pH 7.4, containing the following (in mm): 240 sucrose, 2.0 KCl, 1 $MgCl_2$, 2 $MgSO_4$, 1 $CaCl_2$, 1.25 NaH_2PO_4, 26 $NaHCO_3$ and 10 glucose. Coronal brain slices were cut at 300 μm using a vibrating microtome (Leica VT 1000S) and allowed to recover at room temperature in a submersion holding chamber with ACSF containing the following (in mm): 124 NaCl, 2.5 KCl, 2 $MgCl_2$, 2 $CaCl_2$, 1.25 NaH_2PO_4, 26 $NaHCO_3$, and 17 d-glucose bubbled with 95% O_2 with 5% CO_2. Slices from one hemisphere were incubated in ACSF and slices from the other in ACSF with 0.05 U/ml chondroitinase ABC (ChABC; Sigma-Aldrich C3667) for ≥2 h until they were transferred to a recording chamber and continuously bathed (at 2

ml/min) in normal ACSF at room temperature ([137]). Effectiveness of the chondroitinase treatment was confirmed by staining Amigo2-EGFP slices with WFA as above, except that the 300-μm-thick slices were cleared using 60% thiodiethanol in PBS before imaging ([250]).

Whole-cell recordings were made from pyramidal neurons in either the CA2 or CA1 regions. CA2 neurons in the pyramidal layer were initially identified using Amigo2-EGFP mice. Glass borosilicate pipettes were filled with a potassium gluconate internal solution containing the following (in mm): 120 K-gluconate, 10 KCl, 3 $MgCl_2$, 0.5 EGTA, 40 HEPES, 2 Na_2-ATP, 0.3 Na-GTP, pH 7.2. The pipettes had a tip resistance between 2.5 and 4 MΩ. Baseline synaptic responses were collected for ≥5 min. For long-term potentiation (LTP) experiments, a pairing protocol was used. This protocol consisted of 1.5 min of 3 Hz presynaptic stimulation (270 pulses) paired with postsynaptic depolarization to 0 mV in voltage-clamp mode. Data were collected using Clampex 10.4 and analyzed using Clampfit software (Molecular Devices). Series and input resistances were monitored by measuring the response to a 10 mV step at each sweep and cells were included for analysis if <25% change in series and input resistance was detected. Recordings were not compensated for series resistance.

To determine action potential threshold, whole-cell recordings were performed in current-clamp mode. Current pulses of 180 ms in 0.2 nA steps were delivered and the membrane potential at which the cells first fired action potentials was measured. To assess excitatory transmission, whole-cell recordings were performed in voltage-clamp mode, and EPSCs were isolated using the $GABA_A$ receptor antagonist bicuculline (10 μm) in the bath solution. EPSC amplitudes were measured at increasing stimulation intensities. Paired-pulse facilitation was assessed under similar conditions.

To measure the NMDA receptor (NMDAR)-mediated component of the EPSC, a cesium internal solution was used to block sodium-dependent action potentials, and 5 tetraethylammonium chloride was used for whole-cell recordings conducted in the presence of glycine (5 μm) and bicuculline (10 μm). The cesium internal solution contained the following (in mm): 102 CsOH, 102 d-gluconate, 3.7 NaCl, 10 BAPTA, 0.2 EGTA, 20 HEPES, 4 Mg-ATP, 0.3 Na-GTP, 5 lidocaine *N*-ethyl bromide (QX314). EPSCs were measured at −70 and +40 mV holding potentials. The AMPA receptor (AMPAR)-mediated component of the EPSC was measured 2 ms after stimulation at +40 mV (P1), while the NMDAR-component was measured 50 ms after the same stimulation (P2; [251]). The AMPAR/NMDAR ratio was calculated either as a ratio of the P1/P2 responses at +40 mV or as a ratio of P1 at −70 divided by P2 at +40 mV.

Environmental Enrichment (EE)

One dam (Amigo2-EGFP line) and its litter were singly housed in either standard caging (32 × 21 × 19 cm) or environmental enrichment (EE) caging (50 × 30 × 30 cm). Standard caging included cotton squares (Enviro-Dri, Shepherd's Specialty Papers) for nesting. EE caging consisted of toys of varying shapes and sizes, such as plastic houses and wooden blocks; extra bedding material, such as cotton squares; sunflower seeds, and fruit/bacon-flavored rodent treats for various forms of sensory stimulation. Objects were repositioned/replaced and treats were replenished every other day. Brains were harvested as described above from male mice at ages PN 14, PN 21, and PN 45 and analyzed for staining of WFA during the 12 h light cycle. WFA staining intensity was quantified using measures of pixel luminescence value on ImageJ software (National Institutes of Health) using a region of interest (ROI) contoured around either CA2 pyramidal neurons in stratum pyramidale (SP) or CA2 apical dendrites using GFP fluorescence

in a dorsal hippocampal section. The mean gray value measure of the image background was subtracted from the mean gray value of the CA2 ROI. Each data point represents one mouse. This study was repeated in a separate cohort of animals and the data combined by normalizing each mean gray value–the value for the PN 45 enriched cohort–for each study. For each experiment, fluorescence quantification was repeated and analyzed with the experimenter blinded to condition. The sample number of mice (*N*) was 4, 5, 6, 7, 8, and 9 for the following groups, respectively: PN 14 standard, PN 14 enriched, PN 45 standard, PN 21 enriched, PN 21 standard, and PN 45 enriched.

In situ hybridization

Adult mouse brains were flash frozen and coronal 20-μm-thick sections were cut on a cryostat and mounted on SuperFrost Plus slides (Fisher Scientific 12-550-15). Sections were fixed in 4% paraformaldehyde for 1 h at 4°C, dehydrated in 50, 70, and 100% ethanol, and air-dried at room temperature. Fluorescent RNAscope *in situ* hybridization (ISH) was performed using an RNAscope Fresh Frozen Multiplex Fluorescent kit according to the manufacturer's protocol to perform target probe hybridization and signal amplification (Advanced Cell Diagnostics). Probes were purchased from Advanced Cell Diagnostics: aggrecan mRNA, mm-acan-C1 (catalog #300031-C1) and the CA2-marker Purkinje cell protein 4 (PCP4) mRNA, Mm-Pcp4-C2 (catalog #402311-C2). Fluorescent images were captured on a Zeiss laser-scanning confocal microscope (LSM710).

Statistics

Data in Figures 3 and 4 are expressed as a mean ± SEM. Data in Figure 3 are expressed as a normalized mean ± SEM (the enrichment study was repeated once and data were pooled to increase statistical power). Statistical analyses were performed using GraphPad Prism 6.05

software, and significance was calculated using an α level of 0.05. The Kolmogorov–Smirnov test was used to test normality and variance.

Results

PNNs localize to excitatory synapses on CA2 pyramidal neurons

To confirm our initial impression that PNNs indeed surround CA2 pyramidal neurons and their dendrites, we used tissue from mice expressing EGFP under the promoter of *Amigo2*, a gene highly expressed in area CA2 [252]. Three different PNN markers, WFA, the chondroitin sulfate proteoglycans aggrecan and neurocan, labeled select inhibitory interneurons throughout the hippocampus (Fig.1a), but also intensely labeled EGFP-expressing CA2 pyramidal neurons (Fig. 1b). The origin of PNN matrix components in area CA2 is unknown, so we used fluorescence ISH to determine whether these pyramidal neurons express transcripts for the major PNN component aggrecan. We found that CA2 neurons identified by Purkinje cell protein 4 (*PCP4*) expression, but not CA1 and CA3 neurons, expressed *aggrecan* mRNA (Fig. 1c). Localization of *aggrecan* mRNA in the pyramidal cell layer of area CA2 indicates that CA2 pyramidal neurons synthesize at least one major component of the PNN matrix, identifying such neurons as a novel source of PNNs in the hippocampus.

Figure 1

Figure 1: PNN markers surround CA2 pyramidal neurons and dendrites. ***a***, Fluorescent labeling of WFA (green) localizes with CA2 pyramidal neurons and with GAD67-positive inhibitory neurons (red) in hippocampus. ***b***, Anti-aggrecan (top), WFA (middle), and neurocan (bottom), indicated in green, label EGFP-expressing CA2 pyramidal neurons and their proximal neurites in red (scale bar, 50 μm). ***c***, Fluorescent ISHs showing that *aggrecan* mRNA (green) and a CA2 marker, *Pcp4* mRNA (red), colocalize to the CA2 pyramidal cell layer. Yellow shows the overlapping distribution of these two mRNAs.

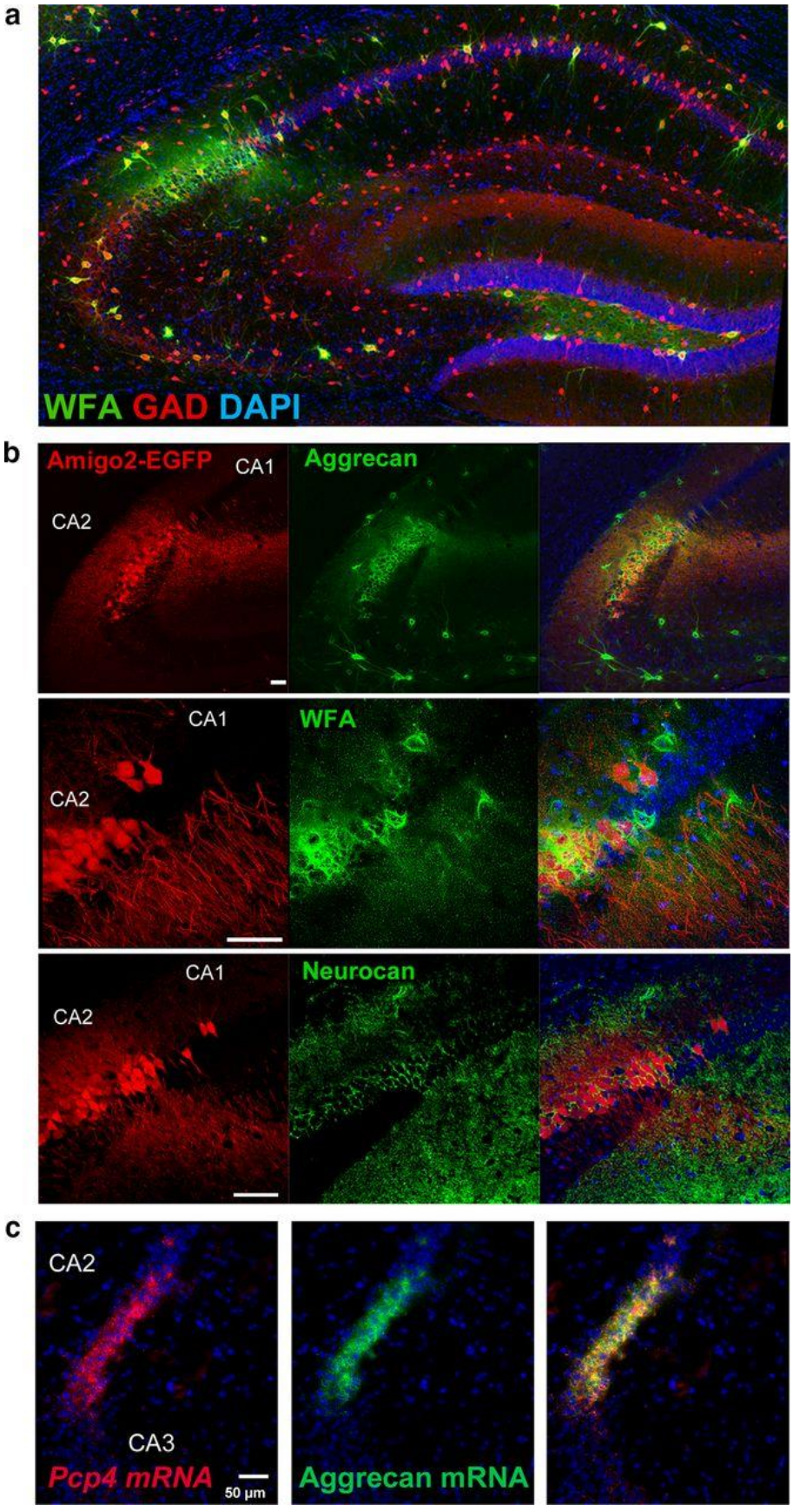
a
WFA GAD DAPI
b
Amigo2-EGFP
CA1
CA2
Aggrecan
CA1
CA2
WFA
CA1
CA2
Neurocan
c
CA2
CA3
Pcp4 mRNA
50 µm
Aggrecan mRNA

WFA also diffusely labeled the CA2 SR and stratum oriens (Fig. 2*a*) near the dendritic spines of excitatory synapses (as defined by label for VGlut1; Fig. 2*b*). To more precisely characterize this diffuse labeling in the CA2 SR, we turned to electron microscopy. We found that electron-dense staining for PNNs appeared around the somata of CA2 pyramidal cells and numerous dendritic spines in the CA2 SR, especially around spine necks and in perisynaptic regions (Fig. 2*c*). In contrast, staining for PNNs in the neighboring CA1 SP and SR layers was sparse (Fig. 2*c*).

Figure 2

Figure 2: PNN markers are associated with excitatory synapses in area CA2. ***a***, WFA immunoperoxidase staining in area CA2 labels CA2 dendrites in the SR in addition to cell bodies in the SP. ***b***, WFA label surrounds excitatory synapses on primary apical dendrites of area CA2 SR; green is GFP expressed in neurons in tissue from a thy1-GFP-M mouse, red is WFA, purple is VGLUT1, and yellow shows where two channels depicted in each panel have overlapped (scale bar, 1 μm). ***c***, Electron micrographs showing WFA staining along dendritic spines of CA2 pyramidal neurons in the SR (top, red arrowheads), and area CA2 somata in the SP (bottom), and sparse labeling of WFA in area CA1 SP and SR (bottom; scale bar, 2 μm).

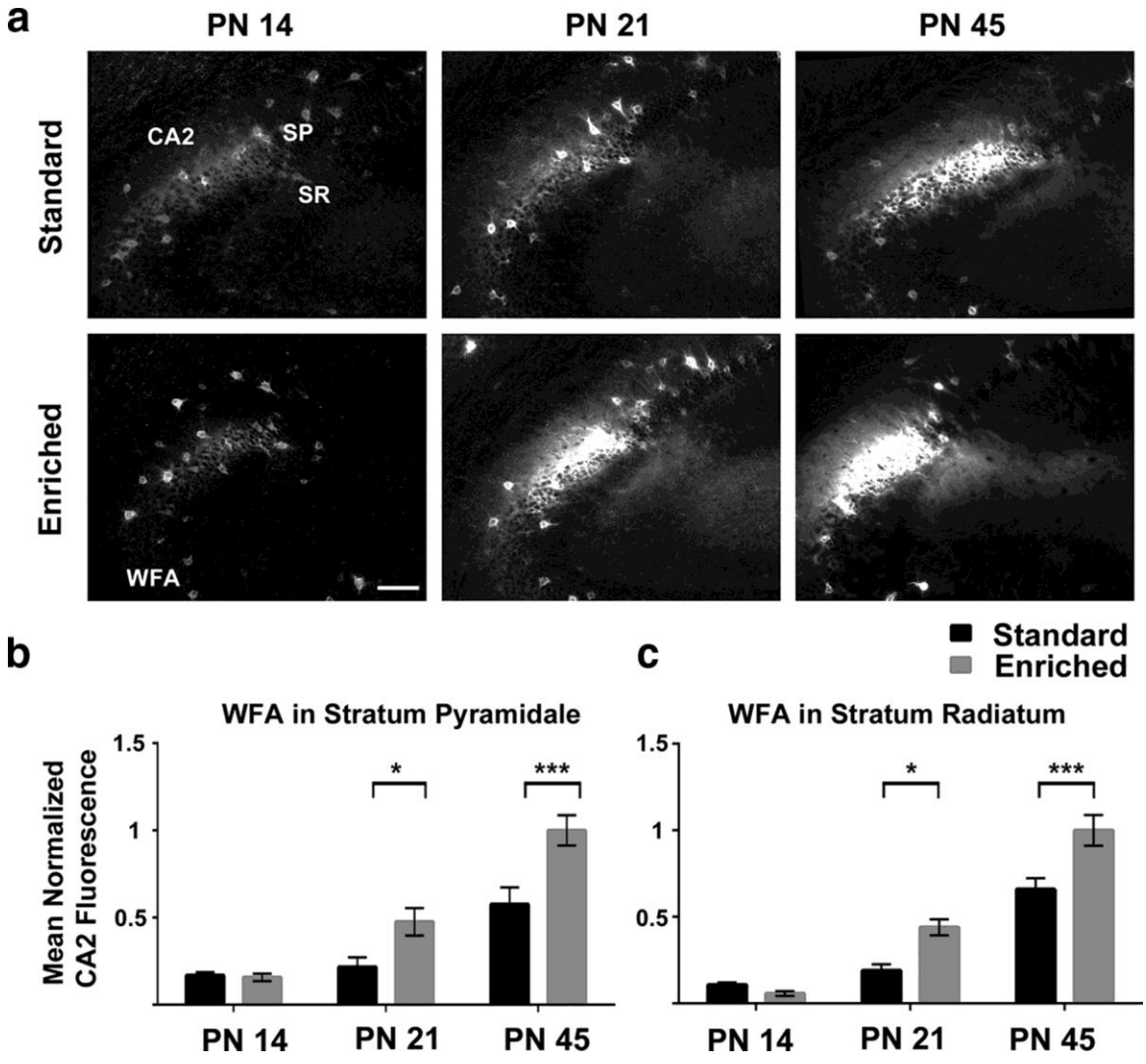
a
PN 14
PN 21
PN 45
Standard
Enriched
CA2
SP
SR
WFA
b
WFA in Stratum Pyramidale
Mean Normalized CA2 Fluorescence
1.5
1
0.5
*
***
PN 14
PN 21
PN 45
c
Standard
Enriched
WFA in Stratum Radiatum
1.5
1
0.5
*
***
PN 14
PN 21
PN 45

PNN development is regulated by experience

Consistent with previous work in other brain regions, including area CA1 [242, 253], we found that PNN staining in CA2 SP and SR increased with age during early postnatal development (Fig. 3*a*), beginning with minimal WFA fluorescence at PN 14, and increasing in intensity with age. Early-life sensory deprivation has been demonstrated to delay and attenuate PNN development in several brain regions [114, 118, 134]. Moreover, in the visual cortex, early-life enrichment has been found to counter effects of dark rearing on PNN development, as well as promote cortical maturation and accelerate the closure of the critical period for plasticity [254, 255]. To investigate whether PNNs are similarly modulated by early-life experience in area CA2, we reared mice in EE conditions. We found that WFA staining intensity in the CA2 SP was significantly greater in EE-exposed animals than those reared in standard housing at PN 21 and PN 45 ($p = 0.047$ and $p = 0.001$ respectively; two-way ANOVA, Bonferroni's *post hoc* test for pairwise comparison), but not at PN 14, the earliest age tested (Fig. 3*b*; $p > 0.05$). WFA staining intensity was similarly significantly greater in the CA2 SR at PN 21 and PN 45 ($p = 0.015$ and $p = 0.001$ respectively; two-way ANOVA, Bonferroni's *post hoc* test for pairwise comparison; Fig. 3*c*).

Figure 3

Figure 3: PNNs increase during postnatal development and are increased with experience. ***a***, WFA staining in area CA2 is increased in animals reared in an enriched environment, compared with animals raised in standard (control) cages. Note that the images have been digitally lightened in all panels equally to better display PNNs at PN 14 in area CA2. ***b***, Normalized WFA fluorescence intensity was significantly greater in CA2 SP of EE mice compared with control at PN 21 (N = 8 and 7 for control and EE respectively) and PN 45 (N = 6 and 9 for control and EE respectively; Bonferroni's *post hoc* test for pairwise comparison after two-way ANOVA,*p < 0.05, ***p = 0.0008). No significant difference was observed at PN 14 (N = 4 and 5 for control and EE respectively). A two-way ANOVA for the two conditions at different ages indicated significant main effects of age ($F_{(2,33)}$ = 32.33), condition ($F_{(2,33)}$ = 11.72), and interaction ($F_{(2,33)}$ = 3.338). Indicated is the mean ± SEM. ***c***, Normalized WFA fluorescence intensity was similarly significantly greater in area CA2 SR at PN 21 and 45 (same N's as reported in ***b***; Bonferroni *post hoc* test for pairwise comparison after two-way ANOVA,*p < 0.05, ***p = 0.0009). A two-way ANOVA for the two conditions at different ages indicated significant main effects of age ($F_{(2,33)}$ = 69.55), condition ($F_{(1,33)}$ = 11.93), and interaction ($F_{(2,33)}$ = 3.940).

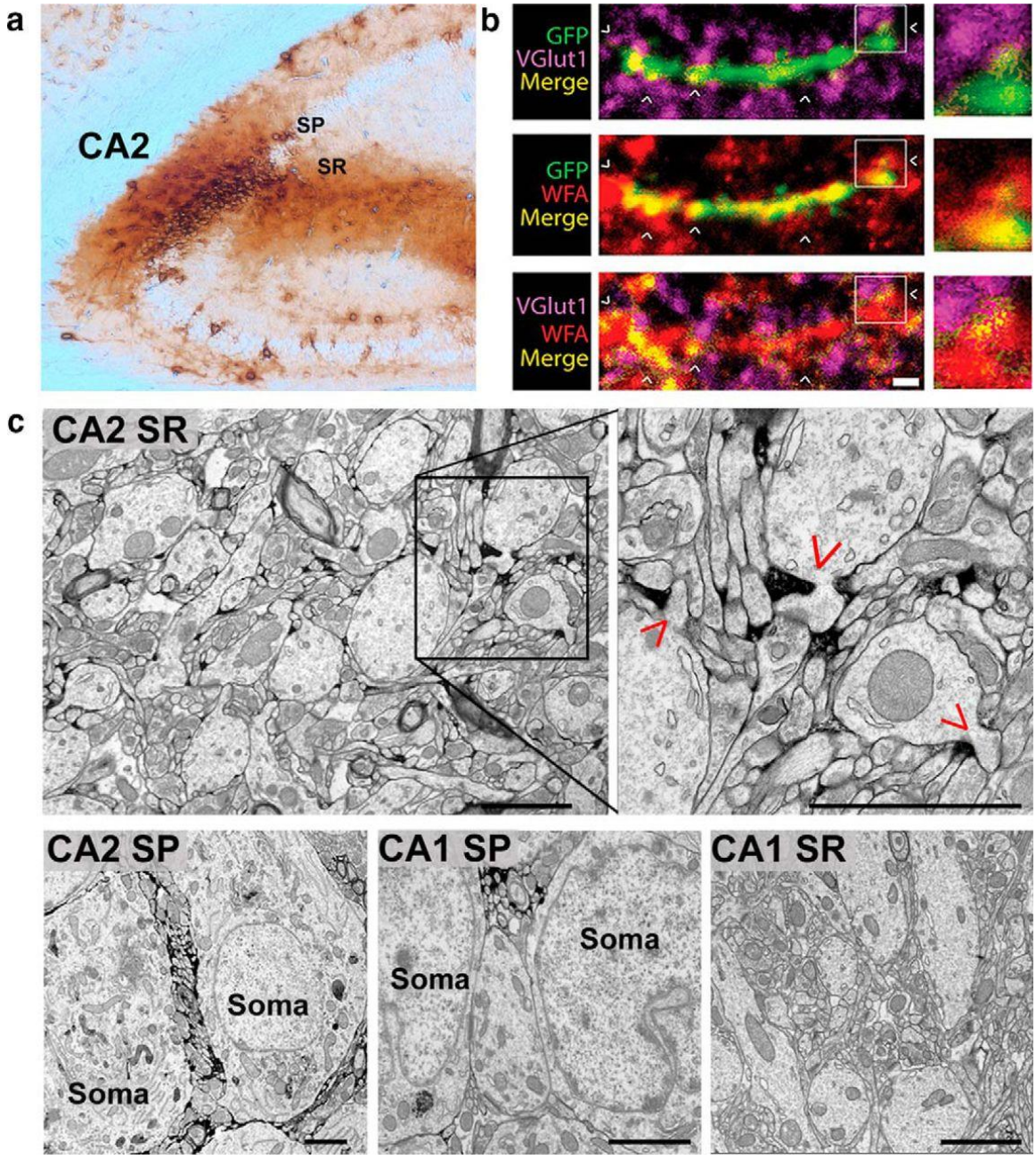
a
CA2
SP
SR
b
GFP
VGlut1
Merge
GFP
WFA
Merge
VGlut1
WFA
Merge
c
CA2 SR
CA2 SP
Soma
Soma
CA1 SP
Soma
Soma
CA1 SR

PNNs suppress synaptic plasticity in area CA2

Excitatory synapses in the CA2 SR fail to express typical LTP [196]. To determine whether PNNs act to restrict this type of plasticity in area CA2, we degraded PNNs with the enzyme ChABC in acute hippocampal slices and attempted to induce LTP at CA2 Schaffer collateral synapses. Similar to what has been reported for area CA1 [137], we found that PNNs are indeed degraded in area CA2 after a 2 h incubation of slices in ChABC (0.05 μl/ml; Fig. 4*a*). As reported previously for untreated slices, synaptic responses recorded from CA2 neurons were not potentiated following an LTP "pairing protocol" (92.0 ± 0.1% baseline, $n = 10$), whereas synaptic responses recorded from CA1 neurons showed typical LTP (140 ± 0.1% baseline, $n = 12$; Fig. 4*b*;[196]). However, a 2 h incubation with ChABC enabled LTP induction of excitatory synaptic responses in the CA2 SR (140 ± 0.2% baseline, $n = 10$), reaching levels comparable to that induced at CA1 synapses ($p = 0.02$, two-tailed unpaired *t* test compared with untreated slices). Similar results were obtained when experiments on ChABC-treated or control-treated slices were performed in the presence of the $GABA_A$-receptor blocker bicuculline (significant difference between ChABC-treated and untreated slices, $p = 0.022$ at 10 min, two-tailed unpaired *t* test compared with untreated slices, $n = 8$ and 4 respectively). Intrinsic properties did not change in a way that could explain this newly uncovered plasticity in area CA2 ($p > 0.05$, two-way ANOVA, Bonferroni's *post hoc* test for pairwise comparison; Fig. 4*c*; Tables 1, 2). Furthermore, in the presence of bicuculline, we found no significant differences in basal excitatory synaptic transmission (Fig. 4*d*), paired-pulse facilitation (Fig. 4*e*), or AMPAR/NMDAR ratio (Fig. 4*f*). These findings are consistent with a previous report showing that ChABC treatment had no effect on basal synaptic transmission and paired-pulse facilitation in area CA1. However, in contrast to our work in area CA2, PNN degradation resulted in an

attenuation of LTP in area CA1 [137]. These findings indicate that PNNs, or another chondroitinase-sensitive component of the ECM, restrict plasticity at the normally plasticity-resistant synapses in CA2 SR.

Figure 4

Figure 4: Disruption of PNNs allows for potentiation of EPSCs in CA2 neurons. ***a***, PNNs are degraded in 300-μm-thick hippocampal slices cleared with thiodiethanol after a 2 h incubation with ChABC compared with control; fluorescent labeling of PNNs with WFA (green) and CA2 neurons with the Amigo2-EGFP mouse (red). Slices shown are from animals at PN 14. ***b***, Plasticity of EPSC amplitudes is enhanced in CA2 neurons treated with the PNN-degrading enzyme ChABC, compared with untreated controls. After baseline, an LTP pairing protocol (270 pulses at 3 Hz paired with postsynaptic depolarization; at time 0), resulted in potentiation of EPSCs in CA2 neurons treated with 0.05 U/ml ChABC (mean over 22–28 min, $n = 10$), but not in untreated CA2 controls ($n = 10$). One-way ANOVA, Bonferroni's *post hoc* test for pairwise comparison, $*p < 0.05$. Indicated is the mean ± SEM. LTP induced in CA1 neurons is shown for comparison. Insets are representative traces of EPSCs from CA2 control and CA2 ChABC-treated neurons before and 20 min after the LTP pairing protocol. ***c***, ChABC treatment did not significantly alter action potential firing frequency in response to indicated current injection ($n =$ 15 per group; two-way ANOVA, $p > 0.05$). Example traces show action potential firing of control (untreated) CA2 neuron (40 pA current steps from −100 to 180 pA displayed). ***d***, ***e***, ChABC did not significantly alter excitatory current amplitude ($n = 6$ per group) or paired-pulse ratio in CA2 neurons (S1, peak of first stimulus response; S2, peak of second stimulus response; $n = 10$ ChABC-treated neurons and $n = 5$ control; two-way ANOVA, Bonferroni's *post hoc* test). ***f***, ChABC did not significantly alter AMPAR/NMDAR ratio measured at +40 mV (left) or at −70 mV ($n = 6$ ChABC-treated neurons and $n = 8$ controls; two-tailed unpaired *t* test). Measurements in ***d–f*** were made in the presence of a $GABA_A$ antagonist bicuculline; see Materials and Methods for details. Insets are representative traces of EPSCs from CA2 control holding at −70 and +40 mV.

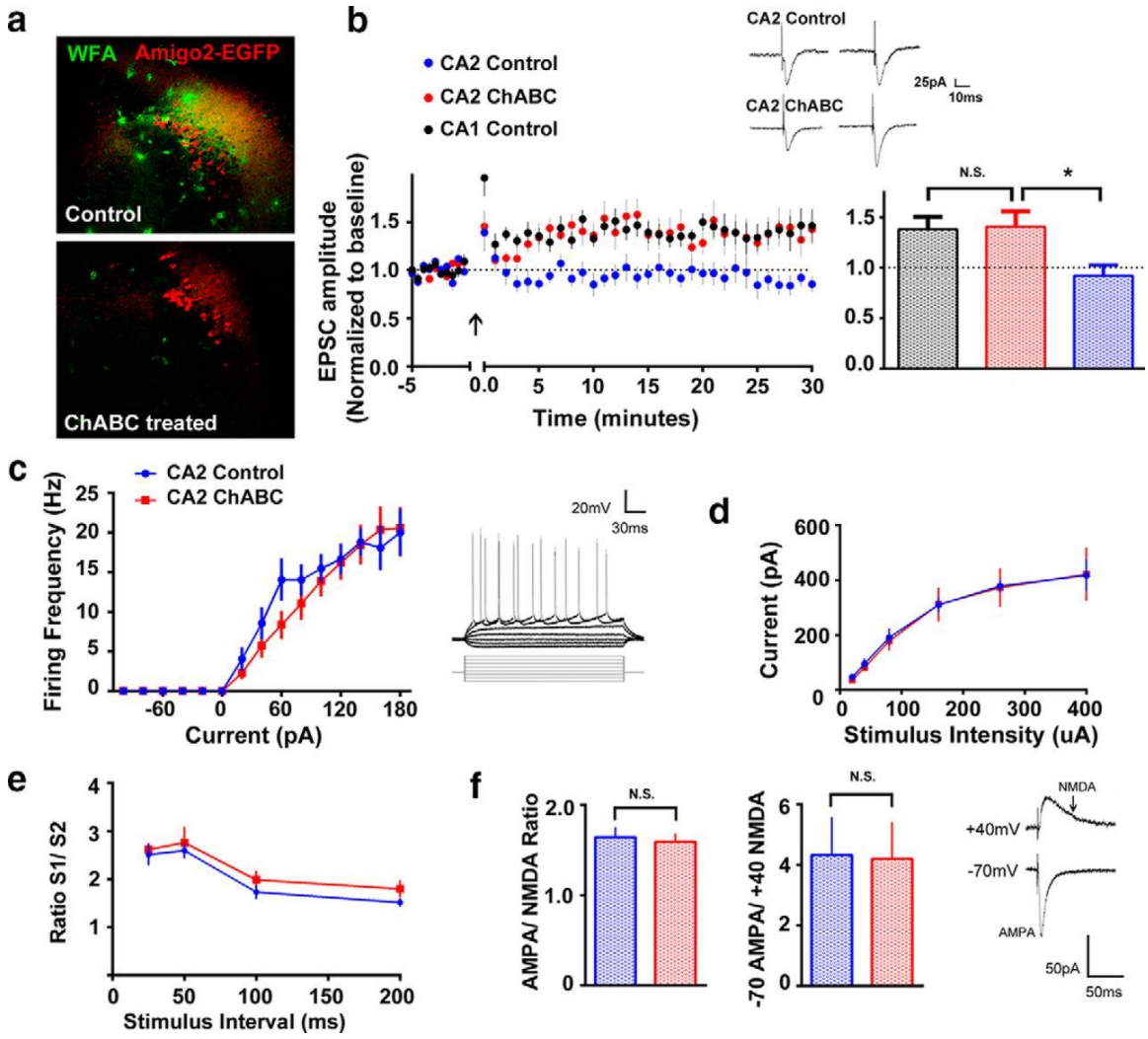
a
WFA
Amigo2-EGFP
Control
ChABC treated
b
CA2 Control
CA2 ChABC
CA1 Control
EPSC amplitude (Normalized to baseline)
Time (minutes)
CA2 Control
CA2 ChABC
25pA
10ms
N.S.
*
c
CA2 Control
CA2 ChABC
Firing Frequency (Hz)
Current (pA)
20mV
30ms
d
Current (pA)
Stimulus Intensity (uA)
e
Ratio S1/ S2
Stimulus Interval (ms)
f
AMPA/ NMDA Ratio
N.S.
-70 AMPA/ +40 NMDA
N.S.
NMDA
+40mV
-70mV
AMPA
50pA
50ms

Table 1

Intrinsic properties of CA2 pyramidal neurons in response to PNN degradation. CA2 neuron input resistance (R_i) is significantly decreased after 0.05 U/mL ChABC treatment (n=11 per group, *P<0.0043, two-tailed unpaired t-test). Significant effects were not detected in other properties, including resting membrane potential, membrane capacitance, and decay time. Indicated are the means ± SEM.

Table 1. Intrinsic properties of CA2 pyramidal neurons in response to PNN degradation.

	Intrinsic Properties			
	RMP (mV)	Cm (pF)	Ri (Mohm)	Tau (ms)
CA2 Control	-63.75 (1.048)	143.1 (9.700)	303.5 (9.989)	1.796 (0.08762)
CA2 ChABC	-66.17 (0.8298)	160.9 (7.917)	*259.0 (10.5)	1.856 (0.06349)

Table 2

Properties of action potentials in CA2 pyramidal neurons, including threshold, peak amplitude, and decay and rise times (tau), were unchanged after ChABC treatment (n = 12 per group, p > 0.05, two-tailed unpaired t test). Indicated are the means ± SEM.

Table 2: CA2 action potential firing properties in response to PNN degradation.

	Action Potential			
	Threshold (mV)	Peak Amplitude (mV)	Decay Tau (ms)	Rise Tau (ms)
CA2 Control	-47.98 (1.014)	90.48 (2.707)	22.23 (1.518)	264.3 (16.88)
CA2 ChABC	-47.87 (0.7022)	98.9 (3.9564)	20.11 (1.262)	241.0 (19.61)

Discussion

PNN degradation can re-open critical windows of plasticity in a number of brain regions, but the mechanism of plasticity suppression by PNNs is unclear [134, 170, 256]. Because PNNs are predominantly associated with inhibitory neurons in the neocortex, it has been suggested that plasticity is altered by a disruption of inhibitory transmission [67]. However, the lack of LTP in area CA2 is unlikely to be due to a disruption of inhibitory transmission, as blockade of GABAergic synaptic transmission is insufficient to restore LTP in area CA2 at excitatory synapses [196, 216] and was not required for the enabling of LTP reported here. In fact, we present evidence that PNNs play a distinct role in suppressing synaptic potentiation at a population of excitatory synapses on pyramidal neurons, perhaps in addition to any roles PNNs may have related to their expression on inhibitory interneurons. Our findings that PNN degradation enables LTP in area CA2 are in contrast with the observation that PNN degradation modestly disrupts LTP in area CA1 [137].

PNNs surrounding CA2 neurons are unlikely to be the only factor contributing to the plasticity resistance in this region. CA2 neurons express high levels of the protein regulator of G-protein signaling 14 (*RGS 14*), which has been implicated in the signaling pathway suppressing LTP in area CA2 [198]. In addition, rodent CA2 neurons have a particularly robust capacity for calcium buffering and extrusion. Raising external calcium levels to 4 mm is insufficient to induce LTP in area CA2, but the very high concentration of 10 mm allows for the induction of LTP, indicating that CA2 synapses have the cellular machinery for LTP, but that calcium is limited in the postsynaptic neurons [209]. Interestingly, both vasopressin and oxytocin, acting through AVPR1b and Oxtr receptors respectively, reinstate ability to induce calcium-dependent

LTP in CA2 [203]. Both receptors are known to be coupled to the 'Gq' type G-proteins and therefore can take part in regulating calcium levels in CA2 spines.

PNNs might act through a number of possible plasticity-limiting mechanisms; for example, they may provide a physical barrier for new synaptic contacts, restrict surface receptor mobility, or buffer ions surrounding fast-firing neurons [140, 257-260]. PNN proteoglycans are highly negatively charged and may function to buffer and restrict diffusion of cations like calcium [3]. Taken together, it might not be coincidental that cation binding to PNNs was found to be saturated at 10 mM [141], a concentration of extracellular calcium that is able to restore plasticity in CA2 neurons [209] Alternatively, PNNs may serve to stabilize the postsynaptic density and limit AMPAR insertion into the synapse [140]. PNNs have also been linked to neuroprotective functions [258, 261], and neurons in area CA2 have long been noted as being remarkably resistant to cell death from both seizure and ischemic insult [194]. The role of PNNs in neuroprotection, however, has been less well defined. Therefore, if PNNs act to limit calcium accumulation in CA2 neurons, we would predict that their disruption would lead to damage susceptibility in area CA2 similar to that in areas CA1 and CA3.

We have also identified CA2 pyramidal neurons as a novel source for a major component of PNNs in the hippocampus, suggesting that these excitatory neurons have the capacity to modulate PNN composition throughout development. We show here that PNNs in area CA2 are upregulated by early-life exposure to EE. Interestingly, other studies have reported a decrease in PNNs after exposure to enrichment in adulthood in several brain regions, suggesting that PNNs may be differentially regulated depending on the age that the animal is exposed to enrichment. For example, amblyopic rats exposed to EE in adulthood had reduced PNNs in the visual cortex[262]; likewise, adult mice exposed to enrichment had reduced PNN density around

cerebellar neurons [263]. In contrast, early postnatal enrichment was found to rescue PNN development in dark-reared animals and promote critical period maturation [254], similar to the findings in this study. Further investigation into intrinsic factors that modulate PNNs, such as direct manipulation of CA2 activity, or early-life seizure at different developmental stages should provide critical insight into how PNNs in area CA2 may be differentially regulated throughout development [242].

Considering that the development of PNNs in hippocampal area CA2 pyramidal neurons parallels the expression timeline of PNNs located in brain regions noted for their critical periods for plasticity, our data raise the intriguing possibility of an early critical period for synaptic plasticity in area CA2. Although the behavioral functions of area CA2 are only beginning to emerge, recent reports implicate area CA2 in social aggression and social recognition memory [203, 223, 224]. Developmental regulation of PNNs in area CA2 may therefore represent a therapeutic target for PNN-associated developmental disorders, such as schizophrenia and Rett syndrome [264, 265].

CHAPTER III– PERINEURONAL NETS PREMATURELY RESTRICT PLASTICITY IN HIPPOCAMPAL AREA CA2 IN A RETT SYNDROME MOUSE MODEL

Introduction

Rett syndrome is a neurodevelopmental disorder caused by a loss-of-function mutation in the gene methyl-CpG-binding protein 2 (MeCP2) [266-268]. *Mecp2* is located on the X chromosome and affects about 1 in 10,000 to 23,000 young girls worldwide [269 270]. A defining feature of Rett symptomology is the apparent normal development for the first year of life, followed by a rapid, profound regression in cognitive function. Rett children progressively lose their motor and language abilities, develop stereotypic hand movements, suffer from autonomic dysfunction, and 7 out of 10 eventually develop seizures [268, 271-275]. MeCP2 protein functions as a transcriptional activator/ repressor, regulates synaptic plasticity and can regulate gene expression post-translationally (via micro-RNAs) [276-278]. The many cellular functions of MeCP2 is correlated with its various binding partners and downstream targets [279]. MeCP2 is first expressed during embryonic development and increases in expression during postnatal development [280, 281]. Early studies of postmortem brain tissue from Rett patients reveal reduction in dendritic spine number and presynaptic markers; rodent studies reveal deficits in adult neurogenesis and synaptic plasticity [270, 282-284]. Although symptoms develop approximately one year into postnatal life, abnormalities in brain development were discovered earlier (embryonic/ early postnatal stages prior to the presentation of symptoms) [285-292]. Much effort in the field has been put towards

understanding the initiation and progression of the disease, and how a *Mecp2* mutation may disrupt critical early learning and memory function.

The specialized extracellular matrix, perineuronal nets (PNNs), are altered in several psychiatric and neurological disorders, such as Rett syndrome [265, 293 294]. PNNs are activity-dependent and first appear in the brain during postnatal development and gradually increase until they are fully expressed in adulthood [118, 295-297]. Staining for PNNs was described as being overexpressed in postmortem brain tissue of Rett individuals in motor cortices, but decreased in number in frontal and temporal cortices [265]. PNNs associated with inhibitory neurons are elevated in auditory and visual cortices in the mouse models of Rett, consistent with human Rett pathology [298, 299]. Because PNNs function to limit plasticity during critical windows of development, a recent study looked at the effect of degrading PNNs in the auditory cortex of *Mecp2*$^{-/x}$ mothers, and found improvements in maternal care (pup gathering behavior) [298]. PNNs however have yet to be described in the hippocampus of either Rett postmortem tissue or mouse models or in association with a population of excitatory pyramidal neurons.

Several transgenic knockout mouse models of Rett have been generated that mimic human Rett symptomology, exhibiting both neurological and behavioral impairments [283, 300]. The MeCP2-null mouse model has been integral in identifying various molecular mechanisms behind both structural and plasticity deficits [300, 301]. These mice exhibit decreased spine number and impairments in excitatory/ inhibitory transmission, neurogenesis, and axonal fiber disorganization [286, 302-304]. The majority of MeCP2-null studies use *Mecp2*$^{-/Y}$ males because they exhibit more severe behavioral phenotypes and pathology than females, although *Mecp2*$^{-/x}$ females eventually exhibit similar deficits [283]. *Mecp2*$^{-/Y}$ males develop severe neurological symptoms around six weeks of age and *Mecp2*$^{-/x}$ females display behavioral symptoms after

several months. The delay in developing neurological deficit in the mouse model nicely mimics the apparent normal early development that is characteristic of Rett. Overall, both human and rodent studies observe the majority of Rett pathology after infancy (>5 weeks in the rodent), however we and others describe pathology in early neonates [287, 290, 305].

Disruptions in synaptic plasticity in the mouse MeCP2-null hippocampus is a leading candidate underlying the hippocampal-dependent learning deficits in Rett syndrome. In the *Mecp2*$^{-/Y}$ hippocampus, synaptic plasticity is impaired at CA1 Schaffer collateral (SC) synapses in an age-dependent manner [286]. Electrophysiological measurements synaptic plasticity, long-term potentiation (LTP) and long-term depression (LTD), at Rett CA1 SC synapses in acute hippocampal slices reveal reduced LTP and LTD. In field recordings, basal synaptic transmission, as assessed with stimulus-response curves, is unchanged between symptomatic mice (18-22 weeks of age) and pre-symptomatic mice (3-5 weeks old); however, more recent studies find deficits in both inhibitory and excitatory transmission (more later) [286, 306, 307]. MeCP2-null mice display significant learning and memory deficits in tasks such as hippocampal-dependent spatial memory, contextual fear conditioning, and long-term social memory [300, 308, 309] [286]. Furthermore, homeostatic synaptic scaling also appears to be disrupted in the Rett hippocampus [310] [72]. Several molecular mechanisms have been proposed to explain these deficits in activity-dependent plasticity.

The plasticity impairment in Rett hippocampus has been linked altered NMDA receptor (NMDAR) subunit composition, which may underlie the profound effects on NMDAR-dependent forms of synaptic plasticity. NR2A levels were significantly decreased and NR2B levels were increased in symptomatic mice; NR1 was unaffected [286]. During development, NR2A subunit gradually replaces the NR2B subunit at the postsynaptic cell in an activity-dependent

manner and NR2A functions to drive 'mature' NMDAR currents [311-313]. Alternatively, or in addition, MeCP2 was initially thought to act as a transcriptional repressor of BDNF, a key molecule in brain development and plasticity [314, 315]. Loss of MeCP2 increased BDNF protein levels in the hippocampus (primary cultures) [314, 316]; however, others have reported a decrease of BDNF in MeCP2 mutant brain lysates [317, 318]. MeCP2 is now thought to also act as an activator of *Bdnf* transcription through binding to the promoter region of *Bdnf.* Upon neuronal depolarization, MeCP2 would be released, allowing *Bdnf* transcription and subsequent activity-dependent gene regulation [318, 319 314]. Interestingly, overexpression of BDNF rescues locomotor and electrophysiology deficits (in cortex) and extended lifespan of MeCP2-null mice [317].

Electrophysiological studies of the Rett mouse models reveal a critical role for MeCP2 in maintaining synaptic excitatory and inhibitory transmission in cortical regions [320]. Both enhanced inhibition and reduced excitation have been observed in the Rett mouse [303, 321], however the effects are complicated because the Rett mouse hippocampus also displays hyperexcitability on a global scale [306]. Neurological deficits, like seizure, were initially linked to glutamatergic activity due to neuronal hyperexcitability [322]. More recent work, however, has focused on the role of MeCP2 exclusively in inhibitory neurons [323, 324]. Targeted expression of MeCP2 in only excitatory neurons of a MeCP2-null mouse was unable to rescue most Rett phenotypes [325]. However, a conditional deletion of MeCP2 in GABAergic inhibitory neurons was sufficient to recapitulate most Rett phenotypes [302] and even abolish critical plasticity [326]. Overall, the variability in cell-type specific deficits associated with the loss MeCP2 suggests that MeCP2 is likely acting cell-autonomously in response to activity.

Although morphological defects have been described in the human Rett hippocampus, PNN pathology in human or rodent hippocampus has yet to be studied. In Rett postmortem

tissue, hippocampal CA3/4 pyramidal cells neurons appeared hypochromic (described as cellular degradation/ 'ghost cells') while CA1 cells appeared normal [327]. In rodent *Mecp2*$^{-/Y}$ CA2, neurons are reported to be smaller than those in wildtype mice [305, 317, 328], although this decrease in size was certainly not limited to neurons in CA2. In this study, I aimed to determine whether PNNs associated with a population of excitatory neurons in area CA2 were altered or disrupted in a mouse model of Rett. I then investigated whether *Mecp2* deletion resulted in any functional consequences in CA2, particularly regarding synaptic plasticity. CA2 SC synapses are normally resistant to the induction of long-term potentiation (LTP) and as outlined in a previous chapter, I identified PNNs as a negative regulator of LTP in acute hippocampal slices of P14-18 day old mice. Here I describe experiments showing that PNNs develop prematurely in area CA2 of *Mecp2*$^{-/Y}$ and in a conditional knockout of *Mecp2*. Furthermore, I found that the plasticity at CA2 SC synapses prior to the development of PNNs is prematurely restricted at P8-11 in CA2 of a MeCP2-null mouse. I also found that normal plasticity in immature CA2 can be rescued by degrading PNNs *in vitro* at P8-11. The results of these studies support the hypothesis that MeCP2 can regulate PNNs cell-autonomously in CA2 neurons, and that the premature development of PNNs in Rett CA2 results in an early closure of a plasticity 'critical period' there. The results of these studies are suggestive of a novel critical window of plasticity in CA2 that is altered in Rett syndrome.

Materials and Methods

Animals in all experiments were housed under a 12:12 light/dark cycle with access to food and water *ad libitum*. All procedures were approved by National Institute of Environmental Health Sciences Animal Care and Use Committee and were in accordance with the National Institutes of Health guidelines for care and use of animals.

Rett Syndrome mouse model:

Mice used in this study were hemizygous MeCP2-deficient males (*Mecp2*$^{-/Y}$; B6.129P2(C) -Mecp2$^{tm1.1Bird}$, The Jackson Laboratory, stock # 003890, donated by Adrian Bird, University of Edinburgh [300]). *Mecp2*$^{-/Y}$ mutant males exhibit severe Rett-like characteristic at 3-8 weeks of age, whereas heterozygous females exhibit symptoms much later around 6 months of age. This mouse line is maintained by breeding heterozygous *Mecp2*$^{-/x}$ females with C57BL/6 males. No special breeding conditions were used.

Conditional deletion of MeCP2:

For deletion of Mecp2 in CA2 pyramidal neurons, we used commercially available mice with an X-linked mutation, *loxP* sites flanking exons 3-4 of the *Mecp2* gene (floxed-MeCP2; *Mecp2*^{flox} ; B6.129P2(C) -Mecp2$^{tm1.1Bird}$/J , The Jackson Laboratory, stock # 006847, donated by Adrian Bird, University of Edinburgh [300])

This mouse line was maintained by breeding heterozygous *Mecp2*$^{flox/x}$ with C57BL/6 males; the hemizygous males *Mecp2*$^{flox/y}$ are infertile. To delete MeCP2 in CA2 neurons, we crossed heterozygous floxed-MeCP2 females with *Amigo2-Cre*$^{+}$ males. MeCP2 is excised upon the recombination of the *loxP* sites in neurons expressing Cre recombinase.

CA2 Cre-expressing line:

The *Amigo2-Cre* mouse line was generated in house at the NIEHS, see Supplemental Methods Fig. S13-17 for genetic and histology details [230]. The *Amigo2* gene (adhesion molecule

with Ig like domain 2) is expressed in CA2/3a, the fasciola cinereum, the cerebellum, the accessory olfactory bulb, and the premammillary nucleus (*in situ* hybridization data, Allen Brain Atlas, Seattle, WA; [252] To gain selective genetic access to molecularly-defined CA2, we used an *Amigo2-Cre* line that expresses Cre recombinase predominantly in CA2 neurons in adult mice. This mouse was generated from a bacterial artificial chromosome (BAC) transgene (Rp23-288P18); as in *Tg(Amigo2-EGP)LW244Gsat*2 (GENSAT[2]) [329]. Amigo2-cre mice were maintained as hemizygous by breeding *Amigo2-Cre+* mice with C57BL/6 mice. Only Cre^{+} males were used in this study and brains harvested >3 weeks old.

Immunohistochemistry:

Mice were deeply anesthetized with Fatal-Plus and perfused with cold phosphate-buffered saline (PBS), followed by 4% paraformaldehyde in PBS (pH 7.4). Brains were removed and post-fixed overnight at 4°C and submerged in 30% sucrose. Forty μm-thick sections were cut on a sliding microtome, blocked in 5% normal goat serum and incubated in biotin-conjugated WFA lectin (1:1000, Sigma Aldrich L1516), or rabbit anti-MeCP2 (07-013, Millipore, 1:500), or mouse anti-STEP (Cell Signaling, 4817, 1:500), or mouse anti-regulator of G-protein signaling 14 (UC Davis/NIH NeuroMab Facility, AB_10698026, 1:1,000), or rabbit anti-PCP4 (SCBT, sc-74186, 1:500 overnight at 4^{0} C. Sections were washed 3 times in PBS and incubated in secondary antibody at 1:500 for 40 minutes at room temperature: streptavidin Alexa-568, or goat anti-rabbit H+L A568, or goat anti-mouse Alexa-568 (Invitrogen). Sections were mounted with Vectashield anti-fade mounting medium with DAPI (Vector laboratories). Images were acquired on a Zeiss laser scanning confocal (LSM510 NLO) or a Zeiss light microscope using controlled camera settings.

[2] The Gene Expression Nervous System Atlas (GENSAT) Project, NINDS Contracts N01NS02331 & HHSN271200723701C to The Rockefeller University (New York, NY).

Electrophysiology

Mice (Charles River Laboratories, Raleigh, NC) were deeply anesthetized with Fatal-Plus, decapitated, and their brains removed and submerged into oxygenated ice-cold sucrose-substituted artificial cerebrospinal fluid (ACSF) of pH 7.4 (in mM): 240 sucrose, 2.0 KCl, 1 $MgCl_2$, 2 $MgSO_4$, 1 $CaCl_2$, 1.25 NaH_2PO_4, 26 $NaHCO_3$ and 10 glucose. Brain slices were cut coronally at 300 μm using a vibrating microtome (Leica VT 1000S) and allowed to recover at room temperature in a submersion holding chamber with artificial cerebral spinal fluid (ACSF) (in mM): 124 NaCl, 2.5 KCl, 2 $MgCl_2$, 2 $CaCl_2$, 1.25 NaH_2PO_4, 26 $NaHCO_3$, and 17 D-glucose bubbled with 95% O_2 with 5% CO_2.

Whole-cell recordings were made from pyramidal neurons in area CA2, which were identified visually using differential interference contrast (DIC) optics (CA2 neurons were verified in earlier, separate experiments using a CA2-specific fluorescent reporter mouse line, see methods [295]). Glass borosilicate pipettes were filled with a potassium gluconate internal solution (in mM) 120 K-gluconate, 10 KCl, 3 $MgCl_2$, 0.5 EGTA, 40 HEPES, 2 Na_2-ATP, 0.3 Na-GTP, pH 7.2), with a tip resistance between 3-4.5 MOhms. Data were collected using Clampex 10.4 and analyzed using Clampfit software (Axon Instruments). Series and input resistances were monitored by measuring the response to a 10mV step at each sweep and cells were included for analysis if <30% change in series and input resistance. Recordings were not compensated for series resistance.

To assess excitatory transmission in P14-18 slices, whole-cell recordings were performed in voltage-clamp mode, and postsynaptic currents (PSCs) were evoked with a bipolar stimulating electrode placed in the stratum radiatum. Excitatory PSCs (EPSCs) were isolated using the $GABA_A$ receptor antagonist bicuculline in the bath solution. Paired-pulse facilitation (PPF) was

assessed under similar conditions. Inhibitory transmission was not blocked in P8-11 slices because pilot experiments with bicuculline in the bath solution resulted in epileptic activity during recordings (data not shown). To determine action potential threshold, whole-cell recordings were performed in current-clamp mode. Current pulses of 180 ms in 0.2 nA steps were delivered and the membrane potential at which the cells first fired action potentials was measured. For long-term potentiation (LTP) experiments, baseline EPSCs were collected every 15 seconds for at least 5 minutes after which a pairing protocol was used, consisting of 1.5 minutes of 3 Hz presynaptic stimulation (270 pulses) paired with postsynaptic depolarization to 0 mV in voltage-clamp mode [330, 331]. Data were averaged and normalized to baseline.

Immunoblotting:

Neurons in single hippocampal hemispheres were lysed with RIPA buffer (Thermo) with Halt™ protease/phosphatase inhibitor cocktail (Thermo). Lysate was briefly sonicated and incubated on ice for 30 minutes while rocking. The lysate was centrifuged and resolved by gel electrophoresis and transferred to a nitrocellulose membrane using the iBlot gel transfer apparatus (Invitrogen). Immunoblots were incubated with primary antibody overnight, washed 3X in PBS with 0.01% Tween for five minutes each and incubated in secondary for two hours. They were again washed 3X in PBS with 0.01% Tween for five minutes each. Blots were visualized with an Odyssey infrared scanner (Li-COR Biosciences) after immunolabeling primary antibodies with infrared fluorophore–tagged secondary antibody (LiCor). Images were analyzed using the ImageJ; the mean gray value of the band of interest was measured and background was subtracted (defined as a region in close proximity to the band of interest).

Equal amounts of protein (25 ug) from each sample were loaded on 4-12% bis-tris NuPage gels (Invitrogen) and transferred to nitrocellulose membranes. The following antibodies

were used: rabbit antibody to NR2A (04-901, Millipore, 1:4000), rabbit antibody to glutamate receptor 1 protein (GluR1) (ab1504, Millipore, 1:1000), rabbit antibody to MMP-9 (PA5-13199, Invitrogen, 1:1000), rabbit antibody to meCP2 (07-013, Millipore, 1:500), mouse antibody to β-actin (MA5-15739, Invitrogen, 1:10,000), donkey secondary antibody to rabbit IgG IRDye680RD® (925-68073, LiCor, 1:500), and goat secondary antibody to mouse IgG (H+L) IRDye800CW® (924-32210, LiCor).

Results

LTP is expressed at CA2 SR synapses at P8-11

Excitatory synapses in CA2 stratum radiatum (SR) of P14-18 acute hippocampal slices normally fail to express typical LTP, but PNN degradation *in vitro* enables LTP [295]. Whether LTP can be induced at CA2 SR synapses at an age prior to PNN development (<P14) has yet to be tested. First, I characterized the expression of several putative negative regulators of plasticity in CA2 at P10 compared to P60. I found RGS14, which had been shown to inhibit LTP in CA2, was minimally detected at P10 and strongly expressed at P60, consistent with a previous study [198]. Similarly, STEP, WFA and PCP4 were either not detected (WFA) or minimally detectable at P10 (Fig. 3.1a), and highly expressed at P60. Next, I tested whether LTP could be induced at CA2 SR synapses at an age when PNNs as assessed with WFA staining, and these other proteins are not yet detectable (P8-11) compared to P14-18 when PNNs have begun to develop (Fig. 3.1b). Stimulating CA2 SR synapses with an LTP pairing protocol (3 Hz stimulation while depolarizing the cell to 0 mV) was sufficient to induce LTP at P8-11 CA2 SR synapses (143 ± 0.2% baseline, *P=0.0011, two-tailed unpaired t-test at 25-30 min. Fig. 3.1c*).*

Intrinsic properties did not change in a way that could explain LTP in at P8-11 (Table 3.1, unpaired t-test, P>0.05). I found no significant differences in paired-pulse facilitation (Fig. 3.1d), but did observe higher basal excitatory transmission at P8-11 compared to P14-18 CA2 neurons (**P= 0.0011 at the highest current stimulation intensity, 320 uA, two-way ANOVA, Bonferroni *post-hoc* test, Fig. 3.2d). Because inhibitory transmission was not blocked during P8-11 recordings, I repeated EPSC stimulus-response and PPF experiments without inhibitory blockers and replicated results in Fig. 3.2d (data not shown). The action potential firing frequency of CA2 neurons was also higher at P14-18 compared to P8-11 (**P= 0.0036 at 180 pA of injected current, Bonferroni *post hoc* test for pairwise comparison, two-way ANOVA, Fig. 3.1d). Developmental changes in CA2 action potential firing frequency at P8-11 does not explain the LTP in CA2. The enhanced excitatory transmission (stimulus-response curve) at high intensity stimuli at P8-11 CA2 SR synapses compared to P14-18 is similarly unlikely to a factor because the LTP experiments were typically performed using stimulation intensities between 15-30 μA.

PNNs are increased in CA2 of a mouse model of Rett Syndrome

Previous work has shown that PNNs, presumably around PV neurons, are higher in brain tissue from both individuals with Rett Syndrome and *Mecp2*$^{-/Y}$ mice [265]. To determine whether PNN maturation is also altered in hippocampal area CA2 in postnatal development, I quantified PNNs at P14, 21 and 45 in a *Mecp2*$^{-/Y}$ mice. I found that staining for the PNN marker, WFA, is increased in P14, 21 and 45 in CA2 stratum pyramidale (SP) of *Mecp2*$^{-/Y}$ compared to wildtype littermates (Fig. 3.2a), Bonferroni *post hoc* test for pairwise comparison, two-way ANOVA, **P< 0.005, ***P<0.0001. WFA staining was however unchanged around PNN+ inhibitory neurons in area CA1 and in overlying somatosensory cortex, P > 0.05 (Fig. 3.2a). This finding in

somatosensory cortex was in contrast to the results reported in another study looking at PNNs in somatosensory cortex in a MeCP2-null mice, which showed PNN staining to be increased [284]. We also investigated whether another CA2 plasticity inhibitor may be increased in the MeCP2-null mouse, RGS14. Staining for RGS14 protein was unchanged in CA2 SP at P14, 21, and P45 of the MeCP2-null males compared to wildtype littermates, $P > 0.05$ (Fig. 3.2b). I next sought to determine whether this premature overexpression of PNNs in CA2 prematurely inhibits synaptic plasticity.

PNNs in CA2 are increased in a targeted deletion of MeCP2 in CA2

Lastly, I sought to determine whether the increase in PNNs in CA2 of Rett is cell-autonomous to pyramidal neurons, or is dependent on a global loss of MeCP2 in the hippocampus, perhaps by way of glial cells or inhibitory network properties [302, 325].To test this, we ablated MeCP2 from CA2 neurons and quantified PNN expression levels in the hippocampus. We used a mouse strain expressing Cre recombinase (Cre) in CA2/3 neurons, *Amigo2-Cre*$^{+}$, to gain selective genetic access to molecularly-defined CA2 pyramidal cells. To conditionally delete MeCP2 from CA2 neurons, we crossed *Amigo2-Cre*$^{+}$ mice with a Cre-dependent MeCP2 mouse line, floxed-MeCP2 (*Mecp2*$^{flox/x}$) (Fig. 3.3a). The loss of MeCP2 protein was observed in all CA2 pyramidal neurons and sparsely in CA3 pyramidal neurons and dentate gyrus (DG). No apparent loss of MeCP2 protein was observed in extra-hippocampal brain structures, however it is likely that regions where *Amigo2* is expressed were also affected (eg. Cerebellum; [252]. MeCP2 protein was not altered in *Amigo2-Cre*$^{-}$; floxed-MeCP2 animals compared to C57BL/6 (data not shown). Staining for PNNs revealed a greater staining intensity of WFA in CA2 SP compared to three different controls: Cre^{+} WT, Cre-Floxed, Cre^{+} WT (***$P = 0.0001$, one-way ANOVA, Tukey for *post-hoc* test, Fig. 3.3b), replicating the findings in the

global *Mecp2*$^{-/Y}$ mouse (Fig. 3.2a). We also found that PNNs were not different around PNN+ neurons in CA1 or overlying somatosensory cortex (Fig. 3.3b). These data support the idea that MeCP2 is likely acting cell-autonomously in pyramidal neurons to upregulate PNNs in CA2.

LTP is prematurely restricted at CA2 SR synapses in a mouse model of Rett and degradation of PNNs restores plasticity

Because we found that LTP is expressed at CA2 SR synapses at P8-11 before PNNs are detectable, we next asked whether the higher expression of PNNs in Rett CA2 may disrupt the potentiation we can induce at early postnatal ages. We quantified WFA staining intensity in CA2 at P11 in MeCP2-null males compared to age-matched wildtype littermates. WFA staining was indeed was higher in CA2 at P11 in the MeCP2-null compared with WT littermates at that age (**P=0.0043, two-tailed, unpaired t-test, Fig. 3.4a). Note: to capture optimal images of WFA fluorescence at P11, I had increased the camera exposure settings (relative to settings for P14-45 images in Fig. 3.1a). Next, I tested whether LTP could be induced at CA2 SR synapses in P8-11 MeCP2-null males like in wildtype animals. Consistent with the idea that premature PNN development interferes with LTP, I found that LTP is indeed prematurely restricted at P8-11 CA2 SR synapses in *Mecp2*$^{-/Y}$ compared to wildtype littermates (111 ± 0.1% baseline at 20 minutes versus 1670.1% ± 0.3% baseline in wildtype baseline at 20 minutes), **P= 0.005, two-tailed unpaired t-test, Fig. 3.4*b*. Intrinsic properties did not differ in a way that could explain the premature restriction of plasticity in CA2 (Table 3.1, P>0.05, unpaired t-test). I also found no significant differences in action potential firing frequency or paired-pulse facilitation at P8-11 between *Mecp2*$^{-/Y}$ and wildtype littermates (p>0.05, two-way ANOVA, Fig. 3.4c). Basal excitatory transmission, as assessed with a stimulus-response curve, was however smaller at P8-11 CA2 synapses of Mecp2$^{-/Y}$ compared to wildtype littermates (*P= 0.014 at 320pA current

stimulation, two-way ANOVA, Bonferroni post-hoc test, Fig. 3.4c). This may provide a possible explanation for the premature loss of LTP at P8-11 CA2 Rett synapses if synapses were 'maximally potentiated' prior to slice preparation, as proposed by Pozzo-Miller and colleagues [332]. To determine whether it is indeed the aberrant PNNs that are functioning to prematurely restrict LTP in Rett CA2, I degraded PNNs in an acute hippocampal slice with the exogenous enzyme chondroitinase (ChABC). I found that degradation of PNNs with ChABC apparently restored the ability to induce LTP at CA2 SR synapses of P8-11 MeCP2-null males to the level of wildtype littermates (178 ± 0.4% baseline versus 1.11 ± 0.4% baseline of WT 20 minutes, *P= 0.038, two-tailed unpaired t-test, Fig. 3.4*d).*

Global loss of MeCP2 alters plasticity-regulating molecules in the hippocampus

I next explored a few other possible mechanisms that may explain PNN upregulation and disrupted plasticity in the Rett syndrome mouse model. One endogenous ECM-degrading enzyme, MMP-9, was worth investigating as it has been shown to regulate structural and functional plasticity in the visual cortex and postnatal reduction of MMP-9 levels promotes PNN formation [160, 166, 333-335]. Immunoblot analyses of MMP-9 protein levels in the adult hippocampus revealed a significant decrease in MMP-9 in MeCP2-null males compared to wildtype littermates (*P=0.034, one-tailed, unpaired, t-test, Fig. 3.5b). Note that we confirmed a complete loss of MeCP2 protein in *Mecp2*$^{-/Y}$ hippocampal lysate (Fig. 3.5a). Furthermore, glutamatergic receptor subunits GluR-1 (AMPAR) and NR2a (NMDAR) have been implicated as a mechanism for disrupted plasticity in CA1 hippocampal neurons of the MeCP2-null mouse [286]. Consistent with previous reports, we show that NR2a protein is decreased in the *Mecp2*$^{-/Y}$ males compared to wildtype littermates (Fig. 3.4c) and GluR-1 is unchanged (Fig. 3.5d). The critical next experiments, though, will be to measure these plasticity-associated molecules (and the CA2

plasticity-restricting molecules) in the hippocampus of pre-symptomatic P8-11 *Mecp2*$^{-/Y}$ mouse. These future experiments will provide valuable insight into the mechanisms underlying premature closure of what seems is a critical period for plasticity in CA2.

Figure 5- Fig. 3.1

Figure 3.1: LTP is expressed at CA2 SR synapses at P8-11

a) CA2 markers RGS14, STEP, PCP4, WFA at P10 and P60 in the hippocampus. At P10, WFA staining in CA2 is the weakest relative to staining of RGS14, STEP and PCP4, which area also show weak staining. At the adult age of P60, staining for all four protein markers are strongly expressed in CA2. b) WFA staining at P11 and P14 in the hippocampus; the age of acute slices used in electrophsyiology recorings in c). Staining for WFA immunofluorescence is detectable and morphologically mature in area CA2 at P14 but not at P11 (left). Image of a 300-µm hippocampal slice where a CA2 neuron is patched with a glass recording electrode and a stimulating electrode is placed in CA SR. c) LTP is expressed at CA2 SR synapses in early postnatal development in a hippocampal slice, before PNNs are detectable in CA2. Plasticity of excitatory postsynaptic current (EPSC) amplitudes is present in CA2 neurons at PN 8-11, but disappears by the second postnatal week. After baseline, an LTP pairing protocol (270 pulses at 3 Hz paired with postysnpatic depolarization; at time 0), resulted in potentiation of EPSCs in P8-11 CA2 neurons. Right: mean over 22-28 minutes of recovery, *P=0.0011, two-tailed unpaired t-test (n=8 and 9 for P14-18 and P9-11 respectively). Arrow indicates induction of the LTP pairing protocol. Indicated is the mean +/- SEM, normalized to baseline. d) Excitatory postsynaptic currents in response to indicated current stimulation is increased at P11 CA2 synapses compared to P14, **P= 0.0011 at 320pA current stimulation, two-way ANOVA, Bonferroni *post-hoc* test (n=9 and 8, P8-11 and P14-18, respectively). Paired-pulse ratio at CA2 synapses is unchanged (S1= peak of first stimulus response, S2= peak of second stimulus response). Action potential firing frequency of P11 CA2 neurons is increased compared to P14, **P= 0.0036 at 180pA of injected current, two-way ANOVA (n= 13 and 20, P8-11 and P14-18), respectively

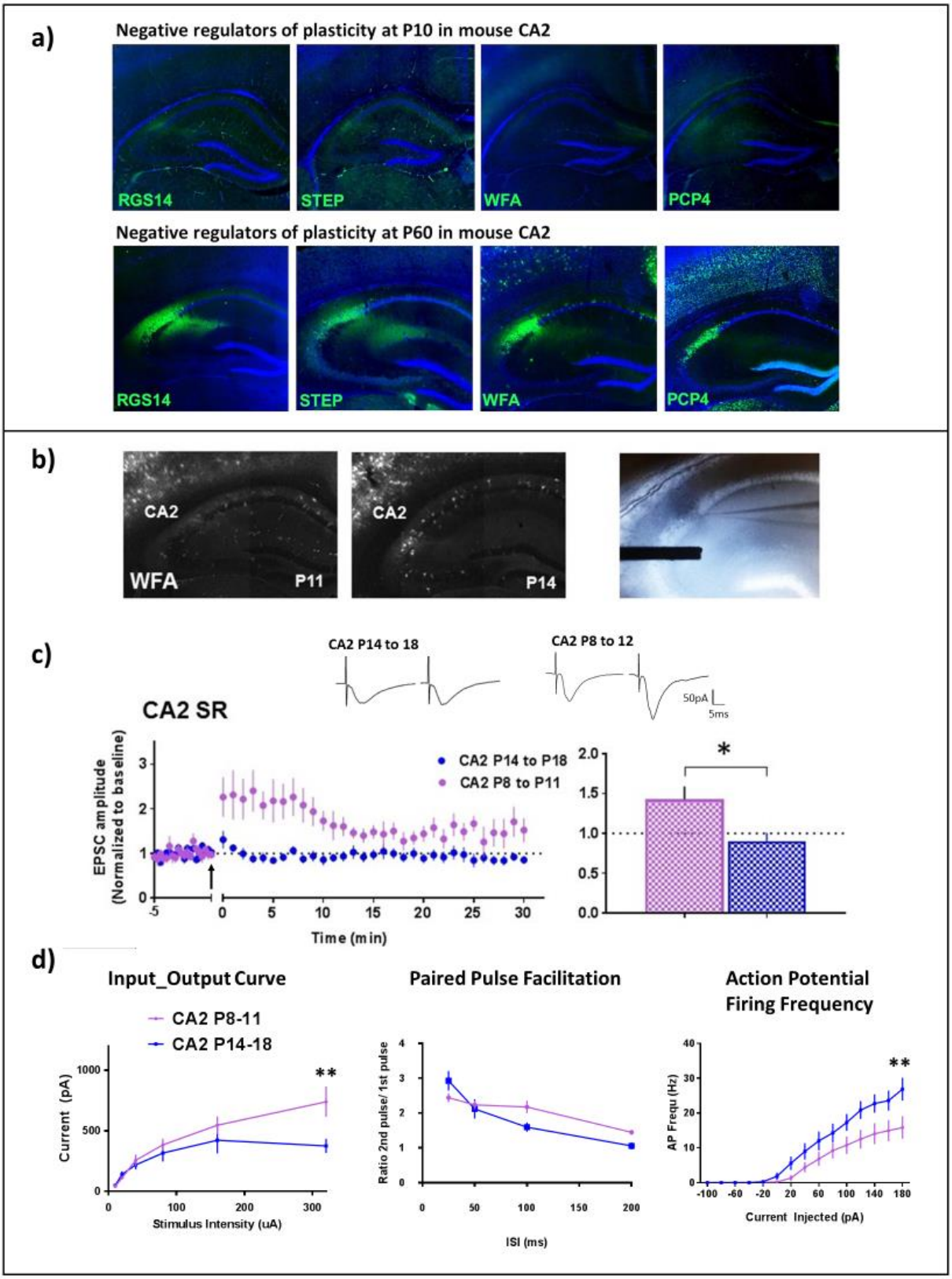
a)
Negative regulators of plasticity at P10 in mouse CA2
RGS14
STEP
WFA
PCP4
Negative regulators of plasticity at P60 in mouse CA2
RGS14
STEP
WFA
PCP4
b)
CA2
WFA
P11
CA2
P14
c)
CA2 P14 to 18
CA2 P8 to 12
50pA
5ms
CA2 SR
EPSC amplitude (Normalized to baseline)
CA2 P14 to P18
CA2 P8 to P11
Time (min)
*
d)
Input_Output Curve
CA2 P8-11
CA2 P14-18
Current (pA)
Stimulus Intensity (uA)
**
Paired Pulse Facilitation
Ratio 2nd pulse/ 1st pulse
ISI (ms)
Action Potential Firing Frequency
AP Frequ (Hz)
Current Injected (pA)
**

Figure 6- 3.2

Figure 3.2: PNNs are increased in CA2 of a mouse model of Rett Syndrome during postnatal development

a) Staining for PNN marker WFA (green) is increased in CA2 of *Mecp2*$^{-/Y}$ males compared to wildtype littermates. Top) Normalized WFA fluorescence intensity was signficatly greater in CA2 SP of *Mecp2*$^{-/Y}$ males (N=4, 4, 5 for ages P14, 21, 45 respectivietly), compared to wildtype littermates (N=4, 3, 5 for ages P14, 21, 45 respectivietly), Bonferroni *post hoc* test for pairwise comparison after two-way ANOVA, **P< 0.005, ***P<0.001. A two-way ANOVA for the two conditions at different ages indicated significant main effects of age $F(2,19)=194.8$, condition $F(1,19)=110.5$, and interaction $F(2,19)=4.913$.) WFA surrounding PNN+ inhibitory neurons in CA1 was unchanged in *Mecp2*$^{-/Y}$ males compared to wildtype littermates, (P>0.05). WFA staining in overlying somatosensory cortex was unchanged in *Mecp2*$^{-/Y}$ males compared to wildtype littermates, (P>0.05). Indicated is the mean ± SEM. b) RGS14 staining in CA2 is unchanged in MeCP2 compared to wildtype littermates. Normalized RGS14 fluorescence intensity was not significantly different in CA2 SP at any age (Bonferroni *post hoc* test for pairwise comparison after two-way ANOVA, P> 0.05. Indicated is the mean ± SEM.

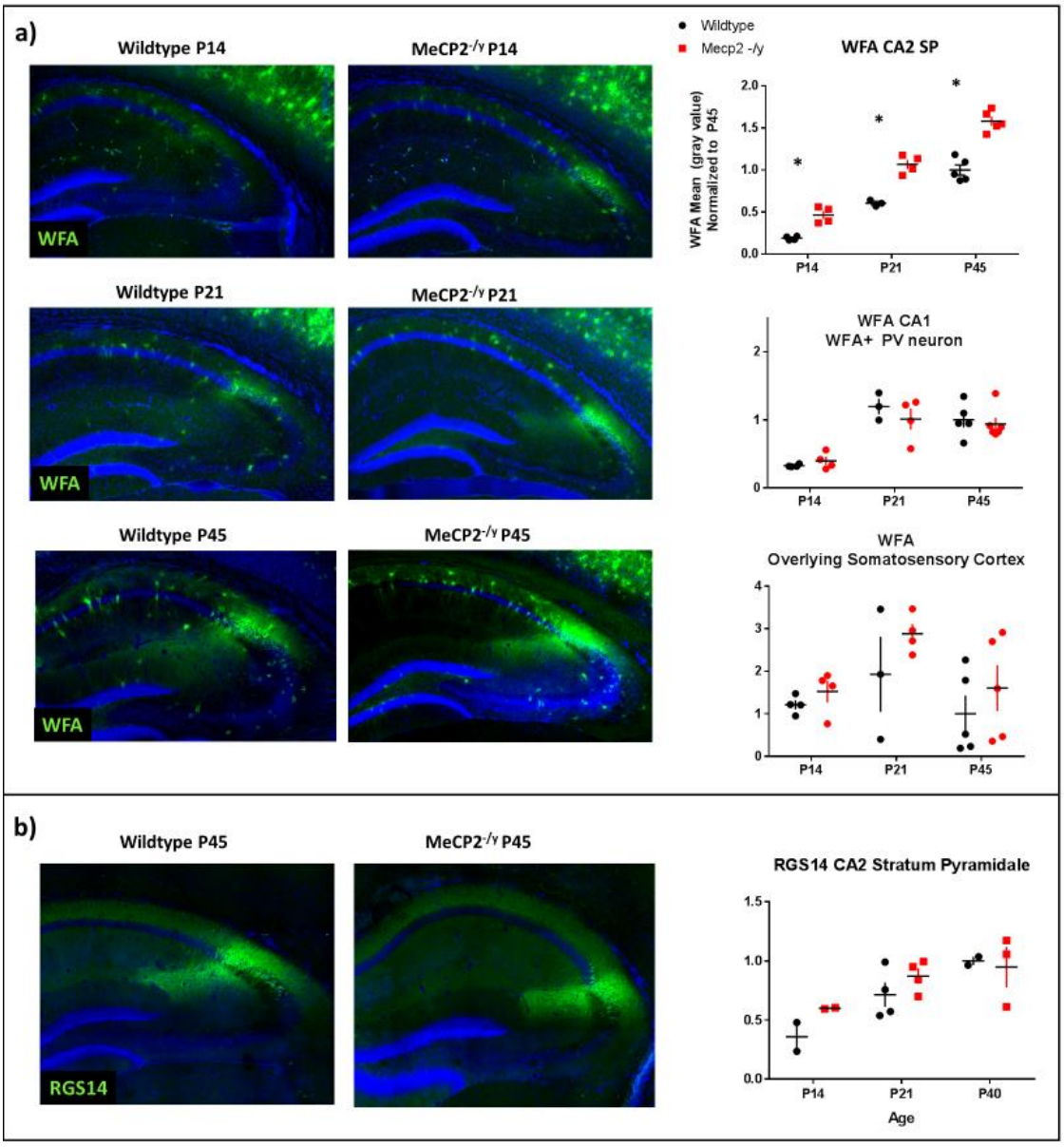
a)
Wildtype P14
MeCP2-/y P14
WFA
Wildtype P21
MeCP2-/y P21
WFA
Wildtype P45
MeCP2-/y P45
WFA
Wildtype
Mecp2 -/y
WFA CA2 SP
WFA Mean (gray value) Normalized to P45
P14
P21
P45
WFA CA1
WFA+ PV neuron
WFA
Overlying Somatosensory Cortex
b)
Wildtype P45
MeCP2-/y P45
RGS14
RGS14 CA2 Stratum Pyramidale
P14
P21
P40
Age

Figure 7- 3.3

Figure 3.3: PNNs in CA2, not in CA1 or overlying cortex, are increased in a targeted deletion of MeCP2 in CA2.

a) To conditionally delete MeCP2 from CA2 neurons, we crossed *Amigo2-Cre*$^{+}$ mice with a Cre-dependent MeCP2 mouse line, floxed-MeCP2 (*Mecp2*$^{flox/x}$). Staining for the MeCP2 protein (red) is absent from the CA2 SP and attenuated in CA3 and DG of the *Amigo2-Cre*$^{+}$; floxed-MeCP2 mouse. The PNN marker WFA appears increased in area CA2 in the *Amigo2-Cre*$^{+}$; floxed-MeCP2 mouse compared to control (*Amigo2-Cre*$^{-}$; *Mecp2*$^{flox/Y}$). b) Quantification of WFA fluoresence in CA2 SP, PNN+ neurons in CA1, and overlying somatosensory cortex of *Amigo2-Cre*$^{+}$; floxed-MeCP2 mouse compared to controls, Cre- wildtype, Cre+ wildtype, *Amigo2-Cre*$^{-}$; floxed-MeCP2. WFA fluorescence intensity is significantly increased in the *Amigo2-Cre*$^{+}$; floxed-MeCP2 mouse in CA2 SP compared to controls, ***P = 0.0001, one-way ANOVA, Tukey for *post-hoc* test, (N= 3 per group). All other regions were not significant, Tukey *post-hoc* test.

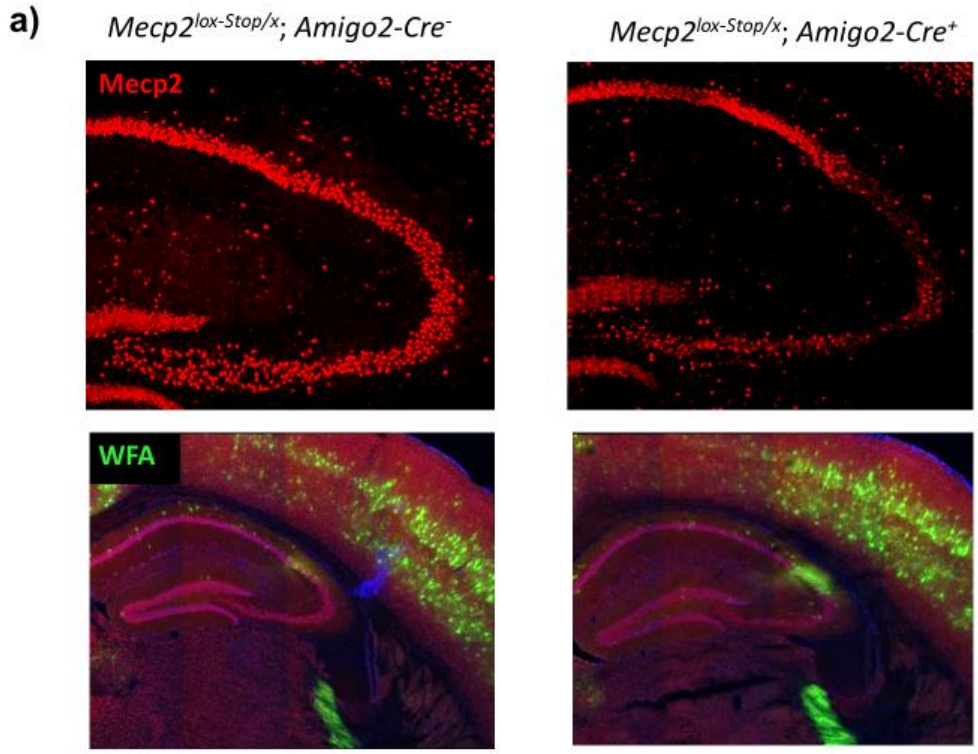
a)
Mecp2lox-Stop/x; Amigo2-Cre-
Mecp2lox-Stop/x; Amigo2-Cre+
Mecp2
WFA

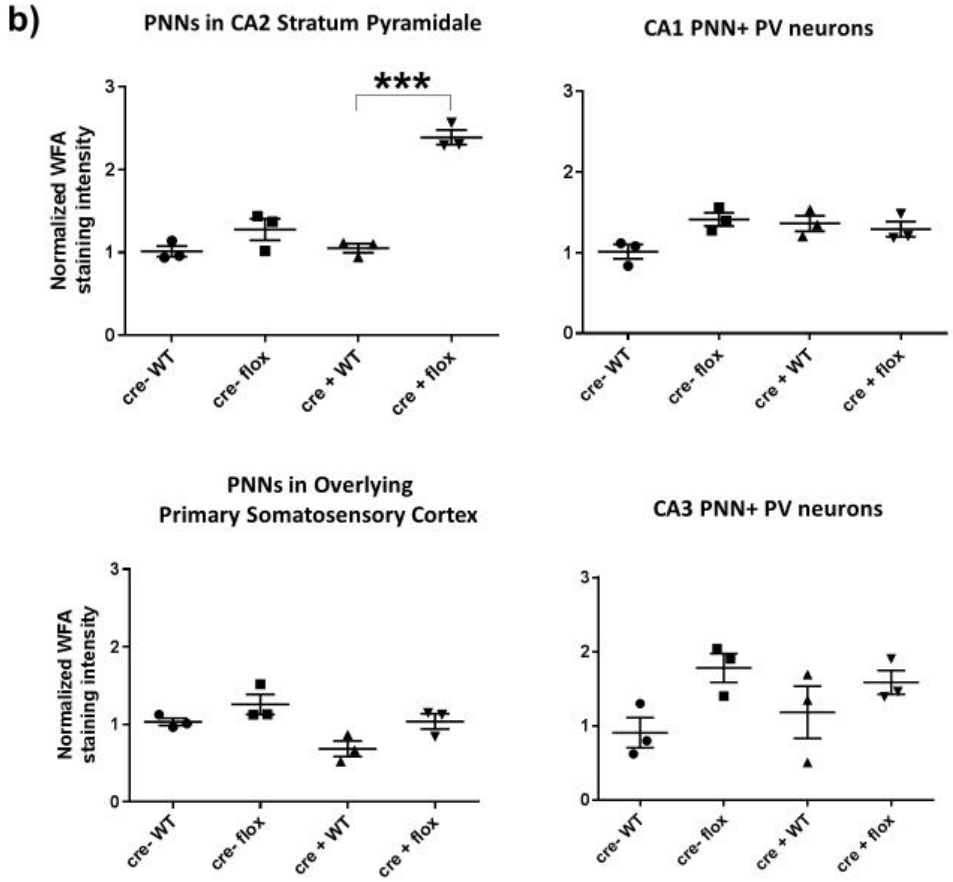
b)
PNNs in CA2 Stratum Pyramidale
***
Normalized WFA staining intensity
cre- WT
cre- flox
cre + WT
cre + flox
CA1 PNN+ PV neurons
PNNs in Overlying Primary Somatosensory Cortex
CA3 PNN+ PV neurons

Figure 8- 3.4

Figure 3.4: Plasticity of excitatory postsynaptic current (EPSC) amplitudes is prematurely restricted at P8-11 CA2 SR synapses of *Mecp2*$^{-/Y}$ neurons and restored upon PNN degradation. a) Staining for WFA is detecable and increased in area CA2 of *Mecp2*$^{-/Y}$ at P11 compared to wildtype littermate, **P=0.0043, two-tailed, unpaired t-test, (N= 6 and 4, wildtype littermate and *Mecp2*$^{-/Y}$ respectively). Note that fluorescent intensity was amplified by camera expsoure settings for quantification purposes. b) LTP is restricted at CA2 SR synpases in P8-11 *Mecp2*$^{-/Y}$ (red) in acute hippocampal slices compared to wildtype littermates (gray). Right: mean at 20 minutes of recovery, **P= 0.005, two-tailed unpaired t-test, (n= 14 and 16, wildtype littermate and *Mecp2*$^{-/Y}$ respectively). Arrow indicates induction of the LTP pairing protocol. Indicated is the mean +/- SEM, normalized to baseline. c) Excitatory postsynaptic currents in response to indicated current stimulation is decreased at P8-11 *Mecp2*$^{-/Y}$ CA2 synapses compared to wildtype littermate, two-way ANOVA, Bonferroni *post-hoc* test, *P= 0.014 at 320pA current stimulation (n= 9 and 6, wildtype littermate and *Mecp2*$^{-/Y}$, respectively). Paired-pulse ratio at CA2 synapses and action potential firing frequency is unchanged, p>0.05. d) Degradation of PNNs after a 2-hour ChABC treatment restores EPSC potentiation in P8-11 CA2 *MeCP2*$^{-/Y}$ neurons (pink) compared to controls of the same age (red). Right: mean at 20 minutes of recovery, *P= 0.038, two-tailed unpaired t-test (n= 16 and 11, *Mecp2*$^{-/Y}$ and +ChABC *Mecp2*$^{-/Y}$). Arrow indicates induction of the LTP pairing protocol. Indicated is the mean +/- SEM, normalized to baseline.

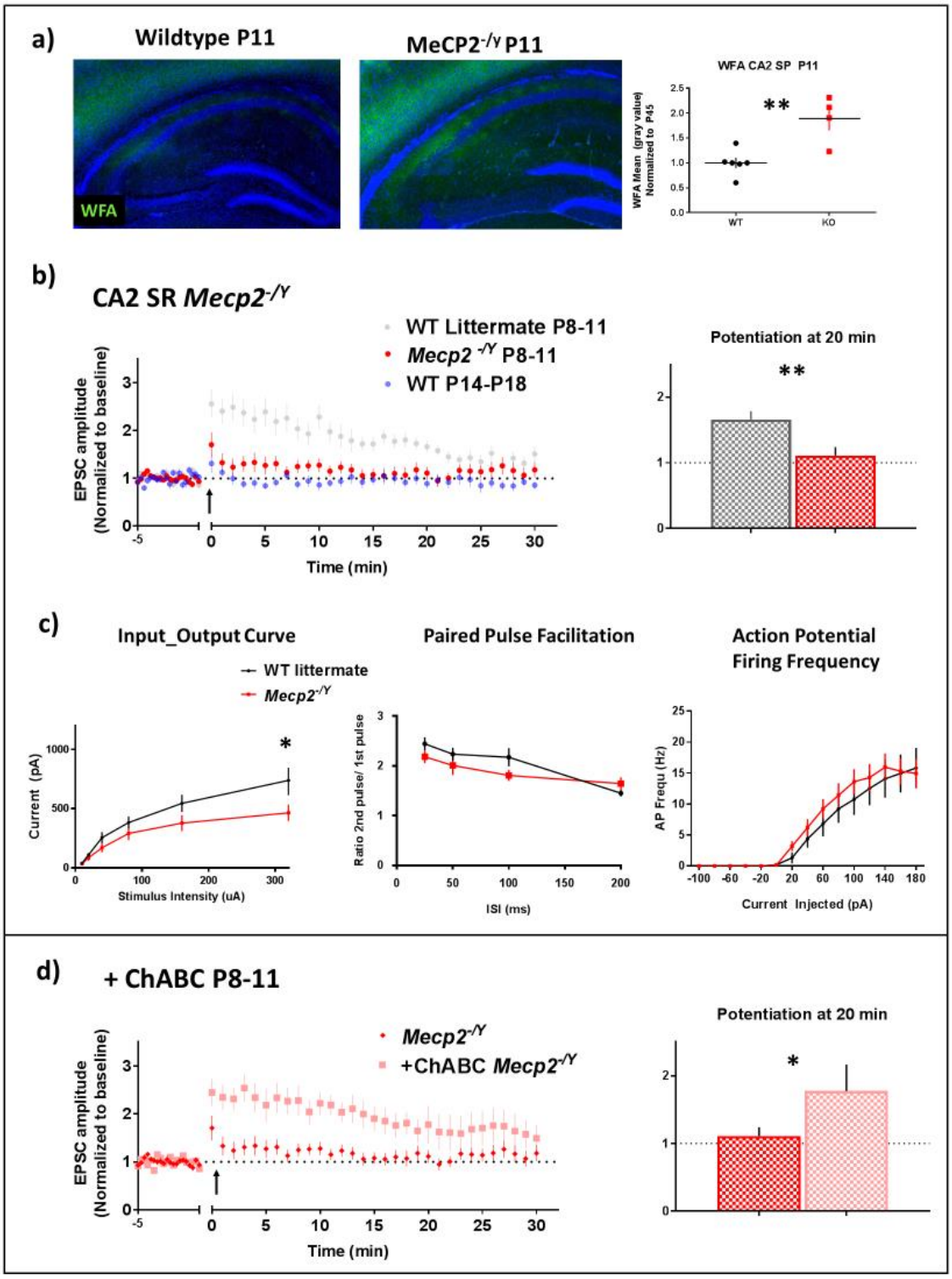
a)
Wildtype P11
MeCP2-/y P11
WFA
WFA CA2 SP P11
WFA Mean (gray value) Normalized to P45
**
WT
KO
b)
CA2 SR Mecp2-/Y
WT Littermate P8-11
Mecp2 -/Y P8-11
WT P14-P18
EPSC amplitude (Normalized to baseline)
Time (min)
Potentiation at 20 min
**
c)
Input_Output Curve
WT littermate
Mecp2-/Y
Current (pA)
Stimulus Intensity (uA)
*
Paired Pulse Facilitation
Ratio 2nd pulse/ 1st pulse
ISI (ms)
Action Potential Firing Frequency
AP Frequ (Hz)
Current Injected (pA)
d)
+ ChABC P8-11
Mecp2-/Y
+ChABC Mecp2-/Y
EPSC amplitude (Normalized to baseline)
Time (min)
Potentiation at 20 min
*

Table 3-3.1

Table 3.1: CA2 P8-11 intrinsic properties including RMP, Cm and Ri, as well as action potential threshold are unchanged in MeCP2-null males compared to widtype littermates (n=17 and 13, respectively), P>0.05, two-tailed unpaired t-test. CA2 P14-18 intrinsic properties including RMP, Cm, Ri, and action potential threshold are unchanged in MeCP2-null males compared to widtype littermates (n=23 and 8), P>0.05, two-tailed unpaired t-test. Indicated is the mean ± SEM. *Voltage threshold to fire action potential (AP) minus resting membrane.

P8-11	Intrinsic Properties			
	RMP (mV)	Cm (pF)	Ri (Mohm)	AP threshold (mV)
CA2 Control	-64.33 (1.97)	115.7 (5.812)	337.3 (16.49)	-20.6 (1.907)
CA2 *Mecp2*$^{-/Y}$	-66.44 (1.464)	120.5 (5.912)	317.7 (24.32)	-16.32 (1.46)
P14-18				
CA2 Control	-65.66 (1.575)	179.8 (12.26)	174.5 (14.38)	-16.29 (1.85)
CA2 *Mecp2*$^{-/Y}$	-64.05 (0.8062)	186.5 (7.605)	223 (14.99)	-12.01 (1.145)

Figure 9- 3.5

Figure 3.5: Global loss of MeCP2 alters plasticity-regulating molecules in the hippocampus. a) Immunoblot of MeCP2 protein (75 kDa) in *Mecp2*$^{-/}$ compared to wildtype littermate (left). The ratio of MeCP2 protein over loading control is signficantly decreased in *Mecp2*$^{-/Y}$ compared to wildtype littermate (right). ***P=0.0003, two-tailed, unpaired, t-test, n=3 for each group. b) Immunoblot of MMP-9 protein (92 kDa) in *Mecp2*$^{-/}$ compared to wildtype littermate (left). The ratio of MMP-9 protein over loading control is decreased, in *Mecp2*$^{-/}$ compared to wildtype littermate (right). *P=0.034, one-tailed, unpaired, t-test, n=3 for each group. c) Immunoblot of NR2a protein (170 kDa) in *Mecp2*$^{-/}$ compared to wildtype littermate (left). The ratio of NR2a protein over loading control is signficantly decreased in *Mecp2*$^{-/}$ compared to wildtype littermate (right). *P=0.024, two-tailed, unpaired, t-test, n=3 for each group. d) GluR-1 protein (107 kDa) in *Mecp2*$^{-/}$ compared to wildtype littermate (left). The ratio of GluR-1 protein over loading control is signficantly lower in *Mecp2*$^{-/}$ compared to wildtype littermate (right), $P > 0.05$.

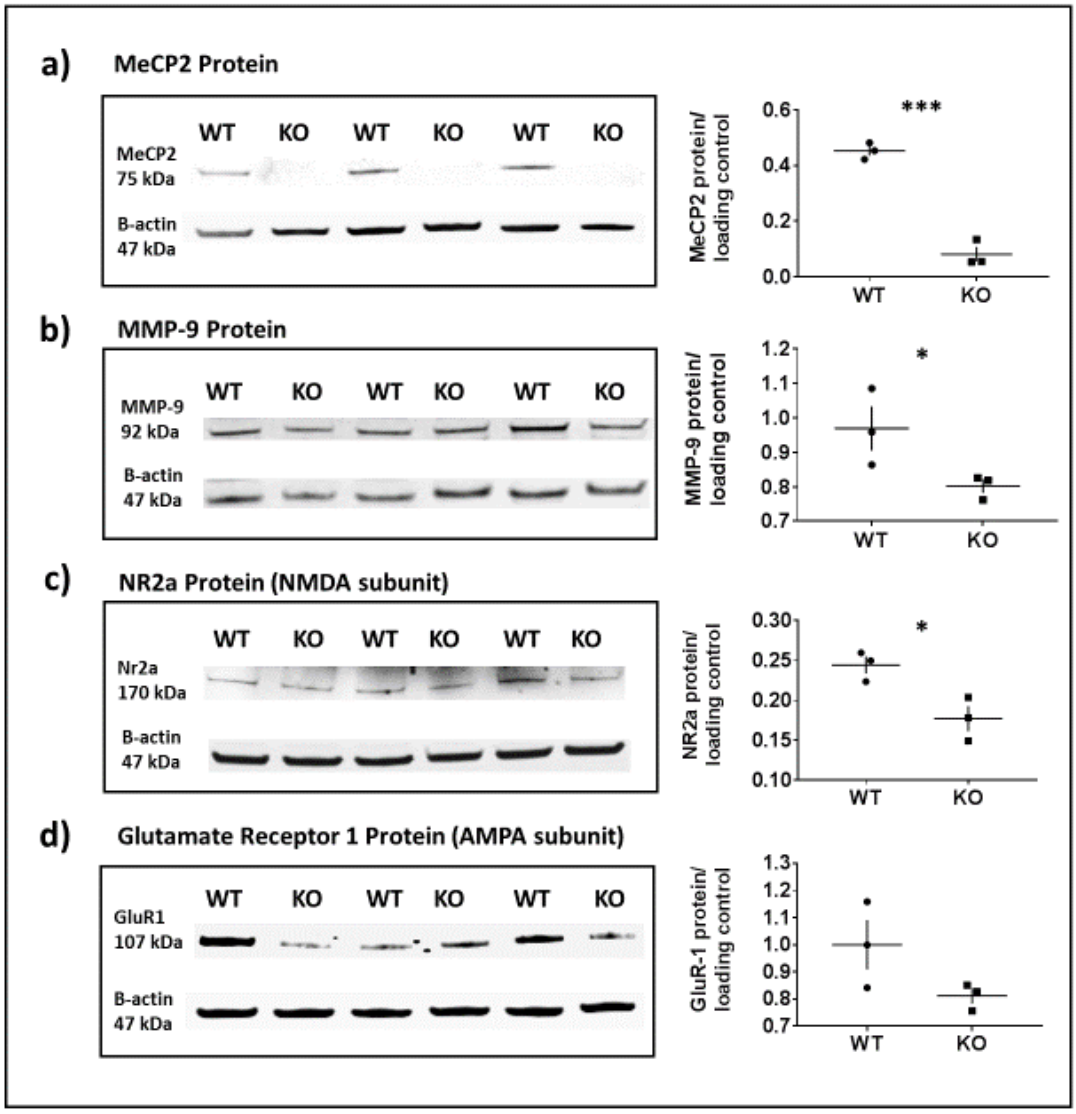
a)
MeCP2 Protein
WT KO WT KO WT KO
MeCP2
75 kDa
B-actin
47 kDa
MeCP2 protein/
loading control
***
0.6
0.4
0.2
0.0
WT KO
b)
MMP-9 Protein
WT KO WT KO WT KO
MMP-9
92 kDa
B-actin
47 kDa
MMP-9 protein/
loading control
*
1.2
1.1
1.0
0.9
0.8
0.7
WT KO
c)
NR2a Protein (NMDA subunit)
WT KO WT KO WT KO
Nr2a
170 kDa
B-actin
47 kDa
NR2a protein/
loading control
*
0.30
0.25
0.20
0.15
0.10
WT KO
d)
Glutamate Receptor 1 Protein (AMPA subunit)
WT KO WT KO WT KO
GluR1
107 kDa
B-actin
47 kDa
GluR-1 protein/
loading control
1.3
1.2
1.1
1.0
0.9
0.8
0.7
WT KO

Discussion

A key challenge for understanding the pathogenesis of Rett syndrome is identifying molecular targets and understanding when and how they cause synaptic dysfunction. PNNs are functionally implicated in inhibiting structural and synaptic plasticity in the developing brain [296]. Moreover, PNNs are elevated in several cortical regions in postmortem Rett individuals, as well as in the mouse model of Rett, MeCP2-null [265, 284, 336, 337]. Because, PNNs have yet to be described in the hippocampus or during early postnatal life, I characterized the development of PNNs in the hippocampus between ages P11 to P45 in *Mecp2*$^{-/Y}$ males. I found that staining for PNNs develops prematurely and is increased in adulthood in hippocampal area CA2 of *Mecp2*$^{-/Y}$ males compared to wildtype littermates. Because the maturation of PNNs closely track the closing of critical windows of plasticity, I reasoned that the normal absence of PNNs at P11 in CA2 may be correlated with a yet-to-be described developmental window of plasticity at CA2 synapses.

In the visual system, PNNs first appear around inhibitory neurons after eye opening, ~P15 and are fully matured by P30, tracking the closure of critical period plasticity in mice [298]. PNNs first develop in area CA2 around P14 in the rodent. Hippocampal CA2 neurons are normally resistant to LTP induction at CA2 SR synapses in mice older than P14 [196]. Because I previously found that degrading PNNs in an acute hippocampal slice was sufficient to enable plasticity in CA2 at P14-18 [295], I tested whether I could induce plasticity in CA2 at in P8-11, an age before PNNs develop in CA2. I found that potentiation could indeed be induced at CA2 SR synapses in the neonatal hippocampus, discovering a previously unknown window of synaptic plasticity in the hippocampus that correlates precisely with the onset of PNN appearance. Next, I investigated whether PNNs and/or plasticity may be altered in the developing brain at P8-11 in Rett CA2 neurons.

I hypothesized that because PNNs are at least one brake on CA2 plasticity, premature development of PNNs may be correlated with premature restriction of plasticity at CA2 SR synapses. Indeed, I found that plasticity is suppressed prematurely in CA2 of a mouse model of Rett (at P8-11). Premature restriction of CA2 LTP may be due to. An alternative hypothesis could be that, because others have found inhibitory transmission developing prematurely, as in the visual system; LTP in CA2 may be prematurely restricted by inhibition [298]. However, this is unlikely considering GABA transmission is normally excitatory at P8-11 [105], although not validated at CA2 synapses. Our data rules out CA2 excitability as a possible explanation because action potential firing frequency is unchanged in *Mecp2*$^{-/Y}$ males. Moreover, I found that degradation of PNNs *in vitro* with ChABC rescues early plasticity restriction, strongly implicating PNNs as a regulator of premature plasticity in *Mecp2*$^{-/Y}$ CA2. To explain the ChABC-induced LTP restoration, I proposed to examine whether ChABC treatment at P8-11 in *Mecp2*$^{-/Y}$ hippocampi enhances CA2 excitatory synaptic strength or increases intrinsic excitability. Overall, the restoration of CA2 plasticity by ChABC treatment in the Rett mouse hippocampus convincingly point to PNNs as a premature molecular brake on plasticity in CA2.

PNNs function to stabilize synapses in the developing brain, therefore premature PNN maturation in Rett CA2 may be disrupting normal synapse/ circuit development [296]. PNN development is activity-dependent and is modulated by normal experience in early-life in several brain regions including motor [116] and visual [113, 117, 118] systems. In general, sensory deprivation from birth delays and attenuates PNN maturation but are unaffected by similar manipulations in adulthood. This begs the question, could pathological increases in activity explain the premature development of PNNs in Rett CA2? Although we did not directly test this, a recent study would suggest that indeed aberrant activity in early life can increase PNN expression levels. A single

seizure at P10 increases PNNs around inhibitory neurons in the hippocampus [242]; whereas a single seizure in adulthood reportedly attenuates PNNs [243]. In contrast to pathological activity, I report that PNNs are increased at P21 and P45 but not at P14 in CA2 after rearing mice in an enriched environment (EE) [295]. In fact, PNNs may even be lower in CA2 at P14 (see Fig. 3, Chap. 2). In future experiments, I propose to characterize the effects of EE on PNN expression at P14, and earlier, to better understand how aberrant versus 'appropriate' activity may differently regulate PNNs during neonatal development of normal and *Mecp2*$^{-/Y}$ brains.

Approximately 70% of Rett children develop partial and generalized convulsive seizures by the age of 7 [266, 270]. In symptomatic *Mecp2*$^{-/Y}$ males, pyramidal neurons in the somatosensory cortex and thalamus of *Mecp2*$^{-/Y}$ males have reduced excitatory synaptic transmission [303, 306, 320, 338, 339]. However, the hippocampus in Rett model mice is reported to be hyper-excitable and more susceptible to seizure [306]. Voltage sensitive dye experiments in acute hippocampal slices reveal increased neuronal depolarizations in response to SR electrical stimulation in Rett CA1 and CA3 regions compared to control [306]. The hyper-excitably is thought to originate from a higher frequency of spontaneous activity in CA3 pyramidal neurons and impaired synaptic inhibition (smaller mIPSC amplitude) [306, 339]. These data indicate that both excitatory and inhibitory impairments contribute to overall hippocampal hyperexcitability observed in symptomatic Rett mice, however this pathophysiology has yet to be studied in the neonate hippocampus.

I found that excitatory synaptic transmission is decreased at CA2 SR synapses in P8-11 *Mecp2*$^{-/Y}$ males compared to wildtype littermates, but only at high stimulation intensities. Interestingly, I also found that excitatory transmission is increased by P14-18 in MeCP2 mice (data not shown), which is consistent with previous reports of hippocampal hyperexcitability in *Mecp2*$^{-/Y}$ males. These data indicate a possible abnormal weakening and subsequent

strengthening of CA2 synapses during *Mecp2*$^{-/Y}$ postnatal development. Interestingly, *Mecp2*$^{-/Y}$ CA1 neurons display a 46% reduction in excitatory synaptic response at 2 weeks of age, which has been attributed to a reduction in glutamatergic terminals on CA1 pyramidal neurons (note- glutamatergic release probability is unchanged) [303]. I did not observe any differences in PPF, suggesting that at least with this measure, presynaptic release properties are normal. In future experiments, I propose to measure mEPSC frequency to determine whether the number of glutamatergic terminals may be similarly reduced. Taken together, these findings demonstrate abnormal strengthening of excitatory synapses in CA2 (and CA1) during early postnatal development in *Mecp2*$^{-/Y}$ hippocampus.

Glutamate receptor subunits have been identified as one possible mechanism underlying the CA1 plasticity deficit in the Rett mouse model [286]. During the critical period in mouse visual cortex, NR2A subunit expression is modulated by visual experience, leading to the hypothesis that the developmental switch from NR2B to NR2A may act to close critical period plasticity [38, 39, 54 55, 340]. Interestingly, AMPA and NMDA receptor densities were increased in young Rett brains (< 8 years old) but dramatically decreased in older patients [341, 342]. It remains unclear as to whether the abnormality in subunit expression in postmortem Rett tissue is a cause or consequence of developmental defects in Rett, therefore a developmental characterization of glutamatergic subunits in the developing *Mecp2*$^{-/Y}$ brain would be hugely informative. We, and others, show that NR2A expression is high in the symptomatic *Mecp2*$^{-/Y}$ hippocampus. In *Mecp2*$^{-/Y}$ CA1, high NR2A and low NR2B is thought to contribute to LTP deficits, because NR2A is more efficient than NR2B in generating NMDAR-dependent LTP in adult CA1 synapses [343]. NR2B subunit is normally highly expressed at embryonic ages in the cortex, while NR2A appears in the cortex a few days after birth in the rodent [312, 344]. As an example of NMDA

subunit regulation in early windows of plasticity, LTP at thalamocortical synapses in the somatosensory cortex at P3-7 is dependent on NR2B, not on NR2A [345]. Note- LTP is expressed between P8-11 at thalamocortical synapses in somatosensory cortex, at which point LTP is not inducible >P11 [345]. Because LTP in CA2 is NMDAR-dependent, P8-11 LTP at CA2 SR synapses may similarly be NR2B-dependent, in which case alterations in NR2B subunit in neonates of MeCP2-null animals could explain the lack of LTP in CA2 of MeCP2-null animals [203]. To our knowledge, though, the level of NR2b in Mecp2-null mouse hippocampus has only been measured in symptomatic adult animals [286].

Finally, the idea of a premature closure of plasticity is not new to the Rett field. *Mecp2*$^{-/Y}$ visual acuity is comparable to that of WT at the time of eye opening (P13), however rapid and progressive deficits in morphology, connectivity and physiological properties occur by 2-3 days later [299, 346-348]. Krishnan and colleagues also note that PNNs are enhanced at P15 and P30, similarly suggesting an early closure of the critical period. Indeed they found an early onset and closure of ocular dominance plasticity, as well as deficits in visual function, and attribute these findings to a precocious maturation of PV neurons [298]. Interestingly, the loss of MeCP2 from only PV inhibitory neurons abolishes experience-dependent plasticity, but a loss of MeCP2 from glutamatergic cells or somatostatin+ inhibitory neurons has no effect on critical period plasticity[326]. I found that knock-down of MeCP2 in CA2 was sufficient to replicate the overexpression of PNNs. These data would suggest that although loss of MeCP2 in glutamatergic cells in the visual cortex did not alter critical period plasticity, our observation of increased PNNs in CA2 would suggest that selective loss of MeCP2 in glutamatergic CA2 neurons may ultimately be sufficient to prematurely restrict plasticity in CA2. In future experiments, I propose to characterize PNNs in a PV-targeted MeCP2 knock-down mouse,

where an increase in CA2 PNNs would suggest that MeCP2 is not acting cell-autonomously, but instead is regulating PNNs on a global scale of hippocampal activity changes. Either way, these findings ultimately beg the question, what might be the long-term effects on disrupting an early window of critical hippocampal-dependent learning?

Overall, my findings indicate that synaptic function appears to be pre-symptomatically impaired in the hippocampus, particularly in CA2. Interestingly, dendritic spines are reportedly decreased in CA1 *Mecp2*$^{-/Y}$ at P7 but not at P15. Taken together with our findings, the study of plasticity in the *Mecp2*$^{-/Y}$ neonatal hippocampus is critical [332]. Future experiments focusing on the pathophysiology in the pre-symptomatic mouse, as well as developmental studies of MeCP2-reinstatement will be imperative to better understand the timepoint at which cognition declines and, ultimately, identifying an optimal therapeutic window for therapeutic intervention. Taken together, the presence of PNNs in CA2 is highly suggestive of an unknown critical window of plasticity in the hippocampus that may ultimately shed light on hippocampal-dependent learning deficits associated with Rett syndrome infants.

CHAPTER IV–SEIZURE ACTIVITY ALTERS PERINEURONAL NETS IN THE HIPPOCAMPUS OF A MOUSE MODEL OF TEMPORAL LOBE EPILEPSY

Introduction

Temporal lobe epilepsy (TLE) affects an estimated 50 million people worldwide and is among the most difficult form of epilepsy to treat [349, 350]. Epileptogenesis refers to the process whereby a normal brain becomes epileptic and is thought to reflect aberrant plasticity, however, little is known about the underlying mechanisms [351]. Thus, understanding more about the remodeling that takes place during epileptogenesis should lead to more effective therapeutic targets for TLE. During epileptogenesis, massive hippocampal remodeling occurs, including mossy fiber sprouting and long-term changes in functional plasticity [352, 353]. Another observation is that the extracellular matrix (ECM), specifically the specialized ECM perineuronal nets (PNNs), are altered in the hippocampus of humans with epilepsy and in rodent models of seizures [294, 354, 355 356]. TLE patients typically develop recurrent seizures during childhood and studies of human adult post-mortem TLE tissue reveal massive hippocampal synaptic reorganization. Loss of ECM components are thought to be one mechanism by which the cellular environment could become permissive for this axonal remodeling [354, 357].

In rodents, a single prolonged seizure can lead to extensive structural and functional synaptic changes in the adult hippocampus, including mossy fiber sprouting, neuronal cell death and aberrant synaptic plasticity [353, 358-360]. Interestingly, PNNs have be reported to be down-regulated in the rodent hippocampus after an acute seizure in adulthood [243]. One mechanism by

which the seizure-induced degradation of PNNs is that endogenous proteases, enzymes that degrade the ECM, dramatically increase, and have been shown to play a prominent role in modulating epileptogenesis [165, 361, 362] [351]. Many rodent seizure models, however, have neglected to mimic the effects of recurrent seizures that are characteristic of TLE. Because PNNs are implicated in epilepsy and are densely localized to hippocampal region CA2, I sought to characterize the development and plasticity of PNNs around this population of excitatory pyramidal neurons in a mouse model of TLE.

CA2 neurons have been long appreciated as resistant to seizure-induced cell death in TLE individuals and rodents [191, 363-365]. Post-mortem analysis of sclerotic hippocampi of TLE individuals reveals widespread cell death in areas CA1/ 3 and DG but not in are CA2 [191, 363, 366]. The effect of pathological increases in activity on PNN formation in CA2, however, is unknown. Interestingly, PNNs in the hippocampus appear to be differently regulated by acute seizure in the developing brain compared to adulthood; McRae and colleagues found a persistent decrease of PNNs staining around inhibitory neurons in the hippocampus one week to two months after a single seizure that persisted into adulthood [243]. Moreover, the same group found that a single seizure in a neonatal rat (age P10) caused an increase in PNN+ inhibitory neurons four days post status-seizure [242]. Because we previously found that PNN degradation enables potentiation in the normally plasticity-resistant CA2 pyramidal neurons, I reasoned that PNN degradation in response to recurrent seizures in adulthood may alter plasticity there. Interestingly, a recent study in mice reported mossy fiber sprouting in the CA2 region following seizure, suggesting that seizures may allow for a permissive environment in CA2 for aberrant plasticity to occur [367].

To identify the effect of early-onset seizures on PNN expression levels in hippocampal CA2, I used Kv1.1-null mice, in which the Kv1.1 potassium channel gene has been deleted. Kv1.1-null mice display frequent spontaneous seizures beginning early in development and continuing into adulthood. The seizures exhibited by these mice have been characterized behaviorally and electrographically, and mimic limbic seizures observed in human TLE [368]. Homozygous Kv1.1-null mice on a B6/129S genetic background develop seizures around P21, and progress in severity over time limiting the life span to approximately 2 months of age [368]. This TLE mouse model has allowed me to study the effects of early-life seizure on CA2 PNN development, as well as the effects of long-term recurrent seizures on PNNs in adult hippocampus. In addition, this model will help us to disentangle the effects of seizure activity and MeCP2 depletion, as seizures are common in Rett syndrome [282].

The dense localization of PNNs in CA2, CA2's particular resistance to both plasticity and damage from seizure, and the region's central location in hippocampal excitatory circuity make CA2 a compelling region to study how PNNs may be developmentally disrupted in epilepsy. In this section I report that PNNs are indeed attenuated in area CA2 of adult Kv1.1-null mouse, but are unaffected by early-life seizure in these mice. I will also describe a dramatic increase in PNNs in dentate gyrus, which is inconsistent with another study that found aggrecan is decreased in DG after a single seizure [243]. Future investigation into how recurrent seizures modulate PNNs in a mouse model of TLE and subsequently, how alterations of PNNs modulate hippocampal plasticity will be critical for our understanding of the long-term effects of epileptogenesis on hippocampal function.

Next, we sought to investigate how PNNs are regulated by artificial manipulation of CA2 neuronal activity in the adult brain. PNNs are indeed susceptible to damage from injury like

seizure or ischemia in the adult brain; however, non-pathological forms of activity such as environmental enrichment or other learning tasks appear sufficient to also alter expression [125, 295, 369-371]. For example, PNNs in the adult auditory cortex were enhanced 4 hours after tone-shock-paired fear conditioning but returned to baseline after 24 hours in mouse [174]. I previously found enhanced PNNs in area CA2 at P45 in mice reared in an enriched environment, suggesting that PNN modifications can persist on a longer timescale [295]. The age, duration, and degree of neuronal activity changes all appear to be variables in regulating PNNs throughout development.

Here I describe experiments where we directly manipulated CA2 activity using a chemogenetic approach. Chemogenetics is a method by which proteins are engineered to interact with small molecule chemical actuators [372]. One class of engineered proteins that was designed to manipulate neuronal activity is G-coupled Designer Receptors Exclusively Activated by Designer Drugs (DREADDs) [372]. DREADD receptors are activated by their designer drug clozapine N-oxide (CNO) [230, 373, 374]. Depending on the class of DREADDs, activation of the receptor can either increase (Gq-coupled) or decrease (Gi-coupled) neuronal activity by either depolarizing or hyperpolarizing the cell [372]. CNO has been reported to have lasting effects for up to 6-10 hours post administration [374]. Using DREADDs, we increased or decreased activity of CA2 neurons persistently for 5 days and compared PNN levels to that of the TLE mouse model. We found that PNNs staining was significantly lower in CA2 after 5 days of increased activity in CA2 compared to control animals.

Finally, the current methods of experimentally degrading PNNs have several limitations. First, a knockout of the major ECM component, aggrecan, during embryonic development is lethal and is therefore limited to *in vitro* studies [375]. Moreover, loss of a single PNN component, such as tenascin-R, is typically insufficient to fully reduce staining for this matrix, which is

likely due to the redundancy of proteoglycan components [138, 168, 376, 377]. Note however that these mice do exhibit aberrant synaptic and structural plasticity [138, 168, 376]. The chondroitinase enzyme itself is promiscuous in the mammalian brain; direct injection of the enzyme effects a large diffuse area surrounding the site of injection [134, 256]. This commonly used approach also lacks cell-type specificity, considering that all PNN+ neurons within the ChABC-injected area are affected. ChABC has previously been successfully expressed in mammalian neurons using AAV and lentiviral vectors, however the effect has still been diffuse and not cell-type specific [259, 378, 379]. Ultimately, cell-type specific degradation of PNNs would allow for studies of cell-autonomous regulation of PNNs and potentially allow us to better understand whether PNNs are a cause or an effect of pathological changes in activity. Here I describe preliminary data suggesting that targeting PNN-degradation with cell-type specificity *in vivo* is indeed possible. This novel approach will allow me to study PNN function with cell-type selectivity *in vivo* and may ultimately reveal how long-term loss of PNNs (associated with several neurodevelopmental disorders) may disrupt learning and memory processes [265, 380, 381].

Materials and Methods

Animals:

Animals in all experiments were housed under a 12:12 light/dark cycle with access to food and water *ad libitum*. All procedures were approved by National Institute of Environmental Health Sciences NIEHS and were in accordance with the National Institutes of Health guidelines for care and use of animals.

Immunohistochemistry:

Adult male mice were deeply anesthetized with Fatal-Plus and perfused with cold PBS, followed by 4% paraformaldehyde in PBS, pH 7.4. Brains were removed and postfixed overnight at 4°C and submerged in 30% sucrose. Forty-micrometer-thick sections were cut on a sliding microtome, blocked in 5% normal goat serum and incubated in biotin-conjugated *Wisteria floribunda* agglutinin (WFA) lectin (1:1000; Sigma-Aldrich L1516), rabbit anti-PCP4 (1:500, SCBT, sc-74186), rabbit anti-MMP-14 (1:500, Abcam, ab51074), guinea pig anti-ZNT3 antibody (Synaptic systems #197 004, 1:500), overnight at 4°C. Sections were washed three times in PBS and incubated in secondary antibody at 1:500 for 40 min at room temperature: streptavidin Alexa-568 (Invitrogen #S11226) or goat anti-rabbit H+L A568 (Invitrogen). Sections were mounted with Vectashield antifade mounting medium with DAPI (Vector Laboratories). Images were acquired on a Zeiss laser scanning confocal (LSM510 NLO) or a Zeiss light microscope using controlled camera settings.

WFA quantification and statistical analysis:

PNNs were stained and imaged using the protocol described above in the immunohistochemistry section. WFA staining intensity was quantified using measures of pixel luminescence value on ImageJ software (National Institutes of Health) using a region of interest (ROI) contoured around either CA2 pyramidal neurons in stratum pyramidale (SP), PNN+ neurons in CA1 or a square ROI spanning all layers of overlying cortex. This cortical region is defined as primary somatosensory cortex according to an anatomical reference from the Allen Mouse Brain Atlas (Allen Institute, Seattle, WA). The mean gray value measure of background (defined as a region in a fixed anatomical location in the fimbria of each section) was subtracted from the mean gray value of each ROI. Each data point represents one mouse. Fluorescence quantification was repeated and analyzed with the experimenter blinded to condition.

Data in figures are expressed either as a mean ± SEM or a normalized mean ± SEM. Statistical analyses were performed using GraphPad Prism 6.05 software, and significance was calculated using an α level of 0.05. The Kolmogorov–Smirnov test was used to test normality and variance.

Aim 1: PNN regulation in a temporal lobe epilepsy (TLE) mouse mode.

TLE mouse model:

Kv1.1-null mouse (also known as *Kcna1* knock-out mouse), C3HeB.129S7-*Kcna1*^{tm1Tem}/J, The Jackson Laboratory, stock # 003532, donated by Bruce L. Tempel, University of Washington School of Medicine [368]. We crossed heterozygous Kv1.1$^{+/-}$ mice and used homozygous male and female Kv1.1$^{-/-}$ knock-out mice to measure *in vivo* electrophysiology and to quantify PNN staining.

Electrode implantation of a Kv1.1 KO mouse:

A P40 Kv1.1 null mouse was implanted with an electrode wire bundle for *in vivo* electrophysiology recordings to measure potential ictal activity. The mouse was anesthetized with ketamine (100mg/kg, IP) and xylazine (7mg/kg, IP) and placed in a stereotaxic apparatus. An incision was made in the scalp and a hole was drilled over the target region for recording. One ground screw was positioned approximately 4 mm posterior and 2 mm lateral to Bregma over the right hemisphere. The electrode was lowered and implanted in the left dorsal hippocampus targeting CA3 (-2.06 AP, -2.2 ML, -2.1 DV from Bregma). The electrode consisted of one bundle of 8 stainless steel wires (44-µm) with polyimide coating (Sandvik Group, Stockholm, Sweden). The wires were then connected to a printed circuit board (San Francisco Circuits, San Mateo, CA), which was connected to a miniature connector (Omnetics Connector

Corporation, Minneapolis, MN). Electrode placement was confirmed via wire bundle tracks during histological analysis.

Electrophysiology data acquisition:

Five days following electrode implantation, the null mouse underwent electrophysiological recording in the awake, behaving state for a duration of one hour on two consecutive days, and local field potential (LFP) data were analyzed for bouts of ictal activity. Neural activity was transmitted via a 32-channel wireless 10x gain headstage (Triangle BioSystems International, Durham, NC) and was acquired using the Cerebus acquisition system (Blackrock Microsystems, Salt Lake City, UT). Continuous LFP data were band-pass filtered at 0.3-500 Hz and stored at 1,000 Hz. Neurophysiological recordings were referenced to a silver wire connected to the ground screw.

Maximal electroconvulsive Shock (MECS) protocol:

Unanesthetized adult male mice were given a single maximal electroconvulsive shock (MECS) by delivering alternating current through ear clips (60Hz, 45mA for 0.2s with 0.5ms pulse width, UGO BASILE ECT UNIT cat # 57800-001). MECS was characterized by full extension of the hind limbs (tonic phase) for 10–15 sec, followed by repetitive flexion–extension of the forelimbs for 5–10 sec (clonic phase). Sham animals were handled identically except that no current was passed. See Farris et al. (2014) for extended methods [382]. One hour after seizure induction, mice received a lethal dose of fatal plus and the brains were removed and flash frozen in isopentane (chilled to −20°C in a dry ice and ethanol bath) for RNA analysis (below).

In situ hybridization

Adult mouse brains were flash frozen and coronal 20-μm-thick sections were cut on a cryostat and mounted on SuperFrost Plus slides (Fisher Scientific 12-550-15). Sections were

fixed in 4% paraformaldehyde for 1 h at 4°C, dehydrated in 50, 70, and 100% ethanol, and air-dried at room temperature. Fluorescent RNAscope *in situ* hybridization (ISH) was performed using an RNAscope Fresh Frozen Multiplex Fluorescent kit according to the manufacturer's protocol to perform target probe hybridization and signal amplification (Advanced Cell Diagnostics). Probes were purchased from Advanced Cell Diagnostics: aggrecan mRNA, mm-acan-C1 (catalog #300031-C1) and the immediate early gene Rn-Arc-3p (catalogue number 317076) (see design methods[187]. Fluorescent images were captured on a Zeiss laser-scanning confocal microscope (LSM710).

Cell death Staining:

Cell death and degenerating neurons were visualized using the FD Neurosilver kit (FD Neurotechnologies) on 40-µm sections. Tissue was prepped as described in immunohistochemistry manual. See FD Neurotechnologies for protocol, but in brief, the NeuroSilver stain uses diaminobenzodine as a chromogen, which stains degenerating neurons the color silver. Sections were slide-mounted and washed in tap water, dehydrated through a series of ethanol washes (70%, 90%, 100%), for 5-min each, and then finished in a xylene solution. We visually inspected the hippocampus in coronal slices for neuronal damage.
http://www.fdneurotech.com/item/0/41/0/732/FD_NeuroSilver_Kit_II_small

Aim 2: PNN regulation by chemogenetic manipulation of CA2 activity

Animals:

To gain selective genetic access to molecularly-defined CA2, we generated a tamoxifen-inducible mouse line, *Amigo2*-icreERT2. Expression of Cre in CA2 was validated by crossing *Amigo2*-icreERT2+ with a Cre-dependent tdTomato reporter mouse line [383]. Mice expressed

tdTomato in CA2 of *Amigo2-icre*ERT2+; *ROSA*-tdTomato+/- treated with tamoxifen (see Fig. S1 of Alexander et al. (2017) for expression of the Cre indicator [230]). The localization to CA2 pyramidal neurons was characterized by co-labeling with the CA2 pyramidal cell marker, PCP4, and an inhibitory neuron marker, GAD. The expression of Cre was indeed localized to CA2 pyramidal neurons and not inhibitory neurons in the hippocampus. To chemogenetically manipulate CA2 activity, Cre-dependent AAVs encoding either excitatory Gq-coupled or inhibitory Gi-coupled Designer Receptors Exclusively Activated by Designer Drugs (DREADDs) were infused into hippocampi of adult *Amigo2-icre*ERT2+ or *Amigo2-icre*ERT2- mice. Mice were group housed until the time of the AAV infusion, at which point they were singly housed and monitored during recovery from surgery. All procedures were approved by the National Institute of Environmental Health Sciences Animal Care and Use Committee and were in accordance with the National Institutes of Health guidelines for care and use of animals.

Animal numbers:

WFA staining intensity was quantified to measure changes in response to chemogenetic changes in activity. Sample sizes for histological analysis are consistent with those used in the field.

Mice	**Infusion hM3Dq**	**Infusion hM4Di**	**No virus infusion**
*Amigo2-icre*ERT2+	(4 mice)	(6 mice)	1
*Amigo2-icre*ERT2-	(4 mice)	(6 mice)	1

In vivo chemogenetics:

Gq- or Gi-coupled DREADD AAV (hSyn-DIO-hM3D(Gq)-mCherry or hSyn-DIO-hM4D(Gi)-mCherry, respectively; serotype 5) was delivered to hippocampus near CA2 in *Amigo2-icre*ERT2 mice to selectively target CA2 pyramidal neurons. Expression of each DREADD virus was validated previously using the mCherry reporter that is encoded in the AAV construct [230]. The mCherry expressing cells also expressed the CA2 marker PCP4 and pyramidal cell marker CaMKII but not the inhibitory marker GAD.

Virus infusion and tamoxifen treatment:

Viruses listed above were obtained from the viral vector core at the University of North Carolina at Chapel Hill. To prepare mice for the virus-infusion, mice were anesthetized with ketamine (100 mg/kg, IP) and xylazine (7 mg/kg, IP) and placed in a stereotaxic apparatus. An incision was made in the scalp and a hole was drilled over the CA2 target region for AAV infusion. A 27 guage cannula connected to a Hamilton syringe was lowered into the hippocampus (in mm: -2.3 AP, +/-2.5 ML, -1.9mm DV from bregma). Virus were infused unilaterally on the left side for hM3Dq and bilaterally for hM4Di AAV at a rate of 0.1 µl/min for a total of 0.5 µl. The cannula was then left in place for an additional 10 min before removing. Once removed, the scalp was sutured and animals were returned to their cages. Animals were administered buprenorphine (0.1 mg/kg, SQ) for pain preoperatively.

Protocol timeline:

After *Amigo2-icre*ERT2+ and *Amigo2-icre*ERT2- adult mice were infused with Gq or Gi-coupled DREADD AAV, the animals recovered from surgery for 2 weeks. The mice were given daily treatments of tamoxifen (100 mg/kg, IP) for 7 days. One week after the last tamoxifen injection, the mice were administered the DREADD ligand (“designer drug”) clozapine N-oxide

(CNO) subcutaneously (1 mg/kg for Gq DREADD infused mice and 5 mg/kg for Gi DREADD infused mice) twice daily (at 10:00 AM and 2:00 PM) for four days. On the fifth day, mice received one CNO treatment (at 10:00 AM) and were perfused for histology 2 hr later.

Figure 10- Method 4.1

Methods Figure 4.1:

a) Histology of the CA2 marker PCP4 (green) was used to demarcate CA2 SP and SR regions. b)

b) The DG ROI was created using a reference atlas, where DG is highlighted in purpose (Allen Brain Institue, Seattle, WA). Below:

c, d) Example images of WFA fluorescnet staining (white) with ROIs for CA2 SP or SR contoured in red (c), and DG and overlying primary somatosensory cortex (d).

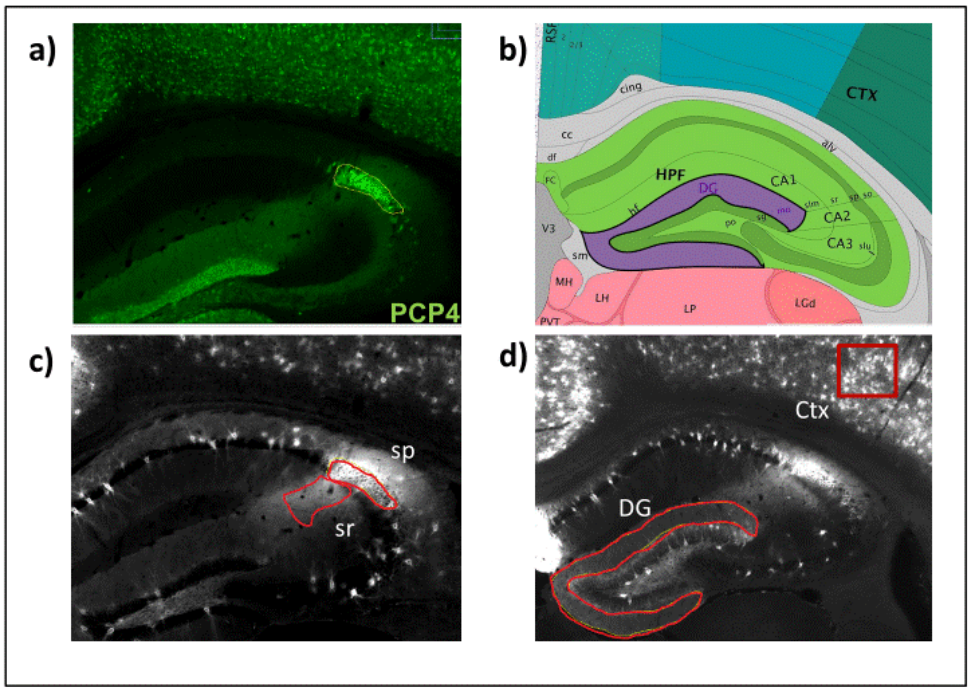

Aim3: Selective degradation of PNNs in CA2 *in vivo* with a Cre-dependent AAV; a pilot study

Generation of AAV-ChABC

To degrade PNNs with cell-type selectively, I sought to create a Cre-dependent AAV that encodes the PNN-degrading enzyme ChABC. AAV and lentiviral vectors encoding a modified ChABC gene have previously been generated, and infusion into the mouse brain has previously been shown to successfully degrade PNNs around the injection site [384, 385]. These viruses for expressing ChABC were not cell-type specific and PNN degradation was widespread around the injection site. They also lacked a tag or reporter to validate expression localization.

Chondroitinase gene:

For the ChABC gene insert, we used the synthetic chondroitinase gene sequence 'Y1330' that was published in lentiviral-ChABC studies [385] and originally optimized for enzymatic secretion from mammalian cells *in vitro* and in tissue culture [386]. The ChABC sequence containing a P2A processing sequence at its 3' end (Methods Fig. 4.1) was cloned into vector pUC57 at the Xba I site (GenScript, Piscataway, NJ).

AAV vector:

A shuttle plasmid containing a double floxed mCherry under the control of human synapsin promoter was used for the viral vector backbone, pAAV-hSyn-DIO-mCherry (courtesy of the Bryan Roth lab at the University of North Carolina Chapel Hill, also commercially available at Addgene, plasmid #50459-AAV5). The ChABC cDNA and P2A sequence were subcloned into the AAV shuttle vector as an Xba I restriction fragment and verified for correct orientation by PCR. DNA sequencing was carried out to assure fidelity of the shuttle plasmid with the original sequence of the vector and insert. AAV particles were generated by

cotransfection of HEK 293 cells with the ChABC shuttle vector, a helper plasmid and capsid encoding plasmid according to a system originally purchased from Agilent Technologies (AAV Helper-Free System Catalog #240071). Viral particles were harvested from HEK 293 cells, purified and concentrated by ultracentrifugation, and the viral pellet was resuspended in 1x PBS/5% glycerol and stored in aliquots at -80℃ at a titer of 4.16E13 GC (genome copies)/ml (Methods Fig. 4.2).

Virus infusion and tamoxifen treatment:

To express ChABC selectively in CA2 pyramidal neurons, I injected the ChABC-AAV into the left hippocampus of mice expressing Cre in only CA2 neurons, *Amigo2-iCre*ERT2+ mice (See Aim 2). Saline was injected into the right hemisphere for a within-subject control. To prepare mice for the virus infusion, mice were anesthetized with ketamine (100 mg/kg, IP) and xylazine (7 mg/kg, IP) and placed in a stereotaxic apparatus. An incision was made in the scalp and a hole was drilled over the hippocampal target region for AAV infusion, adjacent to CA2. A 27-gauge cannula connected to a Hamilton syringe was lowered into the hippocampus (in mm: -2.3 AP, +/-2.5 ML, -1.9mm DV from Bregma). The AAV was infused unilaterally at a rate of 0.1 µl/min for a total of 0.5 µl. Saline was infused with the same parameters into the right hemisphere as a control comparison within mouse. The cannula was then left in place for an additional 10 minutes before removing, at which point the scalp was sutured and animals were returned to their cages, singly housed. Mice were administered buprenorphine (0.1 mg/kg, SQ) for pain preoperatively.

After the virus infusion surgery, mice recovered from surgery for 2 weeks. Mice were then administered tamoxifen for either 1 or 3 days (100 mg/kg, IP) to induce recombination. Two animals per group were used or a preliminary qualitative analysis of ChABC-AAV expression

and PNN degradation. This dosing was based on findings from an earlier pilot study in which we found that 7 days of tamoxifen treatment resulted in a diffuse loss of PNNs that reached extrahippocampal regions. Mice were perfused two weeks after the last tamoxifen injection, and tissue was stained for the PNN-labeling lectin, WFA, and a CA2 marker, anti-PCP4 antibody.

Figure 11- Method 4.2

Method Figure 4.2: ChABC cDNA sequence

Synthetic ChABC cDNA sequence, 3162 base pairs, containing Xba I restriction sties, KOZAK sequence to initiate translation, and P2A sequences to cleave ChABC from mCherry.

Key
XbaI
P2A
Chondroitinase (ChABC)
KOZAK

tctagaTGGGCCAGGATTCTCCTCGACGTCACCGCATGTTAGCAGACTTCCTCTGCCCTC
TCCACTGCCaggcagaggggataacttaatctcctgatgccgaaataggaggtgaaggtgagctcagtgttatccccgcttacctga
tacttcacttcgctgttcttatcagcgctctgccacttcccattaatggtgacgttgattgtgacaggggtagcagctttctgccgggtcatgttca
aatctggtgtaactgcagacacgatcaaggtatccttttggcgatgtgtcatcacaattgctggcttattcacctttttgatccacttatcctcgata
gaagctggctggtaaaaggcgtatcctgtaacgtttgagagcttgtcgagtataatgtgcacgtccttatctttgcggagcacctgatacaacc
cgttgttttctctgaacttctgggccatttctcccattttctcgggagtagcatccaggaacaccatgtattcgtagctggcatctttcggtcttgtg
ctatggtctatccatgctgatgaaaagttcccttctgtaggttgcctgttcttgttttctgctgaaacctgatgttggcgactgacgtttaccttctcg
gcttgcgtgattaggtagccattcccgttactgtcgattaaccaatccccctgttgcagagtcgtctggtagggcatattttcaatcttctgcccat
taatccacagtgtattcaaggtgggcgtaatggcatgctgaaacaaggtagtttccacatttttgttcttatcactagaattgatgttagacccaat
aaagataaggtggttgtcggcggcgagaacgctcttctttgcggtgaagttggggtcaaatctctcaagattcgctggatagatcaggtcgaa
tgccatcatgccatactgcccttctaagcttgaagtgccggagaaaccccctctcgcccctctgcatcagtgtatgcggttttgggctatccaga
tccttcaagggaaggtgtatagtcgtggccccctgcatccggttccaatcccagccttcctgttggtatccctggctaagctgggaaccttggc
tgactatctgggccactccgtgactctggtagcgaccatacctattgtctttgttgtagatctcgctagaccacacattagtattgtaggccttga
gtgtgaccatcttgtcctgccacctgtgtatgccaaaagcaccaccgttaaaggcatagaatccttgaggcagggatgctggcgtaatagtct
ctccaaagatggcggtactctcattctgggtcttgtcgcttatggcaagatagatggaagctaaagtcttatcgggagaggatttcgctgacat
agctagccaatagtagccctgagccacgcttttcagagatgggctgttaaagggatgacggccggccaaaggtaagcccacttccggattg
ctgtaaatccaagcggaaaccatagctttttcagattattccatccactttcgcccactgaaaacggggtatcccgcagtaaataaatcaactg
ggcagcattcttgaaagcgggaaatgagtacccgggatagttgccctcatggcgccaagcagttccatcgggtctgagcccgtcttttccgc
ctgggggaacttgagtaagtgcaccggtgatatagtgagaaaaggtgttcactaggttaatgcgcttttggtcgtctggctctaggagcagca
gagccaggtgctgtctggacaacgtattgaaatagtccagatcgctggaatctgcagataccttcatgtcgaaggaactcttgaactccctact
ataccacagcagggaatcatagacctgggtctgcagatttgcctccttcagggcatctgacatgagcaatgtggagatgtaccaccatcggg
atgagtatccccagtggtgtgtagtaaccagagcagagcccttgacgaacccctggtcgagcagatgttttgtcatcagcaggtacatctgttt
cagctgggctttctgcgtaggatctttctcgagcacgtaagctcgggaaatttggaacatcagtgtagtgtactgtcccaaaatcacgtagttgt
cgaacagctgtttgtcctgggaattgaggttttctggttggtagatgatgatttgcttatcggtaatgaggtgtcgcccctgagttccgccattgg
ctaaagtgtgtatgttaagtgcatcaaagtcggatttcagcttagagatcttctcctcgagggcaagattcgtctcttttttctccacccacaaactc
gttgatgagcctttgccgaatgaggtcgatcgcggccaggttctctggtgtaacgggcagttgaggcttcacgttgtgaaactggatttctgg
ctcagatagccgtgtcttcacctgatagtcagaccactggtatcgggcgtcatcgacgctaaacattatgcggtcaatatagatctcgccctga
gagacattactgggagctttgaaccgtatgctatccacttttgctcccagactcctgccaatagagtcctgtgtaccgtcgctgctggtgttggt\

agcgttgagggtcatctctctattttccaggtcattgttcagagagacgcctacggctctccatcctgtgaagtcaagcttcactttaaagcccg
cttgtgcttcggaggttgaaatcagcttctccccaaaatcgattgtcaggtaaccgtcgataggtttctcgttatagagccagaaggaaaacac
cggtgtgctacttctgccccacgctttgctggcctctttatcggtaggtacaatcagtttcttgtgcagggtgaaactagaacccccttccactt
ccaaagaaggctctgattgcccatgattgaccgcttgtcggacagagtcaagatgctattcttatcactgctgaagtctgcgagaggattattct
gggcgaaatggtagatttcgctctgcatcaggtttttggggtcgaaggcgggattactagttgccgctatggcacgaccaagtagacagcac
agaacgcaaaggacccgcaaagggcctgctagggctccccacgctacacgggcttccatggtggcggctctaga

Figure 12- Method 4.3

Method Figure 4.3: Cre-dependent AAV-ChABC construct

A shuttle plasmid containing a double floxed mCherry under the control of human synapsin promoter was used for viral vector backbone, pAAV-hSyn-DIO-mCherry.

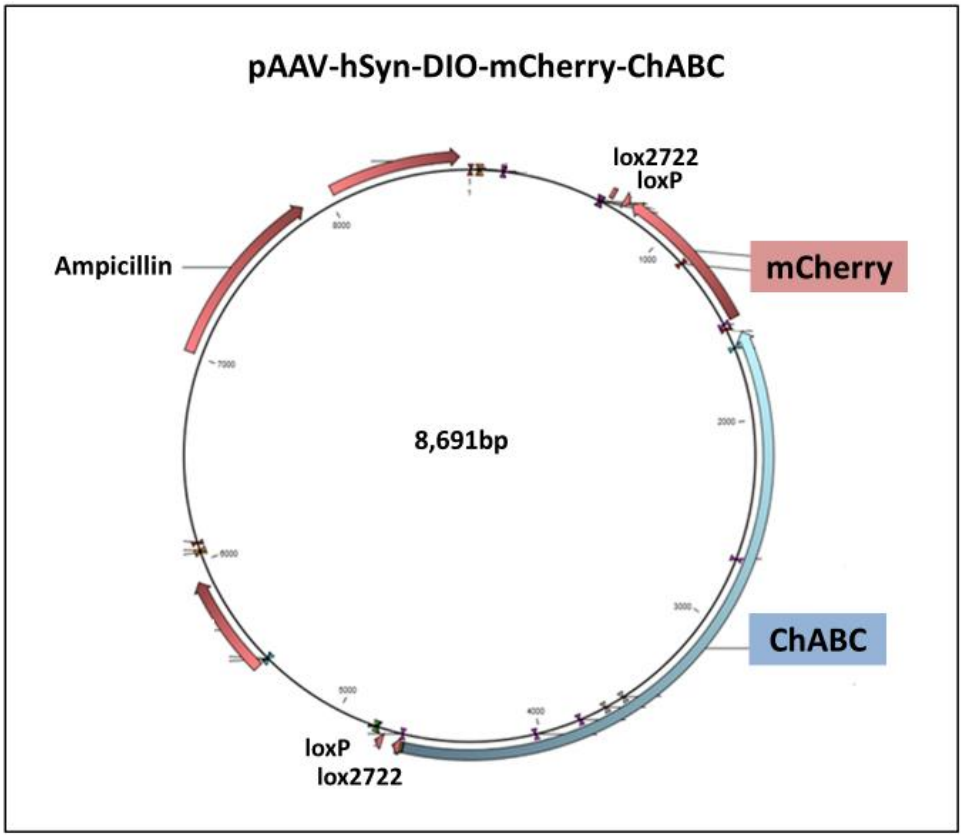

RESULTS

Aim 1: PNN regulation in a temporal lobe epilepsy (TLE) mouse mode.

Spontaneous electrographic seizures were detected in vivo in the hippocampus of a Kv1.1-null mouse.

Prior to characterizing PNNs in our TLE mouse model, we examined electrographic seizure activity recorded from the hippocampus of an adult Kv1.1-null mouse and compared our findings to previously reported electroencephalographic (EEG) data recorded from this mouse strain [368]. We measured local field potential (LFP) data by placing a wire-bundle electrode in area CA3 of a Kv1.1-null mouse (age P40). We recorded hippocampal LFP data for one hour while the mouse was awake and behaving. We observed three episodes of ictal activity (Fig. 4.1a) from the LFP recordings, interspersed between long periods (15 minutes) of non-ictal activity (Fig. 4.1b). Each episode of spontaneous ictal activity lasted approximately 25-30 seconds and was characterized by sudden onset of large amplitude population spikes, polyspikes and burst activity patterns that reversed in polarity and terminated in post-ictal depression [350]. Our observations of three electrographic seizures over the course of a one-hour recording session suggests that at the age of P40, Kv1.1-null mice may have spontaneous seizures approximately every 15-20 minutes. This frequency of seizure activity is consistent with EEG findings from the first Kv1.1-null mutant mouse characterization study [368].

PNNs are altered in the hippocampus in a developmental mouse model of TLE, Kv1.1 mouse

Kv1.1-null mice develop seizures around 21 days old and have spontaneous recurrent seizures into adulthood. Staining for PNN marker WFA is altered in the hippocampus of Kv1.1-null mutant at P60 compared to WT littermates but not at age P28 (Fig. 4.2a). WFA staining is

significantly decreased in area CA2 (compared to WT littermates, *P < 0.05, Bonferroni *post hoc* test for pairwise comparison after two-way ANOVA, Fig. 4.2b) and is robustly increased in DG of P45-60 Kv1.1-null compared to control (***P= 0.0002, Bonferroni *post hoc* test for pairwise comparison after two-way ANOVA, Fig 4.2b). Upon closer inspection, the PNN effect is even more robust if data points are separated by ages P45 and P56-60 (.***P= <0.0001, *P= 0.033, Bonferroni *post hoc* test for pairwise comparison after two-way ANOVA, Fig 4.3). CA2 SP, SR and DG regions of interest (ROI) are outlined in Methods Fig. 4.1.

Molecular indicators of TLE pathology

I next characterized TLE pathology in the Kv1.1 mouse model compared to WT littermate by staining for TLE-associated proteins at P60. Endogenous matrix metalloproteinases (MMPs) are modulated by seizure in human and rodent [163, 164, 333, 334, 361, 387]. MMP-9 protein is increased in young and adult human epilepsy patients, specifically in sclerotic hippocampi [388]. I observe a similar increase in MMP-14 protein levels in the hippocampus, specifically in CA1 and CA2 SP layers (Fig. 4.4a). Mossy fiber sprouting is a classic pathology in the hippocampus of TLE patients [350, 358, 389]. Mossy fibers, labeled with an antibody against zinc transporter 3 (ZNT3), indeed appear increased in surface area in SR region of CA2/ 3 and also in the hilus of the Kv1.1-null mouse compared to WT littermate. Finally, neuronal loss in the TLE hippocampus is another common histopathology (hippocampal sclerosis), where cell death is typically observed in CA1/ 3 and the hilus cells of DG [193, 366]. CA2 neurons are typically resistant to seizure-induced cell death [191, 194, 366]. To stain for cell death and degenerating neurons, we used the proprietary 'NeuroSilver' kit (FD Neurotechnologies). Neurons positive for silver stain indicate cell death or degeneration. Only CA1 neurons in the Kv1.1-null hippocampus were

labeled silver (Fig. 4.4c). No other neurons in the Kv1.1-null mouse or WT littermate show indication of cell death at P60 (Fig. 4.4c).

PNNs appear unaltered in adult WT hippocampus after an acute MECS-induced seizure

I sought to compare the modulation of PNNs in our TLE mouse model (long-term recurrent seizures) to an acute seizure mouse model, a single maximal electroconvulsive shock (MECS)-induced seizure. Note: only mice that exhibited full tonic/ clonic seizure behavior were included. I observed no difference in PNNs in area CA2 or DG in adult MECS hippocampus 18-hours after seizure (Fig. 5a), unlike our adult Kv1.1-null mouse (Fig. 4.1a,b). Furthermore, we probed for transcripts of the immediate early gene *arc* and the major PNN-component *aggrecan* 1-hour after acute seizure. *Arc* expression reflects regions of increased neuronal activity and aggrecan synthesis in activity-dependent [114, 390]. As expected, *arc* mRNA is increased in DG neurons 1-hour post seizure (Fib. 4.5b). Transcripts for *aggrecan* appear increased in DG neurons and weakly attenuated in CA2 (Fig. 4.5b). Although PNNs appear unaltered 18-hours post seizure, the transcript data would suggest that PNNs may be modulated immediately after a single seizure, perhaps on an undetectable protein level. These data give insight into how PNNs may be temporally regulated after a single seizure, versus long-term recurrent seizures exhibited in TLE.

Figure 13- 4.1

Figure 4.1: Spontaneous electrographic seizures were detected *in vivo* in the hippocampus of a Kv1.1-null mouse.

Electrographic seizure activity was detected by LFP recordings from hippocampal area CA3 during a one-hour recording session in a P40 Kv1.1-null male mouse. Three episodes of ictal activity were identified, each lasting 25-30 seconds and followed by non-ictal activity for approximately 15-20 minutes. Traces represent LFP data recorded from a wire-bundle electrode (scale bar indicates time on the x-axis (seconds) and voltage on the y-axis (mV)) (a). Electrographic seizure activity was characterized by large amplitude population spikes, polyspikes and burst activity patterns that reversed in polarity and terminated in post-ictal depression [350]. A period of non-ictal activity during the same recording session is shown for comparison (b).

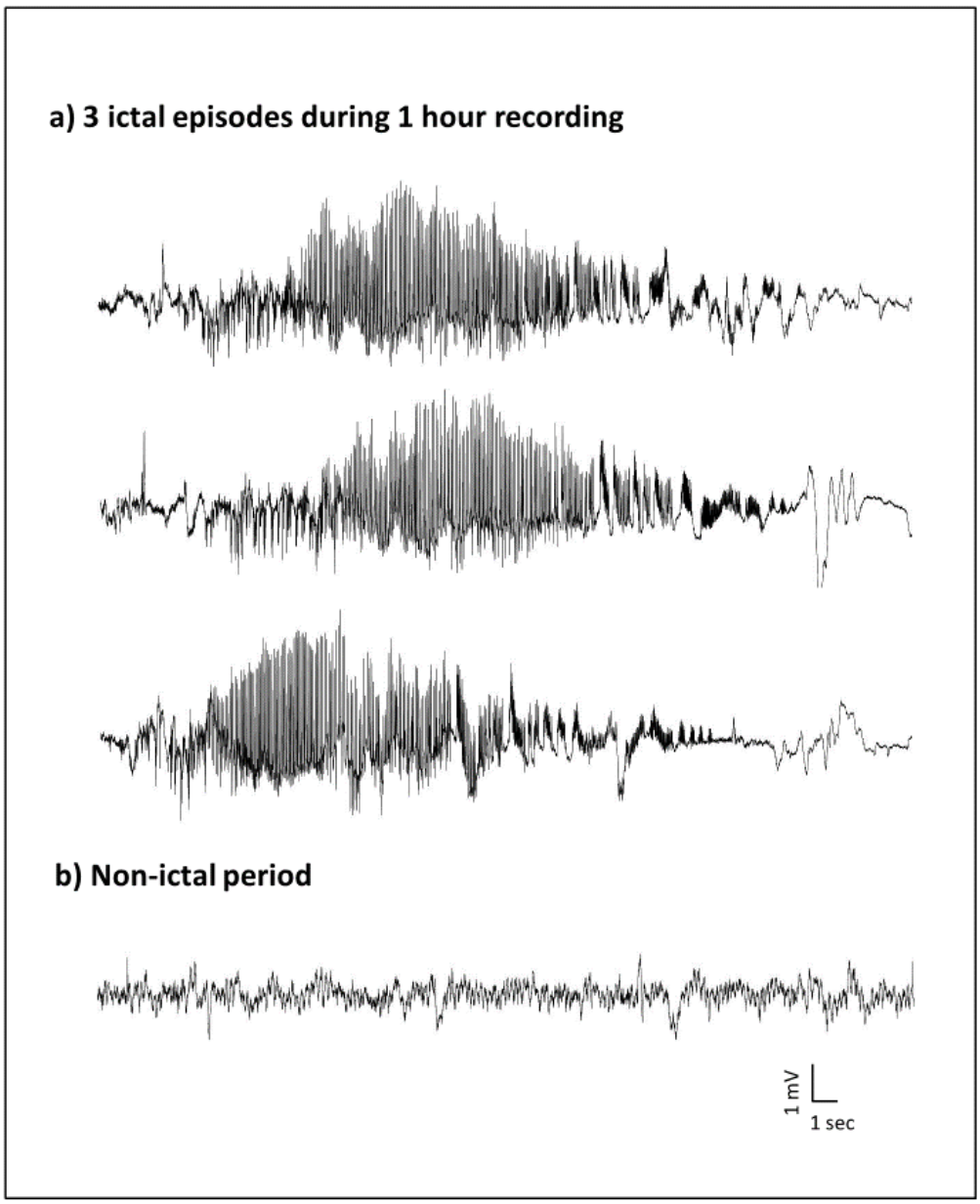
a) 3 ictal episodes during 1 hour recording
b) Non-ictal period
1 mV
1 sec

Figure 14- 4.2

Figure 4.2: PNNs are altered in the hippocampus in a developmental mouse model of TLE, Kv1.1 mouse.

a) Staining for PNN marker WFA (green) is altered in the hippocampus of Kv1.1-null mutant at P60 compared to WT littermates but not at P28. CA2 pyramidal neurons are identified with the CA2-marker PCP4 (red).

b) Normalized WFA fluorescence intensity was decreased at P45-60 in CA2 SP (N=4, 4, 3, and 5 for ages P14, 22, P28 and 45 respectively, per group), compared to WT littermates, *$P < 0.05$, Bonferroni *post hoc* test for pairwise comparison after two-way ANOVA. No significant difference in WFA staining in CA2 SR compared to wildtypes or primary somatosensory cortex ($P > 0.05$). WFA fluorescence intensity was however sinficantly increased at P45-60 in DG compared to WT littermates, ***$P= 0.0002$, Bonferroni *post hoc* test for pairwise comparison after two-way ANOVA. Indicated is the mean ± SEM normalized to P45 WT group.

a)

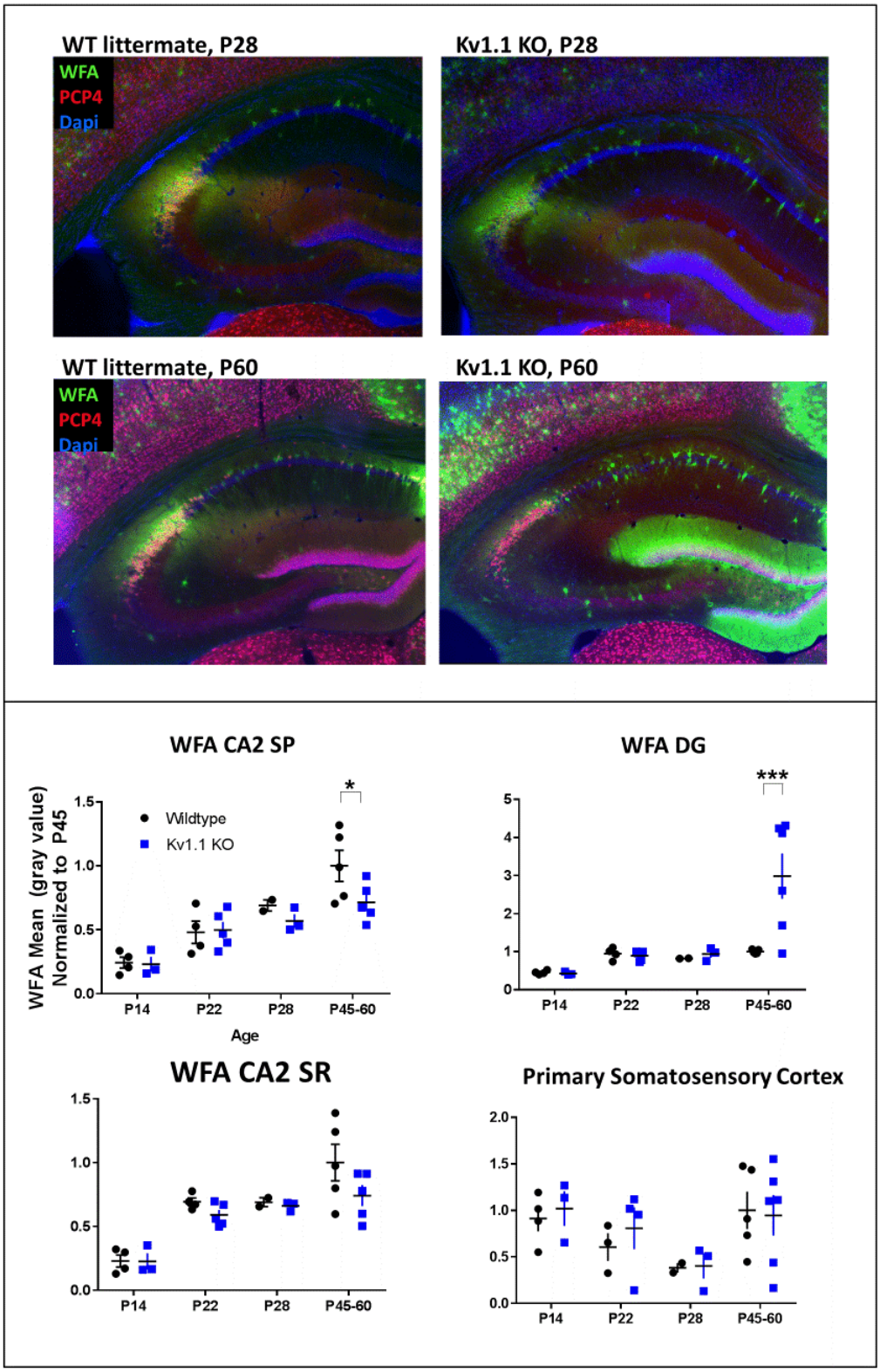
WT littermate, P28
WFA
PCP4
Dapi
Kv1.1 KO, P28
WT littermate, P60
WFA
PCP4
Dapi
Kv1.1 KO, P60
WFA CA2 SP
WFA Mean (gray value) Normalized to P45
Wildtype
Kv1.1 KO
*
P14
P22
P28
P45-60
Age
WFA DG
***
WFA CA2 SR
Primary Somatosensory Cortex

Figure 15- 4.3

Figure 4.3: PNNs in DG in a P56-60 Kv1.1-null are dramatically increased relative to P45 mutant.

WFA intensity in DG analyzed in Fig. 4.1 shows a large spread of WFA staining in the P45-60 group. Upon closer inspection, the P60 Kv1.1-null mice have the strongest increase in WFA staining compared to a still significant increase at P45. ***P= <0.0001, *P= 0.033, Bonferroni *post hoc* test for pairwise comparison after two-way ANOVA. Indicated is the mean ± SEM normalized to P45 WT group.

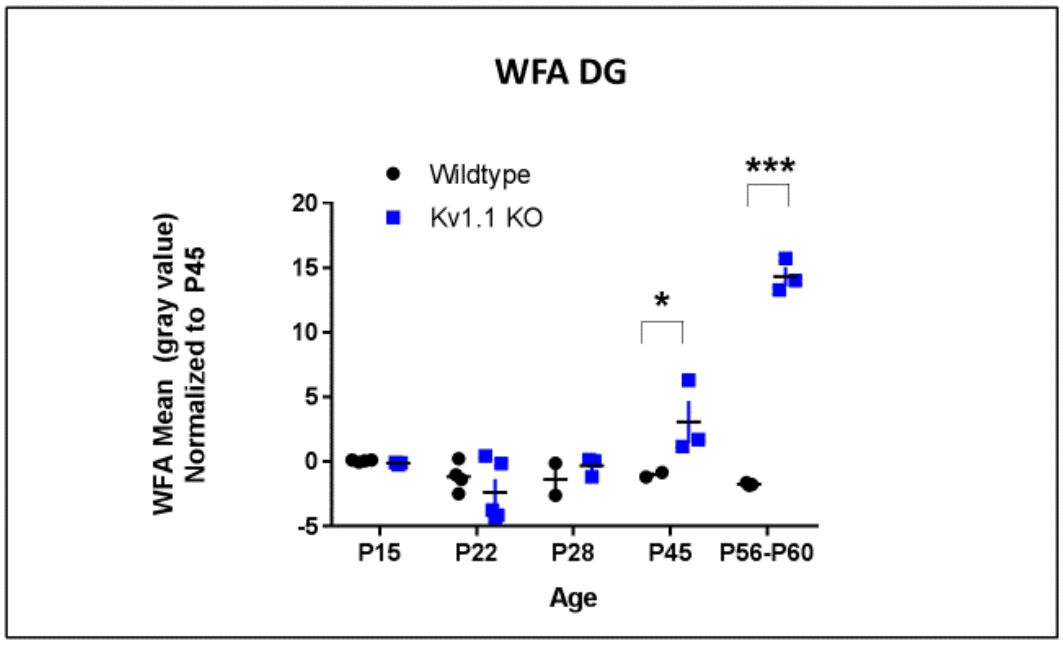

Figure 16- 4.4

Figure 4.4: Molecular indicators of TLE pathology

a) Immunofluorescent staining for the endogenous matrix metalloproteinase, MMP-14 (green), appears increased in CA1 and CA3 SP regions of the Kv1.1-null mouse compared to WT littermate.

b) Staining for mossy fibers with the antibody, anti-ZNT3 (green), reveals mossy fiber sprouting in DG and SR of CA2/ 3 regions. Staining for ZNT3 is increased in area in CA2/ 3 SR region, and in the the hilus. CA2 neurons are labeled with with anit-PCP4 antibody (red).

c) Hippocampal sections of a P60 Kv1.1-null mouse and WT littermate were stained with the 'NeuroSilver' kit to label cell death and degenerating neurons. CA1 neurons in the Kv1.1-null were labeled with silver stain, indicating cell death and degeneration. No neurons were positive for silver stain in the Kv1.1-null or WT.

a) Endogenous Protease: Matrix Metalloproteinase (MMP)

WT littermate, P60

Kv1.1 KO, P60

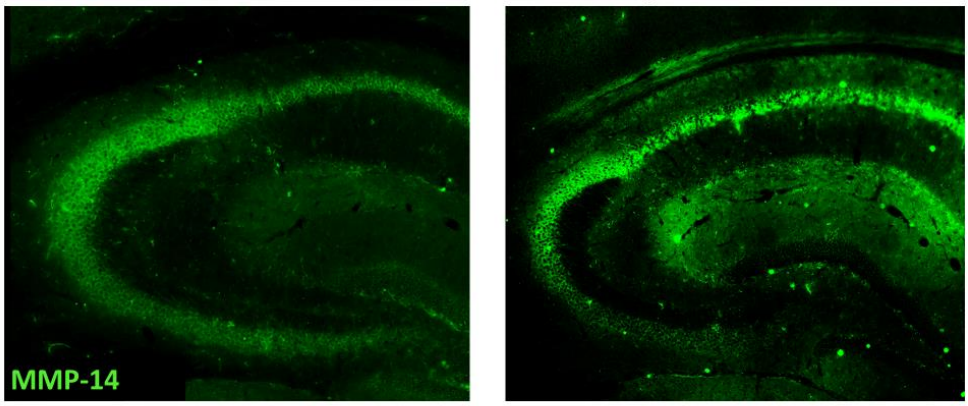

b) Mossy Fiber Sprouting

WT littermate, P60

Kv1.1 KO, P60

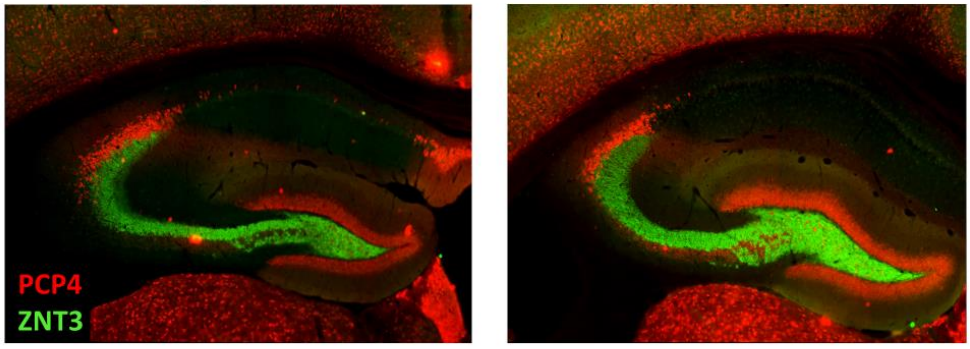

c) Cell Death

WT littermate, P60

Kv1.1 KO, P60

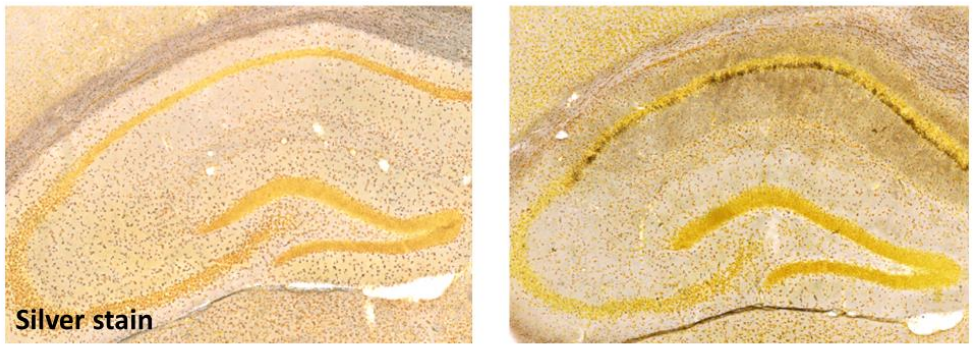

Figure 17- 4.5

Figure 4.5: PNNs appear unaltered in WT hippocampus after an acute MECS-induced seizure

a) PNNs in CA2 are unchanged 18 hours after an acute seizure induced by MECS treatment in an adult WT. WFA staining (green) in CA2 or DG is not observabley different in MECS-treated versus sham control mouse. CA2 neurons are labeled with anit-PCP4 (red).

b) Transcripts for thhe PNN-component aggrecan and the immediate early gene arc were visualized 1 hour after an acute MECS seizure (RNAscope fluorescence *in situ* hybridization). Wildtype controls represent a sham-treated mouse of the same age. Aggrecan mRNA (red) is increased in DG and decreased in CA2 in the seizure mouse compared to sham-treated control. Furthermore, the efficacy of the seizure was validated with an expected robust increase in arc in DG one-hour post status.

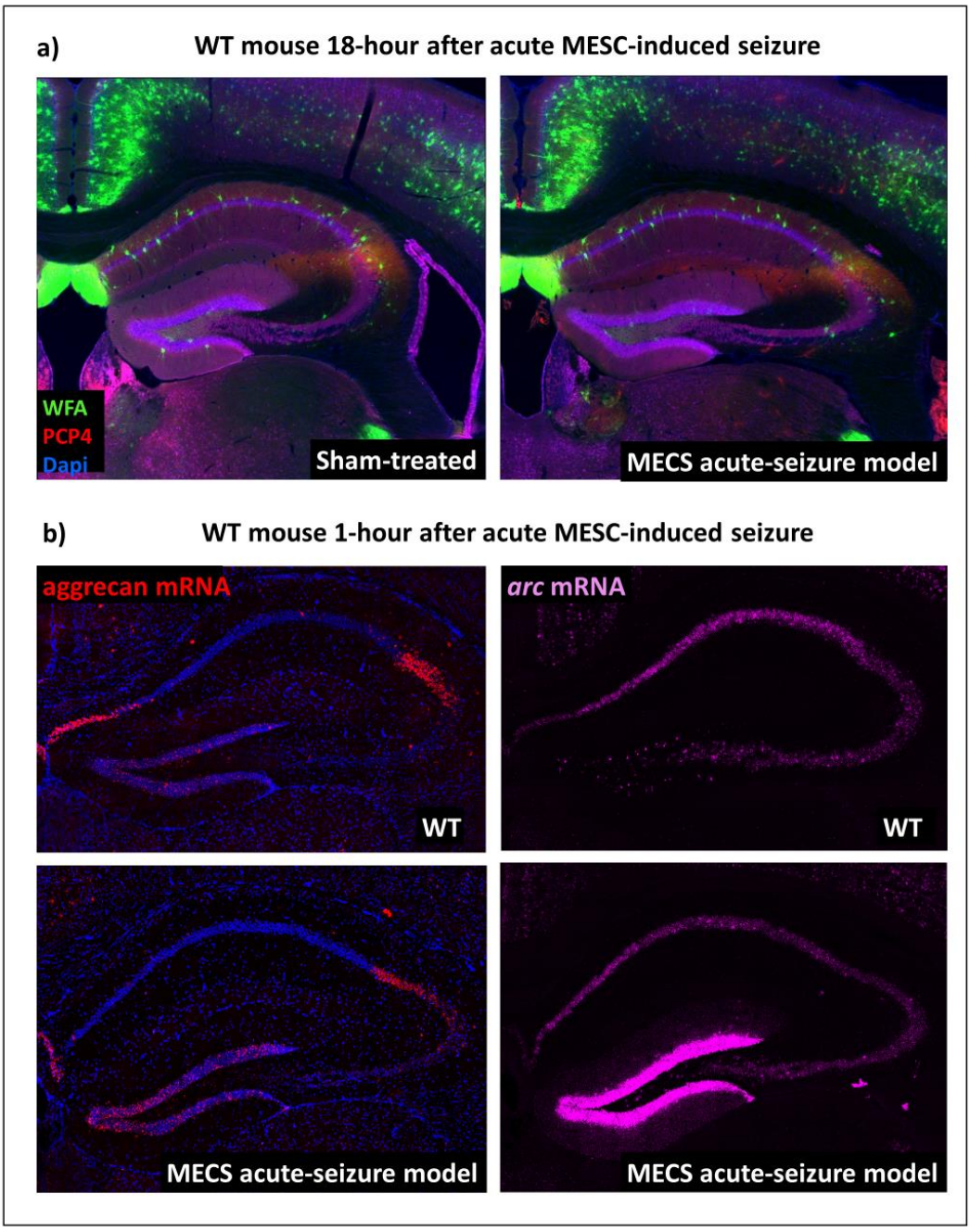
a)
WT mouse 18-hour after acute MESC-induced seizure
WFA
PCP4
Dapi
Sham-treated
MECS acute-seizure model
b)
WT mouse 1-hour after acute MESC-induced seizure
aggrecan mRNA
WT
arc mRNA
WT
MECS acute-seizure model
MECS acute-seizure model

<u>Aim 2:</u> PNN regulation by chemogenetic manipulation of CA2 activity

We previously demonstrated that PNNs are regulated by experience in CA2 during early development [295]. We also found that PNNs are decreased in CA2 but increased in DG in a developmental TLE mouse model (Fig. 4.2b). In this study, we sought to determine whether selectively increasing activity in CA2 over several days is sufficient to change PNNs in CA2. To do so, we used chemogenetics to either increase or decrease CA2 activity for 5 days in an adult mouse. A Cre-dependent AAV expressing either the excitatory Gq- or inhibitory Gi-coupled DREADD was infused into CA2 of mice expressing Cre in CA2, such that DREADDs were selectively express in CA2 neurons (Fig. 4.6a). Cre-negative littermates were also infused with DREADD AAVs. The localized expression of Cre and DREADDs to CA2 was validated previously in our lab with a Cre-dependent reporter mouse and with mCherry-DREADD histology [230]. Importantly, DREADD expression is indeed only expressed in CA2 pyramidal neurons and not in inhibitory neurons; mCherry was not observed in GAD+ neurons.

Mice expressing Gq- and Gi-coupled DREADDs were treated with CNO twice a day for 5 days. Gq/ Gi DREADD activation by CNO has been previously reported to have lasting effects for up to 6-10 hr post administration [230, 373, 374]. I then analyzed regulation of PNNs by quantifying staining intensity of the lectin WFA in the Cre+ Gq and Gi DREADD mice compared to Cre- control animals. I found that PNNs appeared to be increased in CA2 of the Gi DREADD-expressing animals and decreased in the Gq DREADD-expressing animals compared to controls (Fig. 4.6b). Two separate cohorts of mice were tested and data were analyzed and grouped together.

Quantification of WFA florescence intensity revealed that WFA staining intensity was significantly increased in CA2 of Gi DREADD-expressing animals compared to Cre- control

animals (*P= 0.015, one-way ANOVA, multiple comparisons, Tukey post-hoc, Fig. 4.7a). WFA staining in CA2 of Gq Cre^{+} mice showed a downward trend compared to Gq Cre- controls but was not significant by multiple comparisons, (P< 0.0.5, one-way ANOVA, multiple comparisons, Tukey post-hoc, Fig. 4.7a). Direct comparison of Cre+ Gq-DREADD expressing mice with Cre- mice infused with Gq DREADD revealed a significant decrease in WFA intensity among Cre+ mice P=0.0111; two-tailed t-test). Note: when Gq Cre_{+} mice were compared to Gq Cre^{-} controls with an unpaired, two-tailed t-test, Gq DREADD Cre^{+} animals are significantly decreased compared to Cre^{-} controls in CA2 (*P= 0.0111). We also measured WFA expressing in inhibitory neurons in CA1 and CA3. We found that PNN expressing in these neurons was not significantly changed in Gi DREADD or Gq DREADD expressing mice (P > 0.05, one-way ANOVA, Tukey's post hoc test for pairwise comparison, Fig. 4.7b, c). Finally, I quantified WFA staining intensity in the cortical region overlying CA2, primary somatosensory cortex, to assess effects of modifying CA2 activity on an extrahippocampal brain region. Animals expressing Gi DREADD had no change in WFA staining in primary somatosensory cortex compared to Cre^{-} negative controls (P=0.005, one-way ANOVA, multiple comparisons, Tukey post-hoc, Fig. 4.7d). Surprisingly, Gq DREADD mice show a significant increase in WFA staining intensity (*P=0.0012, one-way ANOVA, multiple comparisons, Tukey post-hoc).

Figure 18- 4.6

Figure 4.6: Gq-DREADD AAV was selectively expressed unilaterally in CA2 neurons.

a) Gq-DREADD was infused unilaterally into hippocampus (left side). Immunofluorescent staining of whole brain sections shows mCherry-Gq DREADD only in CA2 neurons; mCherry-Gq DREADD (red) overlaps with the CA2 marker PCP4 (magenta).

b) Images representative of 6 animals showing WFA fluorescence intensity in the hippocampus after 5 days of CNO treatment in Gi and Gq DREADD mice. In total, 8 *Amigo2-icre*ERT2+ mice infused with either Gi or Gq DREADD virus and 12 *Amigo2-icre*ERT2- mice infused. Top row shows WFA fluorescence in green and DREADD expression in red, bottom row shows WFA fluorescence in white to visualize contrast.

a)

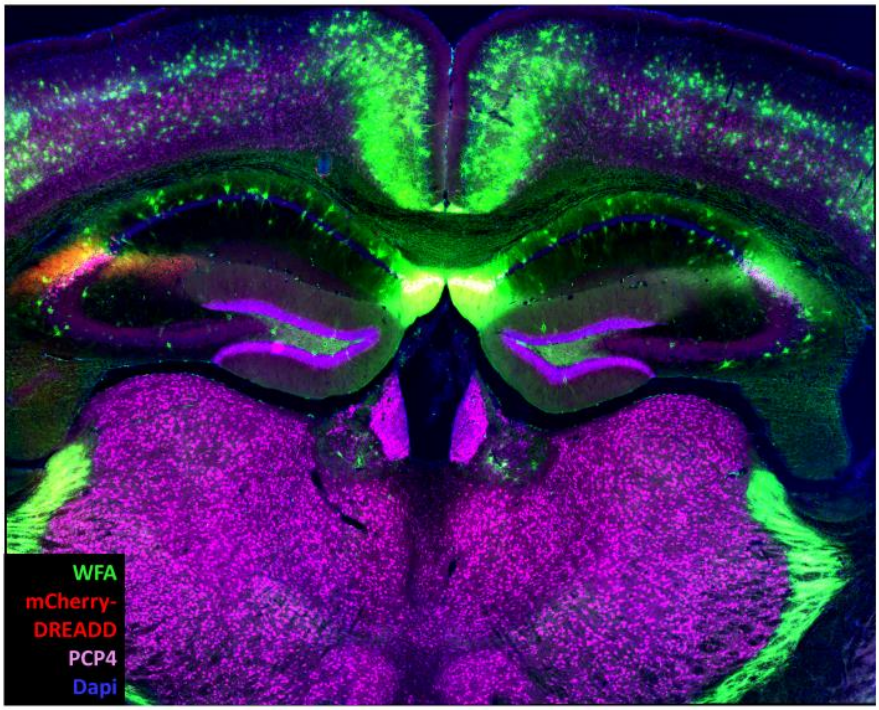

b) WFA staining after 5 days of CNO

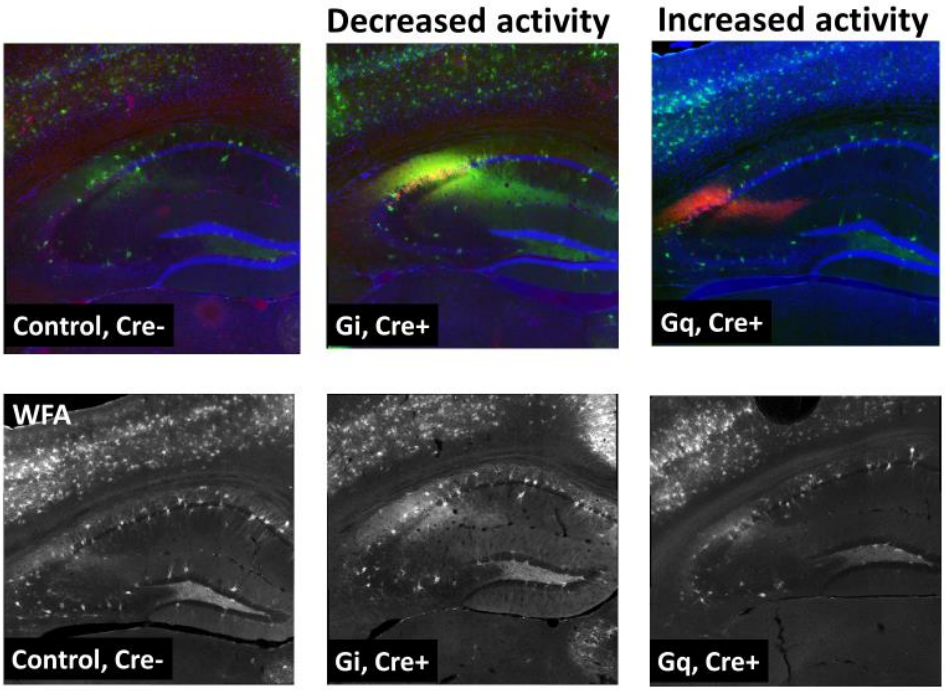

Representative images of 6 adult WT mice

Figure 19- 4.7

Figure 4.7: CA2 neuronal activity negatively regulates PNN staining in adulthood

a) WFA staining in CA2 is increased in neurons expressing Gi DREADD compared to Cre^- Gi control (p= 0.015) and WFA staining in CA2 of neurons expressing Gq DREADD compared to Cre^- Gq control is trending downward (not significant, p> 0.05, Tukey's post hoc test for pairwise comparison). A one-way ANOVA indicated significant main effects of treatment ($F_{(3,17)}$ = 10.19, P=0.0005).

b, c) WFA staining surround PNN+ neurons in CA1(b) and CA3 (c) are unchanged in Cre^+ Gi and Gq DREADD mice compared to Cre^- mice (P>0.05), one-way ANOVA, Tukey's post hoc test for pairwise comparison.

d) WFA staining in overlying primary somatosensory cortex was unchanged in Cre^+ Gi DREADD compared to Cre- Gi (P> 0.05) but increased in Cre^+ Gq compared to Cre^- Gq (*P= 0.0012, one-way ANOVA, Tukey's post hoc test for pairwise comparison). A one-way ANOVA indicated significant main effects of treatment ($F_{(3,17)}$ = 10.24, P=0.0004). Indicated is the mean ± SEM.

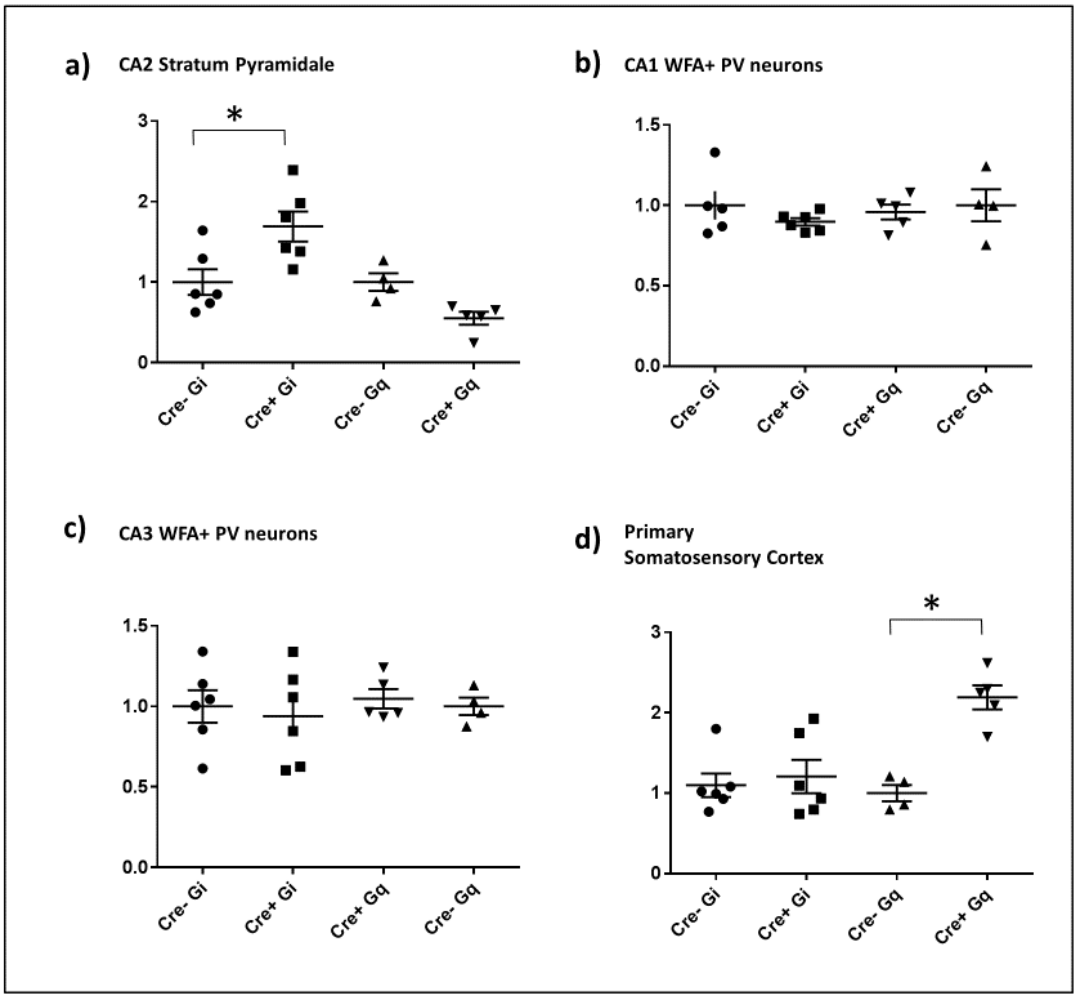
a)
CA2 Stratum Pyramidale
*
3
2
1
0
Cre- Gi
Cre+ Gi
Cre- Gq
Cre+ Gq
b)
CA1 WFA+ PV neurons
1.5
1.0
0.5
0.0
Cre- Gi
Cre+ Gi
Cre+ Gq
Cre- Gq
c)
CA3 WFA+ PV neurons
1.5
1.0
0.5
0.0
Cre- Gi
Cre+ Gi
Cre+ Gq
Cre- Gq
d)
Primary
Somatosensory Cortex
*
3
2
1
0
Cre- Gi
Cre+ Gi
Cre- Gq
Cre+ Gq

<u>Aim3:</u> Selective degradation of PNNs in CA2 *in vivo* with a Cre-dependent AAV; a pilot study

To degrade PNNs selectively in area CA2, ideally only around pyramidal neurons, we generated a Cre-dependent AAV to express the PNN-degrading enzyme ChABC with cell-type specificity. We infused the AAV into hippocampus of CA2 inducible Cre-expressing mice, *Amigo2-iCre*ERT2+ mice (See Aim 2). As a pilot characterization of the expression of ChABC with the AAV-ChABC virus, we tested two different dosing regimens of tamoxifen: 1/day for either 1-day or 3-days. This protocol was based on findings from a previous pilot study in which we administered 7 days of tamoxifen and observed extensive degradation of PNNs in the hippocampus of the contralateral hemisphere (saline-injected side) and ipsilateral extrahippocampal regions (data not shown).

Two weeks after a 1-day treatment with tamoxifen, I observed degradation of PNNs in CA2 of the ChABC-AAV injected (left) hemisphere (Fig. 4.8a). Accordingly, WFA staining was undetectable in the ChABC-AAV injected hippocampus but appeared to be at normal levels in the contralateral saline-injected hemisphere (Fig. 4.8a; see also Fig. 4.8b for another example of PNN degradation in a different mouse treated with 1-day tamoxifen). In comparison, 3 days of tamoxifen treatment resulted in widespread loss of WFA staining in the entire AAV-injected hippocampus, as well as in the saline injected hippocampus (Fig. 4.8c). Similar results were observed in a second mouse treated with tamoxifen for 3 days. I also validated ChABC expression in CA2 neurons using the mCherry reporter that is encoded in the AAV construct. Only CA2 pyramidal neurons (labeled with the CA2 marker PCP4) were fluorescently labeled with mCherry in the hippocampus, indicating successful expression of ChABC in CA2 neurons, as well as CA2 specificity of expression (Fig. 4.8c). However, the effects of the ChABC

expression (i.e. loss of WFA) spread well outside of CA2, indicating a still-too-robust degradation of PNNs. Dosing with a lower concentration of tamoxifen will likely be required to keep the effects of ChABC restricted to CA2.

Finally, I sought to examine an indicator of structural plasticity that may have resulted from sustained degradation of PNNs. I chose to examine mossy fiber sprouting, which reflects granule cell axons in the DG spreading into the inner molecular layer of the DG and is an anatomical pathology that is consistently observed in the hippocampus of postmortem TLE tissue, where granule cell axons in the DG spread into the inner molecular layer of the dentate gyurs [391, 392]. Mossy fiber sprouting has also been linked to ECM components, in that a sustained loss of ECM components has been shown to permit mossy fiber sprouting [362]. Here, I labeled mossy fibers with an anti-ZNT3 antibody and examined the localization of fluorescence in CA2 and CA1. I observed mossy fiber sprouting in the SP layer of CA2 in the ChABC-AAV-injected hemisphere but not in the vehicle-treated hemisphere, 2 weeks post-injection (Fig. 4.9). No obvious mossy fiber sprouting was detected in DG of either hemisphere (Fig. 4.9). Taken together, these data present a novel method to degrade PNNs *in* vivo and suggest that the persistent loss of PNNs in area CA2 permits structural plasticity, including mossy fiber sprouting.

Figure 20- 4.8

Figure 4.8: ChABC is selectively expressed in CA2 neurons and degrades hippocampal PNNs. a) PNNs labeled with the lectin, WFA (green), are undectable in area CA2 and in adjacent CA1 and CA3 subregions. CA2 neurons are labeled with PCP4 antibody (magenta) and ChABC-expressing neurons are labeled with the mCherry reporter encoded in the ChABC-AAV (red). The mCherry labeling of CA2 neurons is also shown in (c). Arrows indicate the site of injection of the ChABC-AAV in the left hemisphere and saline vehicle in the right hemisphere.

b, c) Mice received either 1 day (b) or 3 days (c) of tamoxifen treatment to compare the efficacy of PNN degradation in area CA2. Both 1- and 3-day treatments of tamoxifen was suffient to degrade PNNs in CA2; staining for WFA was undetectable in CA2. However, the radius of undetectable WFA staining from the site of injection was larger following 3 days of tamoxifen treatment than following 1 day of treatment. Three days of tamoxifen treatment resulted in loss of WFA staining from both the ChABC-AAV-injected hemisphere and the vehicle-injected hemiphere. Lastly, staing for CA2 pyramidal neurons, laebled with PCP4 (green), were positive for the mCherry reporter (red), validating that CA2 pyramidal neurons selectively express ChABC (c).

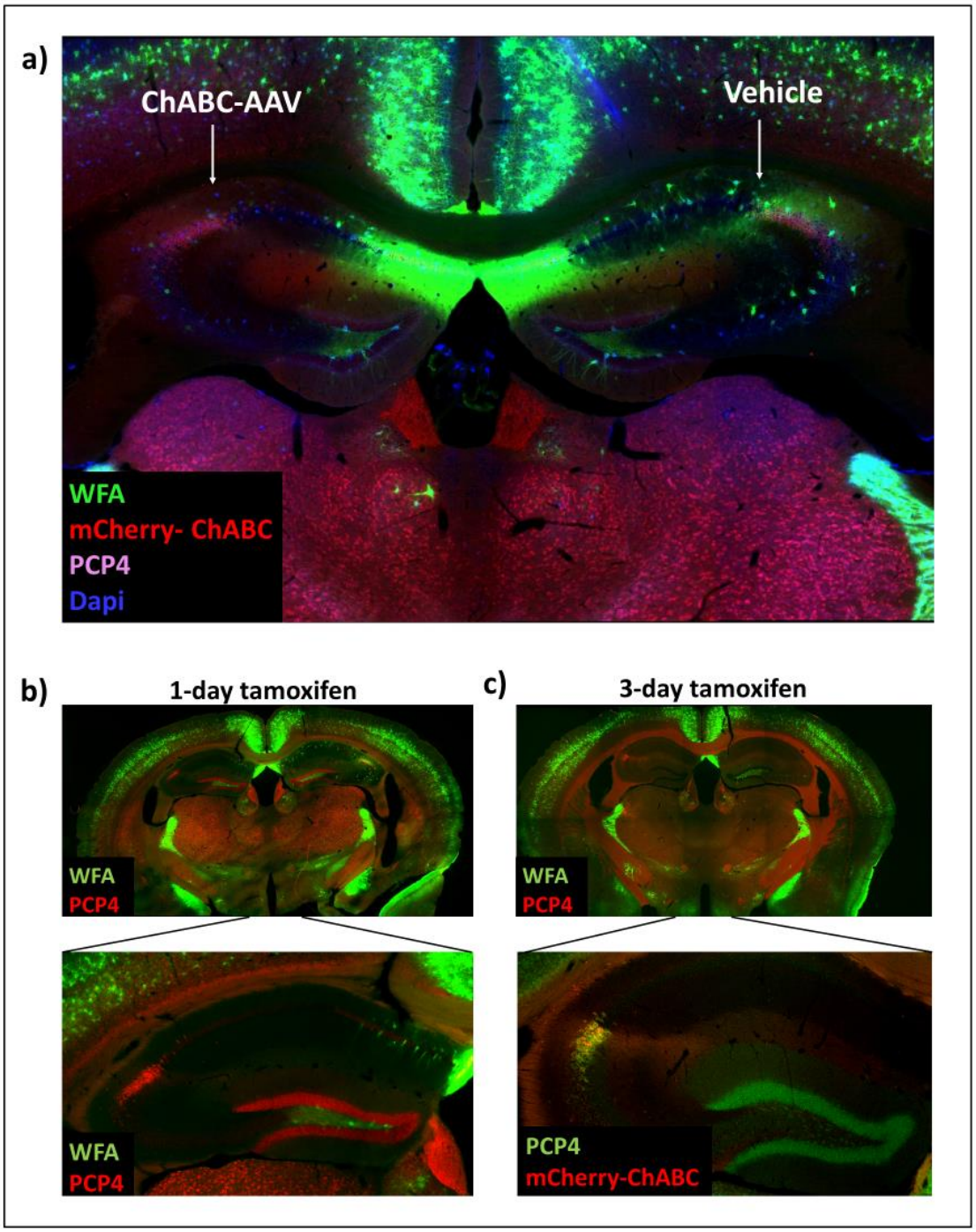
a)
ChABC-AAV
Vehicle
WFA
mCherry- ChABC
PCP4
Dapi
b)
1-day tamoxifen
WFA
PCP4
WFA
PCP4
c)
3-day tamoxifen
WFA
PCP4
PCP4
mCherry-ChABC

Figure 21- 4.9

Figure 4.9: ChABC-AAV injection *in vivo* results in mossy fiber sprouting into CA2 stratum pyramidale.

Staining for mossy fibers with an anti-ZNT3 antibody (green) labels a larger area two weeks after ChABC-injection compared to vehicle-treated hemisphere (1-day tamoxifen treatment). Specifically, ZNT3 staining is evident in CA2 SP in the ChABC-AAV injected hemisphere (arrows) but faint in the vehicle-treated CA2. CA2 cell soma and dentrites are labeled with anit-RGS14 antibody (red) to indicate CA2/ CA3 border.

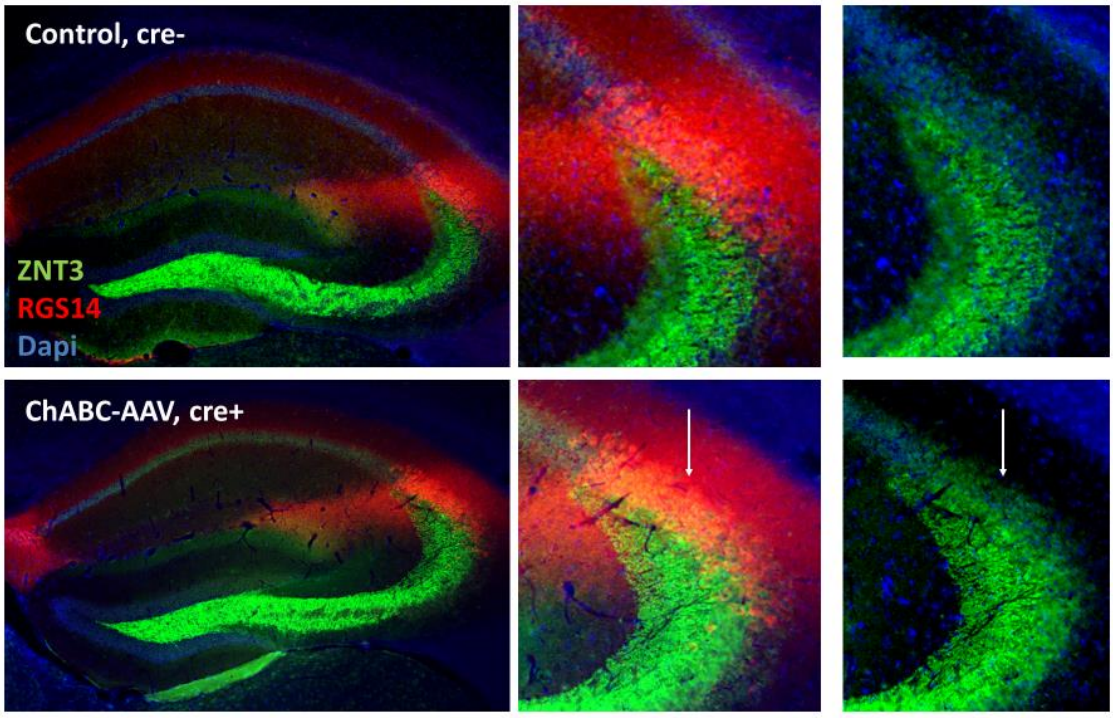

Discussion

Temporal lobe epilepsy (TLE), the most common and refractory form of epilepsy, is characterized by the onset of focal seizures typically early in life, arising mainly from the hippocampus and persisting into adulthood [349, 393]. Recurrent seizures are known to cause massive synaptic reorganization in select regions of hippocampus however little is known about the mechanism behind these changes. Recent studies suggest that these synaptic changes are modulated by the extracellular matrix [355, 357, 394, 395]. CA2 neurons are uniquely resistant to seizure-induced cell death in the hippocampus and have a dense concentration of PNNs [193, 295, 363, 396]. I found that PNNs are reduced in CA2 after prolonged recurrent seizures in our TLE mouse model. Moreover, I found that PNNs are attenuated in CA2 in response to 5 days of elevated CA2 neuronal activity (chemogenetic) and unaffected in other brain regions. Lastly, I generated a Cre-dependent AAV to deliver the PNN-degrading enzyme, chondroitinase (ChABC), selectively to CA2 neurons and found that the AAV-ChABC was sufficient to degrade PNNs in CA2. I also observed mossy fiber sprouting in area CA2 after PNN-degradation by both the AAV-ChABC and in the TLE mouse model. Taken together, these data suggest that decreased PNNs in response to elevated CA2 neuronal activity may cause an aberrant 'opening' of plasticity in the normally plasticity-resistant CA2 region.

CA2 neurons have been long appreciated for their resistance to seizure-induced cell death. Studies of post-mortem hippocampal sclerosis in TLE patients consistently report severe neuronal cell loss in areas CA1 and CA3, with CA2 being relatively unaffected [194, 396]. In a rat model of TLE, electron micrographs confirm that seizure activity damages CA1 and CA3 pyramidal cells but not CA2 [367]. CA2 neurons have many unique cellular properties that likely play a role in their resistance to excitotoxic damage. For example, calcium buffering and

extrusion are both quite robust in CA2 neurons in rodents [209]. In addition, staining for phosphorylated (i.e. active) ERK in response to seizure is substantially lower in CA2 than in neighboring areas of the hippocampus [196]. Interestingly, PNNs are thought to be neuroprotective [397], and may therefore function as an additional mechanism by which CA2 neurons are protected from seizure-induced damage. I examined cell death in CA2 of the Kv1.1-null mouse at P60 and, as expected, observe indication of cell death in CA1, but not CA2. I also examined cell death in hippocampi infused with the CA2-specific AAV-ChABC and observed apparently normal cell survival in CA2 two weeks after infusion of the ChABC-AAV (data not shown). These data suggest that both a partial and complete loss of PNNs in CA2 are not sufficient to cause CA2 cell death and therefore are not consistent with the theory that PNNs are neuroprotective. In future experiments, I propose to examine PNNs several months after the ChABC-AAV viral infusion to determine whether long-term loss of PNNs may induce CA2 cell death. This experiment however would not rule out possible effects of activity changes on CA2 cell survival, considering ChABC-induced PNN degradation in the hippocampus *in vivo* was found to alter hippocampal network activity [175]. Overall, our findings suggest that PNNs are not functioning to protect CA2 neurons from cell death.

PNNs are reportedly reduced in the hippocampus of adult TLE postmortem tissue and in adult rodent seizure models [294, 354, 355 356]. One mechanism to explain the seizure-induced degradation of PNNs is the dramatic increases in endogenous proteases. Enzymes such as matrix metalloproteinases (MMPs) function to post-translationally modify PNNs throughout the brain and are critical for normal development and remodeling of synapses [333]. Moreover, MMPs are activity-regulated in that increased neuronal activity elevates MMP expression, in response to both pathological activity and learning, [157, 158 165, 361, 362]. We found that MMP-14 appears to be

elevated in areas CA1 and CA2 in a P60 Kv1.1-null mouse (N of 1), consistent with other seizure models [361]. However, MMP-14 protein was not uniquely elevated in CA2 and elevated levels around CA1 pyramidal cell somas would suggest that MMP levels are not necessarily correlated with PNN+ neurons. To confirm PNNs are not selectively elevated in CA2, in future experiments I propose to characterize transcripts for *Mmp-9* (the MMP most strongly-implicated in seizure and plasticity[361, 398]) in CA2 of the Kv1.1-null mouse using *in situ* hybridization techniques described in Chapter 2. I would also stain for both the protein and enzymatic activity of active MMP-9 using gelatin-substrate zymography techniques. If MMP-9 levels are indeed not different in CA2, *MMP-9* mRNA localization experiments would still be informative in terms of understanding cell-autonomous regulation of PNNs by MMPs in CA2. Taken together, these data suggest that MMPs may be at least one mechanism by which seizure-induced PNN degradation is regulated in CA2.

An important outstanding question in the field is whether changes in the ECM are a cause or an effect of epileptogenesis. One group found that MMP-9 levels (both protein and enzymatic activity) are strongly increased after seizure, suggesting that PNNs are likely degraded, and MMP-9 deficient mice are less susceptible to epileptogenesis (pentylenetetrazole (PTZ) model of TLE) [361]. If PNNs are indeed increased in the MMP-9 deficient mouse (as expected by the loss of MMP-9), one could speculate that increased PNNs could also correlate with decreased vulnerability to seizure. Indeed, a group recently found that degradation of PNNs with ChABC *in vivo* elevated seizure susceptibility (increased myoclonic seizures in response to PTZ administration) [356]. Moreover, a PNN component knockout mouse, hyaluronan synthase 3, display epileptiform activity in the hippocampus and are more prone to seizure [399]. Although a direct relationship between seizure susceptibility and PNN loss has yet to be identified, these

data provide compelling evidence to further study the role of PNNs in epileptogenesis. In future experiments, I propose to use the Cre-dependent AAV-ChABC to determine whether degrading PNNs in CA2 of the Kv1.1-null mutant, or in a healthy mouse, may increase vulnerability to seizure. Moreover, a critical question surrounding TLE is whether traumatic early-life brain injury is correlated epileptogenesis later in life [349]. To address this, I would conduct a developmental study to determine whether degrading PNNs in early development (using the ChABC-AAV) may increase vulnerability to seizure in adulthood. Taken together, these data suggest that PNNs may play a role both the cause and effect of epilepsy and future developmental studies are needed to determine the exact timing and degree to which aberrant PNNs may be involved in epileptogenesis.

I also compared the Kv1.1-null TLE mouse model to an acute seizure model. One hour after a single MECS-induced seizure, *aggrecan* mRNA is increased in DG but appears decreased in CA2. ECS depolarizes nearly 100% of hippocampal pyramidal cells therefore it is a reliable method to study how activity may affect gene and protein expression [382 {Cole, 1990 #731, 400]. Interestingly, I found that PNNs are not altered in CA2 18 hours after this same seizure protocol. In a recent study, a decrease in aggrecan protein expression around PNN+ PV neurons in the hippocampus was reported 48 hours to 2 months following a single seizure [243, 294]. Interestingly, they also found that the reduction in aggrecan protein precedes a decrease in *aggrecan* mRNA in the hippocampus (whole hippocampal lysates), such that they found no change in *aggrecan* mRNA 48 hours or one week after seizure but a significant decrease in *aggrecan* mRNA 2 months later [114]. These data are not consistent with our finding that *aggrecan* mRNA is altered immediately after seizure however this difference is likely attributable to ‘wash out’ effects from whole hippocampal lysate analysis.

Although seizure onset is around P21 in the Kv1.1-null mouse, we did not observe altered PNNs (compared to wildtype) in CA2/ DG until P45. One possible factor is the degree to which activity is pathologically altered at these different ages. Kv1.1-null seizures progress in severity with age therefore epileptiform activity during the third postnatal week may be insufficient to alter PNNs. Moreover, dramatic increases in excitability by the sixth week of life appear to be sufficient to alter ECM. Our *in vivo* recordings indeed validate that these mice have classic spontaneous electrographic seizures at P40. We observed three ictal episodes over one hour that each lasted approximately 25-30 seconds, indicating that the Kv1.1-null mouse likely has spontaneous recurrent seizures every 15-20 minutes at P40. Note: A previous Kv1.1-null characterization study reported that ictal EEG patters in the cerebral cortex were observed in the absence of apparent seizure behavior [368]. In future experiments, recordings of hippocampal activity in the developing brain before seizure-onset would provide valuable insight into whether pathological activity in TLE may precede seizure initiation. Using methods outlined in Aim 1 of this chapter, I propose to measure LFPs in P14-21 hippocampi to identify possible aberrant activity. Because we found that PNNs are unchanged after the onset of seizure (P21) in the Kv1.1-null mouse, I conclude that either the degree of pathological activity is insufficient to alter PNNs or alternatively, that PNNs are differently regulated by pathological activity in early development, as was previously discussed (Chapter 3).

As an alternative approach, electrophysiological manipulation of activity in acute hippocampal slices could provide valuable insight into the development and mechanism of pathological activity in Kv1.1-null mice. CA3 pyramidal neurons in the Kv1.1-null mouse were previously reported to produce a late burst discharge in response to mossy fiber stimulation [368]. Intrinsic cellular properties, such as resting membrane potential, input resistance, and action

potential amplitude, were unchanged [368]. The generation of epileptiform activity, or ictogenesis, has been proposed to arise from aberrant synchronous activity in CA3, subsequently spreading to other subregions, causing over-synchronous activity of hippocampal pyramidal cell networks [401, 402 403]. In future experiments, I propose to study CA2 intrinsic and synaptic properties in the Kv1.1-null mouse over development to determine whether CA2 neurons may only be abnormal at P45 when PNNs are attenuated.

To better understand whether loss of CA2 PNNs in a TLE mouse model is an effect of global changes in hippocampal activity, or is rather a cell-autonomous effect, we directly manipulated CA2 activity. We show that PNNs are altered in area CA2 in both hM3Dq/ hM4Di-expressing mice after 5 days of twice daily CNO treatment, but that PNNs in CA1 are unaltered, suggesting that targeted manipulation of PNNs in CA2 is sufficient to inversely regulate PNNs in CA2. In future experiments, I propose to test how the age, duration and degree of activity changes in CA2 affect PNN expression in the brain. For example, the duration of changes in CA2 activity can be tested by treating mice with CNO for different lengths of time. Moreover, DREADD-induced voltage changes are CNO dose dependent [230, 374], therefore the degree of activity, although subtle, could be manipulated by altering the dose of CNO. Overall, these future experiments would provide insight into how age, duration and degree of activity changes may differently regulate PNNs and, ultimately, may reveal whether aberrant PNNs are a causative mechanism underlying neurodevelopmental disorders such as TLE.

CHAPTER V – CONCLUSION

Summary of Conclusions:

- PNN in area CA2 function as at least one negative regulator of plasticity in hippocampal CA2 neurons (P14-18 mice).
- LTP is inducible at CA2 SR synapses at an age prior to PNN maturation (P8-11 mice), identifying a novel window of plasticity in CA2.
- In a mouse model of Rett syndrome, PNNs are aberrantly increased and develop prematurely in CA2 during postnatal development.
- LTP is prematurely restricted in CA2 of a Rett mouse model and degradation of PNNs in acute hippocampal slices reinstates LTP in Rett CA2 neurons (P8-11 mice).
- Pathological and chemogenetic increases in CA2 neuronal activity appears to downregulate PNN expression in adult CA2.
- CA2-targeted degradation of PNNs *in vivo* permits structural plasticity in area CA2.

Future Directions:

I describe a function for PNNs in restricting plasticity in a population of excitatory pyramidal neurons. Moreover, I discovered a novel window of early plasticity at CA2 SR synapses in P8-11 mice, an age before PNNs are detectable in CA2. Because PNN degradation with the enzyme ChABC reinstates LTP in CA2 at P8-11, I postulate that the maturation of PNNs functions to, at least in part, close an unknown window of plasticity in CA2. These data are consistent with

previous studies that identify PNNs as a molecular brake on several other windows of plasticity in the brain [113, 114, 116]. The exact behavioral function of area CA2 is not clear, however recent studies find a role for CA2 in social memory and behavior [205, 224, 227-230]. Moreover, a critical window of learning in the hippocampus has yet to be identified, however one specific form of hippocampal-dependent memory that is developmentally regulated is contextual fear learning [73, 233-237]. Fear learning is clinically relevant because childhood trauma has detrimental effects on adult mental health [23]. Understanding the molecular mechanism underlying this potential hippocampal critical period, such as PNNs in CA2, could potentially unveil a therapeutic window of intervention. Moreover, based on findings in this study, developmental regulation of PNNs in area CA2 may represent a therapeutic target for neurodevelopmental disorders, such as TLE and Rett syndrome [264, 265, 349, 350].

A recent focus in the ECM field has been on PNN sulfation patterns, which appear to shift during postnatal development. CSPGs are known to be a class of molecules that are both inhibitory or permissive, depending on their biochemical properties [132, 404].The ratio of carbon 4-sulfated (4S) to 6-sulfated (6S) CSPGs increases in development [405], such that 4S is more prevalent in the PNN matrix in adult rodents while 6S is more strongly expressed in early development. One study found that the transgenic overexpression of 6S in adulthood (decreasing the 4S/ 6S ratio) extended the window of ocular dominance plasticity [405], implicating 6S as an important component of critical period plasticity in the visual cortex. In the future, I propose to characterize the 4S/ 6S ratio in area CA2 to validate a possible window of plasticity. I would predict the 4S/ 6S ratio is low at P8-11 but high by P14-18 in mouse, tracking the closing plasticity in CA2. I would also propose to examine how this ratio may be altered in neurodevelopmental disorders such as Rett syndrome.

As another area of study, I propose to determine whether PNNs in CA2 are distinctly associated with excitatory or inhibitory terminals in CA2 SR. PNNs are enriched along the membrane of CA2 neuron cell bodies and perisynaptically around dendritic spines according to electron micrograph data presented in this study. Interestingly, one study found the PNN marker, WFA, frequently localizes with inhibitory neuron terminal staining, Kv3.1b (voltage-gated potassium channel subunit), in cortical layer V [406]. Using similar methods, I propose to determine whether the PNN-associated terminals along CA2 soma and proximal dendrites are similarly inhibitory, or alternatively excitatory. To determine whether synaptic terminals in CA2 SR are inhibitory or excitatory, I propose to use EM and double-labeling of the PNN marker WFA using the antibody against Kv3.1b and the antibody against VGLUT1 (a vesicular glutamate transporter marking *excitatory terminals*). I would use peroxidase methods and silver-intensified streptavidin-gold particles (demonstrated in Chapter 2) such that I can distinguish the pattern of WFA-immunogold particles from KV 3.1b or VGLUT1 staining in adult CA2. Unlike cortical layer V, I predict that PNNs will be associated with excitatory terminals based on my findings that suggests PNNs function to regulate excitatory plasticity in CA2.

Degrading PNNs with ChABC is a reliable therapeutic approach in spinal cord injury, allowing axon regeneration at the site of injury [378]. However, whether PNNs degradation could serve as a viable therapeutic target in the brain is unclear. Several studies found a correlation between cell survival and PNN+ neurons in a normal brain and in Alzheimer's disease [141, 258]. My data would suggest that PNNs are not playing a neuroprotective role in area CA2 in both a normal mouse brain and in a TLE mouse model. The modulation of PNNs is complicated; they are both overexpressed and 'under-expressed' in several neurological diseases other than Rett syndrome and TLE, eg. schizophrenia, bipolar, prion disease, and

Creutzfeldt-Jakob disease [265, 327, 407]. It is unclear whether alterations in PNNs precedes or follows the onset of disease; however, my findings (PNNs are not altered in the TLE mouse model until two weeks after seizure-onset) would make a case for the latter. In the case of the Rett model mouse, my data show that PNNs are aberrant prior to the onset of symptomology such as behavioral seizures [269 270]. One hypothesis to explain these discrepancies is that the role of PNNs in CA2 is multi-functional, in that their presence is neuroprotective but their degradation may also be critical in recovery from injury.

Overall, the findings presented in this thesis demonstrate a critical role for PNNs in restricting LTP at CA2 synapses. We also identify an undefined window of plasticity in area CA2. The behavioral function of this critical period is unclear. Because CA2 appears to regulate social memory [205, 224, 227-230], this early critical window of plasticity in postnatal may be critical for early social learning. Social deficits are prevalent in many neurodevelopmental disorders, such as in Rett syndrome, where girls display a loss of social interaction and communication [408]. Mouse models of Rett also display sociability impairments [409]. Area CA2 may serve as an integral region for studying mechanisms behind social learning deficits during early development in the Rett brain. Overall, the experience-dependent development of PNNs in CA2 is highly suggestive of an unknown critical period of plasticity in the hippocampus and may ultimately reveal a mechanism behind the severe hippocampal-dependent learning impairments that emerge in many neurodevelopmental disorders such as TLE and Rett syndrome infants [393 269].

REFERENCES

1. Hensch, T.K. Critical period regulation. *Annu Rev Neurosci* **27**, 549-79 (2004).

2. Horii-Hayashi, N., Sasagawa, T., Matsunaga, W. & Nishi, M. Development and Structural Variety of the Chondroitin Sulfate Proteoglycans-Contained Extracellular Matrix in the Mouse Brain. *Neural Plast* **2015**, 256389 (2015).

3. Bruckner, G. et al. Perineuronal nets provide a polyanionic, glia-associated form of microenvironment around certain neurons in many parts of the rat brain. *Glia* **8**, 183-200 (1993).

4. Pyka, M. et al. Chondroitin sulfate proteoglycans regulate astrocyte-dependent synaptogenesis and modulate synaptic activity in primary embryonic hippocampal neurons. *Eur J Neurosci* **33**, 2187-202 (2011).

5. Hebb, D.O. The Organization of Behavior (ed. Wiley) (New York, 1949).

6. Bliss, T.V. & Lomo, T. Long-lasting potentiation of synaptic transmission in the dentate area of the anaesthetized rabbit following stimulation of the perforant path. *J Physiol* **232**, 331-56 (1973).

7. Bliss, T.V. & Gardner-Medwin, A.R. Long-lasting potentiation of synaptic transmission in the dentate area of the unanaestetized rabbit following stimulation of the perforant path. *J Physiol* **232**, 357-74 (1973).

8. Katz, L.C. & Shatz, C.J. Synaptic activity and the construction of cortical circuits. *Science* **274**, 1133-8 (1996).

9. Martin, S.J., Grimwood, P.D. & Morris, R.G. Synaptic plasticity and memory: an evaluation of the hypothesis. *Annu Rev Neurosci* **23**, 649-711 (2000).

10. Kirkwood, A., Lee, H.K. & Bear, M.F. Co-regulation of long-term potentiation and experience-dependent synaptic plasticity in visual cortex by age and experience. *Nature* **375**, 328-31 (1995).

11. Komatsu, Y., Fujii, K., Maeda, J., Sakaguchi, H. & Toyama, K. Long-term potentiation of synaptic transmission in kitten visual cortex. *J Neurophysiol* **59**, 124-41 (1988).

12. Perkins, A.T.t. & Teyler, T.J. A critical period for long-term potentiation in the developing rat visual cortex. *Brain Res* **439**, 222-9 (1988).

13. Kato, N., Artola, A. & Singer, W. Developmental changes in the susceptibility to long-term potentiation of neurones in rat visual cortex slices. *Brain Res Dev Brain Res* **60**, 43-50 (1991).

14. Crair, M.C. & Malenka, R.C. A critical period for long-term potentiation at thalamocortical synapses. *Nature* **375**, 325-8 (1995).

15. Dudek, S.M. & Bear, M.F. Bidirectional long-term modification of synaptic effectiveness in the adult and immature hippocampus. *J Neurosci* **13**, 2910-8 (1993).

16. Dudek, S.M. & Friedlander, M.J. Developmental down-regulation of LTD in cortical layer IV and its independence of modulation by inhibition. *Neuron* **16**, 1097-106 (1996).

17. Blundon, J.A. & Zakharenko, S.S. Presynaptic gating of postsynaptic synaptic plasticity: a plasticity filter in the adult auditory cortex. *Neuroscientist* **19**, 465-78 (2013).

18. Jaynes, J. Imprinting: the interaction of learned and innate behavior. II. The critical period. *J Comp Physiol Psychol* **50**, 6-10 (1957).

19. Hubel, D.H. & Wiesel, T.N. The period of susceptibility to the physiological effects of unilateral eye closure in kittens. *J Physiol* **206**, 419-36 (1970).

20. Lorenz, K. The companion in the bird's world (Auk, 1937).

21. Bateson, P. Sexual imprinting and optimal outbreeding. *Nature* **273**, 659-60 (1978).

22. Bornstein, M.H. Sensitive periods in development: structural characteristics and causal interpretations. *Psychol Bull* **105**, 179-97 (1989).

23. De Bellis, M.D. & Zisk, A. The biological effects of childhood trauma. *Child Adolesc Psychiatr Clin N Am* **23**, 185-222, vii (2014).

24. Harrison, E.L. & Baune, B.T. Modulation of early stress-induced neurobiological changes: a review of behavioural and pharmacological interventions in animal models. *Transl Psychiatry* **4**, e390 (2014).

25. Wiesel, T.N. & Hubel, D.H. SINGLE-CELL RESPONSES IN STRIATE CORTEX OF KITTENS DEPRIVED OF VISION IN ONE EYE. *J Neurophysiol* **26**, 1003-17 (1963).

26. Romens, S.E., McDonald, J., Svaren, J. & Pollak, S.D. Associations between early life stress and gene methylation in children. *Child Dev* **86**, 303-9 (2015).

27. Sperry, R. Optic nerve regeneration with return of vision in anurans. *Journal of Neurophysiology*, 57-69 (1944).

28. Pettigrew, J.D. The effect of visual experience on the development of stimulus specificity by kitten cortical neurones. *J Physiol* **237**, 49-74 (1974).

29. Wiesel, T.N. & Hubel, D.H. Comparison of the effects of unilateral and bilateral eye closure on cortical unit responses in kittens. *J Neurophysiol* **28**, 1029-40 (1965).

30. Fagiolini, M. et al. Separable features of visual cortical plasticity revealed by N-methyl-D-aspartate receptor 2A signaling. *Proc Natl Acad Sci U S A* **100**, 2854-9 (2003).

31. Lewis, T.L. & Maurer, D. Multiple sensitive periods in human visual development: evidence from visually deprived children. *Dev Psychobiol* **46**, 163-83 (2005).

32. Bienenstock, E.L., Cooper, L.N. & Munro, P.W. Theory for the development of neuron selectivity: orientation specificity and binocular interaction in visual cortex. *J Neurosci* **2**, 32-48 (1982).

33. Shatz, C.J. & Stryker, M.P. Ocular dominance in layer IV of the cat's visual cortex and the effects of monocular deprivation. *J Physiol* **281**, 267-83 (1978).

34. Frenkel, M.Y. & Bear, M.F. How monocular deprivation shifts ocular dominance in visual cortex of young mice. *Neuron* **44**, 917-23 (2004).

35. Kirkwood, A., Rioult, M.C. & Bear, M.F. Experience-dependent modification of synaptic plasticity in visual cortex. *Nature* **381**, 526-8 (1996).

36. Smith, G.B., Heynen, A.J. & Bear, M.F. Bidirectional synaptic mechanisms of ocular dominance plasticity in visual cortex. *Philos Trans R Soc Lond B Biol Sci* **364**, 357-67 (2009).

37. Gordon, J.A. & Stryker, M.P. Experience-dependent plasticity of binocular responses in the primary visual cortex of the mouse. *J Neurosci* **16**, 3274-86 (1996).

38. Philpot, B.D., Espinosa, J.S. & Bear, M.F. Evidence for altered NMDA receptor function as a basis for metaplasticity in visual cortex. *J Neurosci* **23**, 5583-8 (2003).

39. Philpot, B.D., Cho, K.K. & Bear, M.F. Obligatory role of NR2A for metaplasticity in visual cortex. *Neuron* **53**, 495-502 (2007).

40. LeVay, S., Wiesel, T.N. & Hubel, D.H. The development of ocular dominance columns in normal and visually deprived monkeys. *J Comp Neurol* **191**, 1-51 (1980).

41. Mioche, L. & Singer, W. Chronic recordings from single sites of kitten striate cortex during experience-dependent modifications of receptive-field properties. *J Neurophysiol* **62**, 185-97 (1989).

42. Doshi, N.R. & Rodriguez, M.L. Amblyopia. *Am Fam Physician* **75**, 361-7 (2007).

43. Trachtenberg, J.T. & Stryker, M.P. Rapid anatomical plasticity of horizontal connections in the developing visual cortex. *J Neurosci* **21**, 3476-82 (2001).

44. Antonini, A. & Stryker, M.P. Rapid remodeling of axonal arbors in the visual cortex. *Science* **260**, 1819-21 (1993).

45. Bear, M.F. & Colman, H. Binocular competition in the control of geniculate cell size depends upon visual cortical N-methyl-D-aspartate receptor activation. *Proc Natl Acad Sci U S A* **87**, 9246-9 (1990).

46. Mataga, N., Mizuguchi, Y. & Hensch, T.K. Experience-dependent pruning of dendritic spines in visual cortex by tissue plasminogen activator. *Neuron* **44**, 1031-41 (2004).

47. Oray, S., Majewska, A. & Sur, M. Dendritic spine dynamics are regulated by monocular deprivation and extracellular matrix degradation. *Neuron* **44**, 1021-30 (2004).

48. Antonini, A., Fagiolini, M. & Stryker, M.P. Anatomical correlates of functional plasticity in mouse visual cortex. *J Neurosci* **19**, 4388-406 (1999).

49. Alvarez, V.A. & Sabatini, B.L. Anatomical and physiological plasticity of dendritic spines. *Annu Rev Neurosci* **30**, 79-97 (2007).

50. Djurisic, M. et al. PirB regulates a structural substrate for cortical plasticity. *Proc Natl Acad Sci U S A* **110**, 20771-6 (2013).

51. Kelly, E.A., Russo, A.S., Jackson, C.D., Lamantia, C.E. & Majewska, A.K. Proteolytic regulation of synaptic plasticity in the mouse primary visual cortex: analysis of matrix metalloproteinase 9 deficient mice. *Front Cell Neurosci* **9**, 369 (2015).

52. Vidal, G.S. & Djurisic, M. Cell-Autonomous Regulation of Dendritic Spine Density by PirB. **3** (2016).

53. Grutzendler, J., Kasthuri, N. & Gan, W.B. Long-term dendritic spine stability in the adult cortex. *Nature* **420**, 812-6 (2002).

54. Philpot, B.D., Sekhar, A.K., Shouval, H.Z. & Bear, M.F. Visual experience and deprivation bidirectionally modify the composition and function of NMDA receptors in visual cortex. *Neuron* **29**, 157-69 (2001).

55. Quinlan, E.M., Olstein, D.H. & Bear, M.F. Bidirectional, experience-dependent regulation of N-methyl-D-aspartate receptor subunit composition in the rat visual cortex during postnatal development. *Proc Natl Acad Sci U S A* **96**, 12876-80 (1999).

56. Carmignoto, G. & Vicini, S. Activity-dependent decrease in NMDA receptor responses during development of the visual cortex. *Science* **258**, 1007-11 (1992).

57. Malinow, R., Mainen, Z.F. & Hayashi, Y. LTP mechanisms: from silence to four-lane traffic. *Curr Opin Neurobiol* **10**, 352-7 (2000).

58. Shi, S., Hayashi, Y., Esteban, J.A. & Malinow, R. Subunit-specific rules governing AMPA receptor trafficking to synapses in hippocampal pyramidal neurons. *Cell* **105**, 331-43 (2001).

59. Takahashi, T., Svoboda, K. & Malinow, R. Experience strengthening transmission by driving AMPA receptors into synapses. *Science* **299**, 1585-8 (2003).

60. Rumpel, S., LeDoux, J., Zador, A. & Malinow, R. Postsynaptic receptor trafficking underlying a form of associative learning. *Science* **308**, 83-8 (2005).

61. Turrigiano, G.G., Leslie, K.R., Desai, N.S., Rutherford, L.C. & Nelson, S.B. Activity-dependent scaling of quantal amplitude in neocortical neurons. *Nature* **391**, 892-6 (1998).

62. Mataga, N., Nagai, N. & Hensch, T.K. Permissive proteolytic activity for visual cortical plasticity. *Proc Natl Acad Sci U S A* **99**, 7717-21 (2002).

63. Maffei, A., Nelson, S.B. & Turrigiano, G.G. Selective reconfiguration of layer 4 visual cortical circuitry by visual deprivation. *Nat Neurosci* **7**, 1353-9 (2004).

64. Maffei, A., Nataraj, K., Nelson, S.B. & Turrigiano, G.G. Potentiation of cortical inhibition by visual deprivation. *Nature* **443**, 81-4 (2006).

65. Morishita, H., Miwa, J.M., Heintz, N. & Hensch, T.K. Lynx1, a cholinergic brake, limits plasticity in adult visual cortex. *Science* **330**, 1238-40 (2010).

66. Beurdeley, M. et al. Otx2 binding to perineuronal nets persistently regulates plasticity in the mature visual cortex. *J Neurosci* **32**, 9429-37 (2012).

67. Dityatev, A., Schachner, M. & Sonderegger, P. The dual role of the extracellular matrix in synaptic plasticity and homeostasis. *Nat Rev Neurosci* **11**, 735-46 (2010).

68. Greenberg, M.E., Xu, B., Lu, B. & Hempstead, B.L. New insights in the biology of BDNF synthesis and release: implications in CNS function. *J Neurosci* **29**, 12764-7 (2009).

69. Dudek, S.M., Bowen, W.D. & Bear, M.F. Postnatal changes in glutamate stimulated phosphoinositide turnover in rat neocortical synaptoneurosomes. *Brain Res Dev Brain Res* **47**, 123-8 (1989).

70. Dudek, S.M. & Bear, M.F. A biochemical correlate of the critical period for synaptic modification in the visual cortex. *Science* **246**, 673-5 (1989).

71. Kirkwood, A., Dudek, S.M., Gold, J.T., Aizenman, C.D. & Bear, M.F. Common forms of synaptic plasticity in the hippocampus and neocortex in vitro. *Science* **260**, 1518-21 (1993).

72. Turrigiano, G.G. & Nelson, S.B. Homeostatic plasticity in the developing nervous system. *Nat Rev Neurosci* **5**, 97-107 (2004).

73. Raineki, C. et al. Functional emergence of the hippocampus in context fear learning in infant rats. *Hippocampus* **20**, 1037-46 (2010).

74. Rudy, J.W. & Morledge, P. Ontogeny of contextual fear conditioning in rats: implications for consolidation, infantile amnesia, and hippocampal system function. *Behav Neurosci* **108**, 227-34 (1994).

75. Esmoris-Arranz, F.J., Mendez, C. & Spear, N.E. Contextual fear conditioning differs for infant, adolescent, and adult rats. *Behav Processes* **78**, 340-50 (2008).

76. Bayer, S.A. Development of the hippocampal region in the rat. II. Morphogenesis during embryonic and early postnatal life. *J Comp Neurol* **190**, 115-34 (1980).

77. Johnson, M.H. Functional brain development in humans. *Nat Rev Neurosci* **2**, 475-83 (2001).

78. Bekenstein, J.W. & Lothman, E.W. An in vivo study of the ontogeny of long-term potentiation (LTP) in the CA1 region and in the dentate gyrus of the rat hippocampal formation. *Brain Res Dev Brain Res* **63**, 245-51 (1991).

79. Harris, K.M. & Teyler, T.J. Developmental onset of long-term potentiation in area CA1 of the rat hippocampus. *J Physiol* **346**, 27-48 (1984).

80. Wilson, D.A. A comparison of the postnatal development of post-activation potentiation in the neocortex and dentate gyrus of the rat. *Brain Res* **318**, 61-8 (1984).

81. Kudryashov, I.E. & Kudryashova, I.V. Ontogeny of synaptic transmission in the rat hippocampus. *Brain Res* **892**, 263-8 (2001).

82. Michelson, H.B. & Lothman, E.W. An in vivo electrophysiological study of the ontogeny of excitatory and inhibitory processes in the rat hippocampus. *Brain Res Dev Brain Res* **47**, 113-22 (1989).

83. Swann, J.W., Smith, K.L. & Brady, R.J. Neural networks and synaptic transmission in immature hippocampus. *Adv Exp Med Biol* **268**, 161-71 (1990).

84. Muller, D., Oliver, M. & Lynch, G. Developmental changes in synaptic properties in hippocampus of neonatal rats. *Brain Res Dev Brain Res* **49**, 105-14 (1989).

85. DiScenna, P.G. & Teyler, T.J. Development of inhibitory and excitatory synaptic transmission in the rat dentate gyrus. *Hippocampus* **4**, 569-76 (1994).

86. Liao, D., Hessler, N.A. & Malinow, R. Activation of postsynaptically silent synapses during pairing-induced LTP in CA1 region of hippocampal slice. *Nature* **375**, 400-4 (1995).

87. Yasuda, H., Barth, A.L., Stellwagen, D. & Malenka, R.C. A developmental switch in the signaling cascades for LTP induction. *Nat Neurosci* **6**, 15-6 (2003).

88. Lisman, J., Schulman, H. & Cline, H. The molecular basis of CaMKII function in synaptic and behavioural memory. *Nat Rev Neurosci* **3**, 175-90 (2002).

89. Smith, G.B. & Bear, M.F. Bidirectional ocular dominance plasticity of inhibitory networks: recent advances and unresolved questions. *Front Cell Neurosci* **4**, 21 (2010).

90. Nicoll, R.A. Expression mechanisms underlying long-term potentiation: a postsynaptic view. *Philos Trans R Soc Lond B Biol Sci* **358**, 721-6 (2003).

91. Busetto, G., Higley, M.J. & Sabatini, B.L. Developmental presence and disappearance of postsynaptically silent synapses on dendritic spines of rat layer 2/3 pyramidal neurons. *J Physiol* **586**, 1519-27 (2008).

92. Abrahamsson, T., Gustafsson, B. & Hanse, E. AMPA silencing is a prerequisite for developmental long-term potentiation in the hippocampal CA1 region. *J Neurophysiol* **100**, 2605-14 (2008).

93. Isaac, J.T., Nicoll, R.A. & Malenka, R.C. Evidence for silent synapses: implications for the expression of LTP. *Neuron* **15**, 427-34 (1995).

94. Malinow, R. & Malenka, R.C. AMPA receptor trafficking and synaptic plasticity. *Annu Rev Neurosci* **25**, 103-26 (2002).

95. Hanse, E. & Gustafsson, B. Quantal variability at glutamatergic synapses in area CA1 of the rat neonatal hippocampus. *J Physiol* **531**, 467-80 (2001).

96. Elias, G.M. et al. Synapse-specific and developmentally regulated targeting of AMPA receptors by a family of MAGUK scaffolding proteins. *Neuron* **52**, 307-20 (2006).

97. Kolleker, A. et al. Glutamatergic plasticity by synaptic delivery of GluR-B(long)-containing AMPA receptors. *Neuron* **40**, 1199-212 (2003).

98. Flint, A.C., Maisch, U.S., Weishaupt, J.H., Kriegstein, A.R. & Monyer, H. NR2A subunit expression shortens NMDA receptor synaptic currents in developing neocortex. *J Neurosci* **17**, 2469-76 (1997).

99. Nase, G., Weishaupt, J., Stern, P., Singer, W. & Monyer, H. Genetic and epigenetic regulation of NMDA receptor expression in the rat visual cortex. *Eur J Neurosci* **11**, 4320-6 (1999).

100. Hayashi, Y. et al. Driving AMPA receptors into synapses by LTP and CaMKII: requirement for GluR1 and PDZ domain interaction. *Science* **287**, 2262-7 (2000).

101. Esteban, J.A. et al. PKA phosphorylation of AMPA receptor subunits controls synaptic trafficking underlying plasticity. *Nat Neurosci* **6**, 136-43 (2003).

102. Yuste, R. & Katz, L.C. Control of postsynaptic Ca2+ influx in developing neocortex by excitatory and inhibitory neurotransmitters. *Neuron* **6**, 333-44 (1991).

103. Cherubini, E., Rovira, C., Gaiarsa, J.L., Corradetti, R. & Ben Ari, Y. GABA mediated excitation in immature rat CA3 hippocampal neurons. *Int J Dev Neurosci* **8**, 481-90 (1990).

104. Ganguly, K., Schinder, A.F., Wong, S.T. & Poo, M. GABA itself promotes the developmental switch of neuronal GABAergic responses from excitation to inhibition. *Cell* **105**, 521-32 (2001).

105. Cherubini, E., Gaiarsa, J.L. & Ben-Ari, Y. GABA: an excitatory transmitter in early postnatal life. *Trends Neurosci* **14**, 515-9 (1991).

106. Rivera, C. et al. The K+/Cl- co-transporter KCC2 renders GABA hyperpolarizing during neuronal maturation. *Nature* **397**, 251-5 (1999).

107. Dityatev, A. & Rusakov, D.A. Molecular signals of plasticity at the tetrapartite synapse. *Curr Opin Neurobiol* **21**, 353-9 (2011).

108. Celio, M.R. Perineuronal nets of extracellular matrix around parvalbumin-containing neurons of the hippocampus. *Hippocampus* **3 Spec No**, 55-60 (1993).

109. Costa, C. et al. Mapping of aggrecan, hyaluronic acid, heparan sulphate proteoglycans and aquaporin 4 in the central nervous system of the mouse. *J Chem Neuroanat* **33**, 111-23 (2007).

110. Yamamoto, M., Marshall, P., Hemmendinger, L.M., Boyer, A.B. & Caviness, V.S., Jr. Distribution of glucuronic acid-and-sulfate-containing glycoproteins in the central nervous system of the adult mouse. *Neurosci Res* **5**, 273-98 (1988).

111. Drake, C.T., Mulligan, K.A., Wimpey, T.L., Hendrickson, A. & Chavkin, C. Characterization of Vicia villosa agglutinin-labeled GABAergic interneurons in the hippocampal formation and in acutely dissociated hippocampus. *Brain Res* **554**, 176-85 (1991).

112. Bruckner, G., Grosche, J., Hartlage-Rubsamen, M., Schmidt, S. & Schachner, M. Region and lamina-specific distribution of extracellular matrix proteoglycans, hyaluronan and tenascin-R in the mouse hippocampal formation. *J Chem Neuroanat* **26**, 37-50 (2003).

113. Lander, C., Kind, P., Maleski, M. & Hockfield, S. A family of activity-dependent neuronal cell-surface chondroitin sulfate proteoglycans in cat visual cortex. *J Neurosci* **17**, 1928-39 (1997).

114. McRae, P.A., Rocco, M.M., Kelly, G., Brumberg, J.C. & Matthews, R.T. Sensory deprivation alters aggrecan and perineuronal net expression in the mouse barrel cortex. *J Neurosci* **27**, 5405-13 (2007).

115. Bruckner, G. et al. Postnatal development of perineuronal nets in wild-type mice and in a mutant deficient in tenascin-R. *J Comp Neurol* **428**, 616-29 (2000).

116. Kalb, R.G. & Hockfield, S. Molecular evidence for early activity-dependent development of hamster motor neurons. *J Neurosci* **8**, 2350-60 (1988).

117. Guimaraes, A., Zaremba, S. & Hockfield, S. Molecular and morphological changes in the cat lateral geniculate nucleus and visual cortex induced by visual deprivation are revealed by monoclonal antibodies Cat-304 and Cat-301. *J Neurosci* **10**, 3014-24 (1990).

118. Kind, P.C., Beaver, C.J. & Mitchell, D.E. Effects of early periods of monocular deprivation and reverse lid suture on the development of Cat-301 immunoreactivity in the dorsal lateral geniculate nucleus (dLGN) of the cat. *J Comp Neurol* **359**, 523-36 (1995).

119. Novak, U. & Kaye, A.H. Extracellular matrix and the brain: components and function. *J Clin Neurosci* **7**, 280-90 (2000).

120. Nicholson, C. & Sykova, E. Extracellular space structure revealed by diffusion analysis. *Trends Neurosci* **21**, 207-15 (1998).

121. Golgi, C. Intorno alla struttura delle cellule nervose. *Med-chir Pavia*, 1-14 (1898).

122. Neame, P.J. & Barry, F.P. The link proteins. *Exs* **70**, 53-72 (1994).

123. Binette, F., Cravens, J., Kahoussi, B., Haudenschild, D.R. & Goetinck, P.F. Link protein is ubiquitously expressed in non-cartilaginous tissues where it enhances and stabilizes the interaction of proteoglycans with hyaluronic acid. *J Biol Chem* **269**, 19116-22 (1994).

124. Watanabe, E., Fujita, S.C., Murakami, F., Hayashi, M. & Matsumura, M. A monoclonal antibody identifies a novel epitope surrounding a subpopulation of the mammalian central neurons. *Neuroscience* **29**, 645-57 (1989).

125. Galtrey, C.M. & Fawcett, J.W. The role of chondroitin sulfate proteoglycans in regeneration and plasticity in the central nervous system. *Brain Res Rev* **54**, 1-18 (2007).

126. Yamaguchi, Y. Lecticans: organizers of the brain extracellular matrix. *Cell Mol Life Sci* **57**, 276-89 (2000).

127. Kwok, J.C., Carulli, D. & Fawcett, J.W. In vitro modeling of perineuronal nets: hyaluronan synthase and link protein are necessary for their formation and integrity. *J Neurochem* **114**, 1447-59 (2010).

128. Asher, R.A. et al. Neurocan is upregulated in injured brain and in cytokine-treated astrocytes. *J Neurosci* **20**, 2427-38 (2000).

129. Moon, L.D. & Fawcett, J.W. Reduction in CNS scar formation without concomitant increase in axon regeneration following treatment of adult rat brain with a combination of antibodies to TGFbeta1 and beta2. *Eur J Neurosci* **14**, 1667-77 (2001).

130. Lin, R., Rosahl, T.W., Whiting, P.J., Fawcett, J.W. & Kwok, J.C. 6-Sulphated chondroitins have a positive influence on axonal regeneration. *PLoS One* **6**, e21499 (2011).

131. Milev, P. et al. Differential regulation of expression of hyaluronan-binding proteoglycans in developing brain: aggrecan, versican, neurocan, and brevican. *Biochem Biophys Res Commun* **247**, 207-12 (1998).

132. Rauch, U. Extracellular matrix components associated with remodeling processes in brain. *Cell Mol Life Sci* **61**, 2031-45 (2004).

133. Bandtlow, C.E. & Zimmermann, D.R. Proteoglycans in the developing brain: new conceptual insights for old proteins. *Physiol Rev* **80**, 1267-90 (2000).

134. Pizzorusso, T. et al. Reactivation of ocular dominance plasticity in the adult visual cortex. *Science* **298**, 1248-51 (2002).

135. Dityatev, A. & Schachner, M. Extracellular matrix molecules and synaptic plasticity. *Nat Rev Neurosci* **4**, 456-68 (2003).

136. Evers, M.R. et al. Impairment of L-type Ca2+ channel-dependent forms of hippocampal synaptic plasticity in mice deficient in the extracellular matrix glycoprotein tenascin-C. *J Neurosci* **22**, 7177-94 (2002).

137. Bukalo, O., Schachner, M. & Dityatev, A. Modification of extracellular matrix by enzymatic removal of chondroitin sulfate and by lack of tenascin-R differentially affects several forms of synaptic plasticity in the hippocampus. *Neuroscience* **104**, 359-69 (2001).

138. Geissler, M. et al. Primary hippocampal neurons, which lack four crucial extracellular matrix molecules, display abnormalities of synaptic structure and function and severe deficits in perineuronal net formation. *J Neurosci* **33**, 7742-55 (2013).

139. Klueva, J., Gundelfinger, E.D., Frischknecht, R.R. & Heine, M. Intracellular Ca(2)(+) and not the extracellular matrix determines surface dynamics of AMPA-type glutamate receptors on aspiny neurons. *Philos Trans R Soc Lond B Biol Sci* **369**, 20130605 (2014).

140. Frischknecht, R. et al. Brain extracellular matrix affects AMPA receptor lateral mobility and short-term synaptic plasticity. *Nat Neurosci* **12**, 897-904 (2009).

141. Morawski, M. et al. Ion exchanger in the brain: Quantitative analysis of perineuronally fixed anionic binding sites suggests diffusion barriers with ion sorting properties. *Sci Rep* **5**, 16471 (2015).

142. Hrabetova, S., Masri, D., Tao, L., Xiao, F. & Nicholson, C. Calcium diffusion enhanced after cleavage of negatively charged components of brain extracellular matrix by chondroitinase ABC. *J Physiol* **587**, 4029-49 (2009).

143. Schuster, T. et al. Immunoelectron microscopic localization of the neural recognition molecules L1, NCAM, and its isoform NCAM180, the NCAM-associated polysialic acid, beta1 integrin and the extracellular matrix molecule tenascin-R in synapses of the adult rat hippocampus. *J Neurobiol* **49**, 142-58 (2001).

144. Bernard-Trifilo, J.A. et al. Integrin signaling cascades are operational in adult hippocampal synapses and modulate NMDA receptor physiology. *J Neurochem* **93**, 834-49 (2005).

145. Huang, Z. et al. Distinct roles of the beta 1-class integrins at the developing and the mature hippocampal excitatory synapse. *J Neurosci* **26**, 11208-19 (2006).

146. Brown, E.J. Integrin-associated proteins. *Curr Opin Cell Biol* **14**, 603-7 (2002).

147. Huber, K.M., Mauk, M.D. & Kelly, P.T. Distinct LTP induction mechanisms: contribution of NMDA receptors and voltage-dependent calcium channels. *J Neurophysiol* **73**, 270-9 (1995).

148. Dityatev, A. et al. Activity-dependent formation and functions of chondroitin sulfate-rich extracellular matrix of perineuronal nets. *Dev Neurobiol* **67**, 570-88 (2007).

149. Kochlamazashvili, G. et al. The extracellular matrix molecule hyaluronic acid regulates hippocampal synaptic plasticity by modulating postsynaptic L-type Ca(2+) channels. *Neuron* **67**, 116-28 (2010).

150. Lundell, A. et al. Structural basis for interactions between tenascins and lectican C-type lectin domains: evidence for a crosslinking role for tenascins. *Structure* **12**, 1495-506 (2004).

151. Briata, P., Ilengo, C., Bobola, N. & Corte, G. Binding properties of the human homeodomain protein OTX2 to a DNA target sequence. *FEBS Lett* **445**, 160-4 (1999).

152. Sugiyama, S. et al. Experience-dependent transfer of Otx2 homeoprotein into the visual cortex activates postnatal plasticity. *Cell* **134**, 508-20 (2008).

153. Vo, T. et al. The chemorepulsive axon guidance protein semaphorin3A is a constituent of perineuronal nets in the adult rodent brain. *Mol Cell Neurosci* **56**, 186-200 (2013).

154. Goretzki, L., Burg, M.A., Grako, K.A. & Stallcup, W.B. High-affinity binding of basic fibroblast growth factor and platelet-derived growth factor-AA to the core protein of the NG2 proteoglycan. *J Biol Chem* **274**, 16831-7 (1999).

155. Shen, Y. et al. PTPsigma is a receptor for chondroitin sulfate proteoglycan, an inhibitor of neural regeneration. *Science* **326**, 592-6 (2009).

156. Shiosaka, S. & Yoshida, S. Synaptic microenvironments--structural plasticity, adhesion molecules, proteases and their inhibitors. *Neurosci Res* **37**, 85-9 (2000).

157. Meighan, S.E. et al. Effects of extracellular matrix-degrading proteases matrix metalloproteinases 3 and 9 on spatial learning and synaptic plasticity. *J Neurochem* **96**, 1227-41 (2006).

158. Szklarczyk, A., Lapinska, J., Rylski, M., McKay, R.D. & Kaczmarek, L. Matrix metalloproteinase-9 undergoes expression and activation during dendritic remodeling in adult hippocampus. *J Neurosci* **22**, 920-30 (2002).

159. Nagy, V. et al. Matrix metalloproteinase-9 is required for hippocampal late-phase long-term potentiation and memory. *J Neurosci* **26**, 1923-34 (2006).

160. Michaluk, P. et al. Matrix metalloproteinase-9 controls NMDA receptor surface diffusion through integrin beta1 signaling. *J Neurosci* **29**, 6007-12 (2009).

161. Nagy, V., Bozdagi, O. & Huntley, G.W. The extracellular protease matrix metalloproteinase-9 is activated by inhibitory avoidance learning and required for long-term memory. *Learn Mem* **14**, 655-64 (2007).

162. Yoshiyama, Y., Asahina, M. & Hattori, T. Selective distribution of matrix metalloproteinase-3 (MMP-3) in Alzheimer's disease brain. *Acta Neuropathol* **99**, 91-5 (2000).

163. Nagel, S. et al. Focal cerebral ischemia induces changes in both MMP-13 and aggrecan around individual neurons. *Brain Res* **1056**, 43-50 (2005).

164. Sole, S., Petegnief, V., Gorina, R., Chamorro, A. & Planas, A.M. Activation of matrix metalloproteinase-3 and agrin cleavage in cerebral ischemia/reperfusion. *J Neuropathol Exp Neurol* **63**, 338-49 (2004).

165. Yuan, W., Matthews, R.T., Sandy, J.D. & Gottschall, P.E. Association between protease-specific proteolytic cleavage of brevican and synaptic loss in the dentate gyrus of kainate-treated rats. *Neuroscience* **114**, 1091-101 (2002).

166. Murase, S. & Lantz, C.L. Light reintroduction after dark exposure reactivates plasticity in adults via perisynaptic activation of MMP-9. **6** (2017).

167. Duffy, K.R. & Mitchell, D.E. Darkness alters maturation of visual cortex and promotes fast recovery from monocular deprivation. *Curr Biol* **23**, 382-6 (2013).

168. Brakebusch, C. et al. Brevican-deficient mice display impaired hippocampal CA1 long-term potentiation but show no obvious deficits in learning and memory. *Mol Cell Biol* **22**, 7417-27 (2002).

169. Zhou, X.H. et al. Neurocan is dispensable for brain development. *Mol Cell Biol* **21**, 5970-8 (2001).

170. Gogolla, N., Caroni, P., Luthi, A. & Herry, C. Perineuronal nets protect fear memories from erasure. *Science* **325**, 1258-61 (2009).

171. Sun, Z.Y. et al. Disruption of perineuronal nets increases the frequency of sharp wave ripple events. **28**, 42-52 (2018).

172. Schlingloff, D. & Kali, S. Mechanisms of sharp wave initiation and ripple generation. **34**, 11385-98 (2014).

173. Kim, J.H. & Richardson, R. A developmental dissociation of context and GABA effects on extinguished fear in rats. *Behav Neurosci* **121**, 131-9 (2007).

174. Banerjee, S.B. et al. Perineuronal Nets in the Adult Sensory Cortex Are Necessary for Fear Learning. *Neuron* **95**, 169-179.e3 (2017).

175. Lensjo, K.K. & Lepperod, M.E. Removal of Perineuronal Nets Unlocks Juvenile Plasticity Through Network Mechanisms of Decreased Inhibition and Increased Gamma Activity. **37**, 1269-1283 (2017).

176. Thompson, E.H. et al. Removal of perineuronal nets disrupts recall of a remote fear memory. *Proc Natl Acad Sci U S A* **115**, 607-612 (2018).

177. Cajal, S.R.y. Sobre un ganglio especial de la corteza esfeno-occipital. *Trab del Lab de invest Biol Univ Madrid* **1**, 189–201 (1902).

178. Lorente de Nò, R. Studies on the Structure of the Cerebral Cortex II. Continuation of the Study of the Ammonic System. *Journal für Psychologie und Neurologie* **113-177**, 113-177 (1934).

179. Bartesaghi, R. & Ravasi, L. Pyramidal neuron types in field CA2 of the guinea pig. *Brain Res Bull* **50**, 263-73 (1999).

180. Gall, C. & Selawski, L. Supramammillary afferents to guinea pig hippocampus contain substance P-like immunoreactivity. *Neurosci Lett* **51**, 171-6 (1984).

181. Zhang, L. & Hernandez, V.S. Synaptic innervation to rat hippocampus by vasopressin-immuno-positive fibres from the hypothalamic supraoptic and paraventricular nuclei. *Neuroscience* **228**, 139-62 (2013).

182. Llorens-Martin, M., Jurado-Arjona, J., Avila, J. & Hernandez, F. Novel connection between newborn granule neurons and the hippocampal CA2 field. *Exp Neurol* **263**, 285-92 (2015).

183. Cui, Z., Gerfen, C.R. & Young, W.S., 3rd. Hypothalamic and other connections with dorsal CA2 area of the mouse hippocampus. *J Comp Neurol* **521**, 1844-66 (2013).

184. Kohara, K. et al. Cell type-specific genetic and optogenetic tools reveal hippocampal CA2 circuits. *Nat Neurosci* **17**, 269-79 (2014).

185. Woodhams, P.L., Celio, M.R., Ulfig, N. & Witter, M.P. Morphological and functional correlates of borders in the entorhinal cortex and hippocampus. *Hippocampus* **3 Spec No**, 303-11 (1993).

186. Hirama, J., Shoumura, K., Ichinohe, N., You, S. & Yonekura, H. Cornu ammonis of the cat: lack of a separate field of CA2. *J Hirnforsch* **38**, 487-93 (1997).

187. Alexander, G.M. et al. Social and novel contexts modify hippocampal CA2 representations of space. **7**, 10300 (2016).

188. Mankin, E.A., Diehl, G.W., Sparks, F.T., Leutgeb, S. & Leutgeb, J.K. Hippocampal CA2 activity patterns change over time to a larger extent than between spatial contexts. *Neuron* **85**, 190-201 (2015).

189. Boehringer, R. et al. Chronic Loss of CA2 Transmission Leads to Hippocampal Hyperexcitability. *Neuron* **94**, 642-655.e9 (2017).

190. Nicoll, R.A. & Schmitz, D. Synaptic plasticity at hippocampal mossy fibre synapses. *Nat Rev Neurosci* **6**, 863-76 (2005).

191. Steve, T.A., Jirsch, J.D. & Gross, D.W. Quantification of subfield pathology in hippocampal sclerosis: a systematic review and meta-analysis. *Epilepsy Res* **108**, 1279-85 (2014).

192. Corsellis, J.A. & Bruton, C.J. Neuropathology of status epilepticus in humans. *Adv Neurol* **34**, 129-39 (1983).

193. Maxwell, W.L. et al. There is differential loss of pyramidal cells from the human hippocampus with survival after blunt head injury. *J Neuropathol Exp Neurol* **62**, 272-9 (2003).

194. Sloviter, R.S., Sollas, A.L., Barbaro, N.M. & Laxer, K.D. Calcium-binding protein (calbindin-D28K) and parvalbumin immunocytochemistry in the normal and epileptic human hippocampus. *J Comp Neurol* **308**, 381-96 (1991).

195. Kirino, T. Delayed neuronal death in the gerbil hippocampus following ischemia. *Brain Res* **239**, 57-69 (1982).

196. Zhao, M., Choi, Y.S., Obrietan, K. & Dudek, S.M. Synaptic plasticity (and the lack thereof) in hippocampal CA2 neurons. *J Neurosci* **27**, 12025-32 (2007).

197. Dudek, S.M., Alexander, G.M. & Farris, S. Rediscovering area CA2: unique properties and functions. *Nat Rev Neurosci* **17**, 89-102 (2016).

198. Lee, S.E. et al. RGS14 is a natural suppressor of both synaptic plasticity in CA2 neurons and hippocampal-based learning and memory. *Proc Natl Acad Sci U S A* **107**, 16994-8 (2010).

199. Evans, P.R., Dudek, S.M. & Hepler, J.R. Regulator of G Protein Signaling 14: A Molecular Brake on Synaptic Plasticity Linked to Learning and Memory. *Prog Mol Biol Transl Sci* **133**, 169-206 (2015).

200. Evans, P.R. et al. Interactome Analysis Reveals Regulator of G Protein Signaling 14 (RGS14) is a Novel Calcium/Calmodulin (Ca2+/CaM) and CaM Kinase II (CaMKII) Binding Partner. *J Proteome Res* (2018).

201. Evans, P.R., Lee, S.E., Smith, Y. & Hepler, J.R. Postnatal developmental expression of regulator of G protein signaling 14 (RGS14) in the mouse brain. *J Comp Neurol* **522**, 186-203 (2014).

202. Donaldson, Z.R. & Young, L.J. Oxytocin, vasopressin, and the neurogenetics of sociality. *Science* **322**, 900-4 (2008).

203. Pagani, J.H. et al. Role of the vasopressin 1b receptor in rodent aggressive behavior and synaptic plasticity in hippocampal area CA2. *Mol Psychiatry* **20**, 490-9 (2015).

204. Young, W.S., Li, J., Wersinger, S.R. & Palkovits, M. The vasopressin 1b receptor is prominent in the hippocampal area CA2 where it is unaffected by restraint stress or adrenalectomy. *Neuroscience* **143**, 1031-9 (2006).

205. Smith, A.S., Williams Avram, S.K., Cymerblit-Sabba, A., Song, J. & Young, W.S. Targeted activation of the hippocampal CA2 area strongly enhances social memory. *Mol Psychiatry* **21**, 1137-44 (2016).

206. Dasgupta, A. et al. Substance P induces plasticity and synaptic tagging/capture in rat hippocampal area CA2. **114**, E8741-e8749 (2017).

207. Choi, W.K. et al. The characteristics of supramammillary cells projecting to the hippocampus in stress response in the rat. *Korean J Physiol Pharmacol* **16**, 17-24 (2012).

208. Ochiishi, T. et al. Cellular localization of adenosine A1 receptors in rat forebrain: immunohistochemical analysis using adenosine A1 receptor-specific monoclonal antibody. *J Comp Neurol* **411**, 301-16 (1999).

209. Simons, S.B., Escobedo, Y., Yasuda, R. & Dudek, S.M. Regional differences in hippocampal calcium handling provide a cellular mechanism for limiting plasticity. *Proc Natl Acad Sci U S A* **106**, 14080-4 (2009).

210. Kirk, I.J. & McNaughton, N. Supramammillary cell firing and hippocampal rhythmical slow activity. *Neuroreport* **2**, 723-5 (1991).

211. Chevaleyre, V. & Siegelbaum, S.A. Strong CA2 pyramidal neuron synapses define a powerful disynaptic cortico-hippocampal loop. *Neuron* **66**, 560-72 (2010).

212. Piskorowski, R.A. & Chevaleyre, V. Delta-opioid receptors mediate unique plasticity onto parvalbumin-expressing interneurons in area CA2 of the hippocampus. *J Neurosci* **33**, 14567-78 (2013).

213. Mercer, A., Trigg, H.L. & Thomson, A.M. Characterization of neurons in the CA2 subfield of the adult rat hippocampus. *J Neurosci* **27**, 7329-38 (2007).

214. Mercer, A., Eastlake, K., Trigg, H.L. & Thomson, A.M. Local circuitry involving parvalbumin-positive basket cells in the CA2 region of the hippocampus. *Hippocampus* **22**, 43-56 (2012).

215. Botcher, N.A., Falck, J.E., Thomson, A.M. & Mercer, A. Distribution of interneurons in the CA2 region of the rat hippocampus. *Front Neuroanat* **8**, 104 (2014).

216. Nasrallah, K., Piskorowski, R.A. & Chevaleyre, V. Inhibitory Plasticity Permits the Recruitment of CA2 Pyramidal Neurons by CA3(1,2,3). *eNeuro* **2** (2015).

217. Leroy, F., Brann, D.H., Meira, T. & Siegelbaum, S.A. Input-Timing-Dependent Plasticity in the Hippocampal CA2 Region and Its Potential Role in Social Memory. *Neuron* **95**, 1089-1102.e5 (2017).

218. Benes, F.M., Kwok, E.W., Vincent, S.L. & Todtenkopf, M.S. A reduction of nonpyramidal cells in sector CA2 of schizophrenics and manic depressives. *Biol Psychiatry* **44**, 88-97 (1998).

219. Piskorowski, R.A. et al. Age-Dependent Specific Changes in Area CA2 of the Hippocampus and Social Memory Deficit in a Mouse Model of the 22q11.2 Deletion Syndrome. *Neuron* **89**, 163-76 (2016).

220. Wintzer, M.E., Boehringer, R., Polygalov, D. & McHugh, T.J. The hippocampal CA2 ensemble is sensitive to contextual change. *J Neurosci* **34**, 3056-66 (2014).

221. Oliva, A., Fernandez-Ruiz, A., Buzsaki, G. & Berenyi, A. Spatial coding and physiological properties of hippocampal neurons in the Cornu Ammonis subregions. *Hippocampus* **26**, 1593-1607 (2016).

222. Lu, L., Igarashi, K.M., Witter, M.P., Moser, E.I. & Moser, M.B. Topography of Place Maps along the CA3-to-CA2 Axis of the Hippocampus. *Neuron* **87**, 1078-92 (2015).

223. Smith, A.S., Williams Avram, S.K., Cymerblit-Sabba, A., Song, J. & Young, W.S. Targeted activation of the hippocampal CA2 area strongly enhances social memory. *Mol Psychiatry* (2016).

224. Hitti, F.L. & Siegelbaum, S.A. The hippocampal CA2 region is essential for social memory. *Nature* **508**, 88-92 (2014).

225. Stevenson, E.L. & Caldwell, H.K. Lesions to the CA2 region of the hippocampus impair social memory in mice. *Eur J Neurosci* **40**, 3294-301 (2014).

226. DeVito, L.M. et al. Vasopressin 1b receptor knock-out impairs memory for temporal order. *J Neurosci* **29**, 2676-83 (2009).

227. Chafai, M., Corbani, M., Guillon, G. & Desarmenien, M.G. Vasopressin inhibits LTP in the CA2 mouse hippocampal area. *PLoS One* **7**, e49708 (2012).

228. Wersinger, S.R., Ginns, E.I., O'Carroll, A.M., Lolait, S.J. & Young, W.S., 3rd. Vasopressin V1b receptor knockout reduces aggressive behavior in male mice. *Mol Psychiatry* **7**, 975-84 (2002).

229. Wersinger, S.R., Temple, J.L., Caldwell, H.K. & Young, W.S., 3rd. Inactivation of the oxytocin and the vasopressin (Avp) 1b receptor genes, but not the Avp 1a receptor gene, differentially impairs the Bruce effect in laboratory mice (Mus musculus). *Endocrinology* **149**, 116-21 (2008).

230. Alexander, G. et al. CA2 Neuronal Activity Controls Hippocampal Oscillations and Social Behavior. *bioRxiv* (2017).

231. Whitlock, J.R., Heynen, A.J., Shuler, M.G. & Bear, M.F. Learning induces long-term potentiation in the hippocampus. *Science* **313**, 1093-7 (2006).

232. Josselyn, S.A. & Frankland, P.W. Infantile amnesia: a neurogenic hypothesis. *Learn Mem* **19**, 423-33 (2012).

233. Fanselow, M.S. Contextual fear, gestalt memories, and the hippocampus. *Behav Brain Res* **110**, 73-81 (2000).

234. Eichenbaum, H. Is the rodent hippocampus just for 'place'? *Curr Opin Neurobiol* **6**, 187-95 (1996).

235. Wiltgen, B.J., Sanders, M.J., Anagnostaras, S.G., Sage, J.R. & Fanselow, M.S. Context fear learning in the absence of the hippocampus. *J Neurosci* **26**, 5484-91 (2006).

236. Bourtchuladze, R. et al. Deficient long-term memory in mice with a targeted mutation of the cAMP-responsive element-binding protein. *Cell* **79**, 59-68 (1994).

237. Daumas, S., Halley, H., Frances, B. & Lassalle, J.M. Encoding, consolidation, and retrieval of contextual memory: differential involvement of dorsal CA3 and CA1 hippocampal subregions. *Learn Mem* **12**, 375-82 (2005).

238. Campbell, B.A. & Spear, N.E. Ontogeny of memory. *Psychol Rev* **79**, 215-36 (1972).

239. Wiskott, L., Rasch, M.J. & Kempermann, G. A functional hypothesis for adult hippocampal neurogenesis: avoidance of catastrophic interference in the dentate gyrus. *Hippocampus* **16**, 329-43 (2006).

240. Treves, A., Tashiro, A., Witter, M.P. & Moser, E.I. What is the mammalian dentate gyrus good for? *Neuroscience* **154**, 1155-72 (2008).

241. Shors, T.J. From stem cells to grandmother cells: how neurogenesis relates to learning and memory. *Cell Stem Cell* **3**, 253-8 (2008).

242. McRae, P.A., Baranov, E., Sarode, S., Brooks-Kayal, A.R. & Porter, B.E. Aggrecan expression, a component of the inhibitory interneuron perineuronal net, is altered following an early-life seizure. *Neurobiol Dis* **39**, 439-48 (2010).

243. McRae, P.A., Baranov, E., Rogers, S.L. & Porter, B.E. Persistent decrease in multiple components of the perineuronal net following status epilepticus. *Eur J Neurosci* **36**, 3471-82 (2012).

244. Fuxe, K., Tinner, B., Staines, W., David, G. & Agnati, L.F. Regional distribution of neural cell adhesion molecule immunoreactivity in the adult rat telencephalon and

diencephalon. Partial colocalization with heparan sulfate proteoglycan immunoreactivity. *Brain Res* **746**, 25-33 (1997).

245. Alpar, A., Gartner, U., Hartig, W. & Bruckner, G. Distribution of pyramidal cells associated with perineuronal nets in the neocortex of rat. *Brain Res* **1120**, 13-22 (2006).

246. Caruana, D.A., Alexander, G.M. & Dudek, S.M. New insights into the regulation of synaptic plasticity from an unexpected place: hippocampal area CA2. *Learn Mem* **19**, 391-400 (2012).

247. Boulanger, L.M. et al. Cellular and molecular characterization of a brain-enriched protein tyrosine phosphatase. *J Neurosci* **15**, 1532-44 (1995).

248. Pelkey, K.A. et al. Tyrosine phosphatase STEP is a tonic brake on induction of long-term potentiation. *Neuron* **34**, 127-38 (2002).

249. Feng, G. et al. Imaging neuronal subsets in transgenic mice expressing multiple spectral variants of GFP. *Neuron* **28**, 41-51 (2000).

250. Aoyagi, Y., Kawakami, R., Osanai, H., Hibi, T. & Nemoto, T. A rapid optical clearing protocol using 2,2'-thiodiethanol for microscopic observation of fixed mouse brain. *PLoS One* **10**, e0116280 (2015).

251. Poncer, J.C. & Malinow, R. Postsynaptic conversion of silent synapses during LTP affects synaptic gain and transmission dynamics. *Nat Neurosci* **4**, 989-96 (2001).

252. Laeremans, A. et al. AMIGO2 mRNA expression in hippocampal CA2 and CA3a. *Brain Struct Funct* **218**, 123-30 (2013).

253. Sur, M., Frost, D.O. & Hockfield, S. Expression of a surface-associated antigen on Y-cells in the cat lateral geniculate nucleus is regulated by visual experience. *J Neurosci* **8**, 874-82 (1988).

254. Bartoletti, A., Medini, P., Berardi, N. & Maffei, L. Environmental enrichment prevents effects of dark-rearing in the rat visual cortex. *Nat Neurosci* **7**, 215-6 (2004).

255. Baroncelli, L. et al. Experience Affects Critical Period Plasticity in the Visual Cortex through an Epigenetic Regulation of Histone Post-Translational Modifications. *J Neurosci* **36**, 3430-40 (2016).

256. Romberg, C. et al. Depletion of perineuronal nets enhances recognition memory and long-term depression in the perirhinal cortex. *J Neurosci* **33**, 7057-65 (2013).

257. Wang, D. & Fawcett, J. The perineuronal net and the control of CNS plasticity. *Cell Tissue Res* **349**, 147-60 (2012).

258. Morawski, M., Bruckner, M.K., Riederer, P., Bruckner, G. & Arendt, T. Perineuronal nets potentially protect against oxidative stress. *Exp Neurol* **188**, 309-15 (2004).

259. Galtrey, C.M., Asher, R.A., Nothias, F. & Fawcett, J.W. Promoting plasticity in the spinal cord with chondroitinase improves functional recovery after peripheral nerve repair. *Brain* **130**, 926-39 (2007).

260. Corvetti, L. & Rossi, F. Degradation of chondroitin sulfate proteoglycans induces sprouting of intact purkinje axons in the cerebellum of the adult rat. *J Neurosci* **25**, 7150-8 (2005).

261. Cabungcal, J.H. et al. Perineuronal nets protect fast-spiking interneurons against oxidative stress. *Proc Natl Acad Sci U S A* **110**, 9130-5 (2013).

262. Sale, A. et al. Environmental enrichment in adulthood promotes amblyopia recovery through a reduction of intracortical inhibition. *Nat Neurosci* **10**, 679-81 (2007).

263. Foscarin, S. et al. Experience-dependent plasticity and modulation of growth regulatory molecules at central synapses. *PLoS One* **6**, e16666 (2011).

264. Mauney, S.A. et al. Developmental pattern of perineuronal nets in the human prefrontal cortex and their deficit in schizophrenia. *Biol Psychiatry* **74**, 427-35 (2013).

265. Belichenko, P.V., Hagberg, B. & Dahlstrom, A. Morphological study of neocortical areas in Rett syndrome. *Acta Neuropathol* **93**, 50-61 (1997).

266. Amir, R.E. et al. Rett syndrome is caused by mutations in X-linked MECP2, encoding methyl-CpG-binding protein 2. *Nat Genet* **23**, 185-8 (1999).

267. Neul, J.L. et al. Rett syndrome: revised diagnostic criteria and nomenclature. *Ann Neurol* **68**, 944-50 (2010).

268. Percy, A.K., Zoghbi, H.Y. & Glaze, D.G. Rett syndrome: discrimination of typical and variant forms. *Brain Dev* **9**, 458-61 (1987).

269. Percy, A.K. et al. Rett syndrome diagnostic criteria: lessons from the Natural History Study. *Ann Neurol* **68**, 951-5 (2010).

270. Armstrong, D.D. Neuropathology of Rett syndrome. *J Child Neurol* **20**, 747-53 (2005).

271. Percy, A.K., Zoghbi, H. & Riccardi, V.M. Rett syndrome: initial experience with an emerging clinical entity. *Brain Dev* **7**, 300-4 (1985).

272. Schultz, R.J. et al. The pattern of growth failure in Rett syndrome. *Am J Dis Child* **147**, 633-7 (1993).

273. Ellison, K.A. et al. Examination of X chromosome markers in Rett syndrome: exclusion mapping with a novel variation on multilocus linkage analysis. *Am J Hum Genet* **50**, 278-87 (1992).

274. Percy, A.K., Zoghbi, H.Y., Lewis, K.R. & Jankovic, J. Rett syndrome: qualitative and quantitative differentiation from autism. *J Child Neurol* **3 Suppl**, S65-7 (1988).

275. Gilby, K.L. & O'Brien, T.J. Epilepsy, autism, and neurodevelopment: kindling a shared vulnerability? *Epilepsy Behav* **26**, 370-4 (2013).

276. Chahrour, M. et al. MeCP2, a key contributor to neurological disease, activates and represses transcription. *Science* **320**, 1224-9 (2008).

277. Cheng, T.L. et al. MeCP2 suppresses nuclear microRNA processing and dendritic growth by regulating the DGCR8/Drosha complex. *Dev Cell* **28**, 547-60 (2014).

278. Qiu, Z. et al. The Rett syndrome protein MeCP2 regulates synaptic scaling. *J Neurosci* **32**, 989-94 (2012).

279. Ebert, D.H. & Greenberg, M.E. Activity-dependent neuronal signalling and autism spectrum disorder. *Nature* **493**, 327-37 (2013).

280. Shahbazian, M.D., Antalffy, B., Armstrong, D.L. & Zoghbi, H.Y. Insight into Rett syndrome: MeCP2 levels display tissue- and cell-specific differences and correlate with neuronal maturation. *Hum Mol Genet* **11**, 115-24 (2002).

281. Mullaney, B.C., Johnston, M.V. & Blue, M.E. Developmental expression of methyl-CpG binding protein 2 is dynamically regulated in the rodent brain. *Neuroscience* **123**, 939-49 (2004).

282. Lyst, M.J. & Bird, A. Rett syndrome: a complex disorder with simple roots. *Nat Rev Genet* **16**, 261-75 (2015).

283. Boggio, E.M., Lonetti, G., Pizzorusso, T. & Giustetto, M. Synaptic determinants of rett syndrome. *Front Synaptic Neurosci* **2**, 28 (2010).

284. Belichenko, P.V., Oldfors, A., Hagberg, B. & Dahlstrom, A. Rett syndrome: 3-D confocal microscopy of cortical pyramidal dendrites and afferents. *Neuroreport* **5**, 1509-13 (1994).

285. Fukuda, T., Itoh, M., Ichikawa, T., Washiyama, K. & Goto, Y. Delayed maturation of neuronal architecture and synaptogenesis in cerebral cortex of Mecp2-deficient mice. *J Neuropathol Exp Neurol* **64**, 537-44 (2005).

286. Asaka, Y., Jugloff, D.G., Zhang, L., Eubanks, J.H. & Fitzsimonds, R.M. Hippocampal synaptic plasticity is impaired in the Mecp2-null mouse model of Rett syndrome. *Neurobiol Dis* **21**, 217-27 (2006).

287. Medrihan, L. et al. Early defects of GABAergic synapses in the brain stem of a MeCP2 mouse model of Rett syndrome. *J Neurophysiol* **99**, 112-21 (2008).

288. Belichenko, N.P., Belichenko, P.V. & Mobley, W.C. Evidence for both neuronal cell autonomous and nonautonomous effects of methyl-CpG-binding protein 2 in the cerebral cortex of female mice with Mecp2 mutation. *Neurobiol Dis* **34**, 71-7 (2009).

289. Tropea, D. et al. Partial reversal of Rett Syndrome-like symptoms in MeCP2 mutant mice. *Proc Natl Acad Sci U S A* **106**, 2029-34 (2009).

290. Zhang, Z.W., Zak, J.D. & Liu, H. MeCP2 is required for normal development of GABAergic circuits in the thalamus. *J Neurophysiol* **103**, 2470-81 (2010).

291. Gantz, S.C., Ford, C.P., Neve, K.A. & Williams, J.T. Loss of Mecp2 in substantia nigra dopamine neurons compromises the nigrostriatal pathway. *J Neurosci* **31**, 12629-37 (2011).

292. Smrt, R.D. et al. Mecp2 deficiency leads to delayed maturation and altered gene expression in hippocampal neurons. *Neurobiol Dis* **27**, 77-89 (2007).

293. Pantazopoulos, H., Woo, T.U., Lim, M.P., Lange, N. & Berretta, S. Extracellular matrix-glial abnormalities in the amygdala and entorhinal cortex of subjects diagnosed with schizophrenia. *Arch Gen Psychiatry* **67**, 155-66 (2010).

294. McRae, P.A. & Porter, B.E. The perineuronal net component of the extracellular matrix in plasticity and epilepsy. *Neurochem Int* **61**, 963-72 (2012).

295. Carstens, K.E., Phillips, M.L. & Pozzo-Miller, L. Perineuronal Nets Suppress Plasticity of Excitatory Synapses on CA2 Pyramidal Neurons. **36**, 6312-20 (2016).

296. Sorg, B.A. & Berretta, S. Casting a Wide Net: Role of Perineuronal Nets in Neural Plasticity. **36**, 11459-11468 (2016).

297. Hockfield, S., Kalb, R.G., Zaremba, S. & Fryer, H. Expression of neural proteoglycans correlates with the acquisition of mature neuronal properties in the mammalian brain. *Cold Spring Harb Symp Quant Biol* **55**, 505-14 (1990).

298. Krishnan, K., Lau, B.Y., Ewall, G., Huang, Z.J. & Shea, S.D. MECP2 regulates cortical plasticity underlying a learned behaviour in adult female mice. *Nat Commun* **8**, 14077 (2017).

299. Krishnan, K. et al. MeCP2 regulates the timing of critical period plasticity that shapes functional connectivity in primary visual cortex. *Proc Natl Acad Sci U S A* **112**, E4782-91 (2015).

300. Guy, J., Hendrich, B., Holmes, M., Martin, J.E. & Bird, A. A mouse Mecp2-null mutation causes neurological symptoms that mimic Rett syndrome. *Nat Genet* **27**, 322-6 (2001).

301. Pelka, G.J. et al. Mecp2 deficiency is associated with learning and cognitive deficits and altered gene activity in the hippocampal region of mice. *Brain* **129**, 887-98 (2006).

302. Chao, H.T. et al. Dysfunction in GABA signalling mediates autism-like stereotypies and Rett syndrome phenotypes. *Nature* **468**, 263-9 (2010).

303. Chao, H.T., Zoghbi, H.Y. & Rosenmund, C. MeCP2 controls excitatory synaptic strength by regulating glutamatergic synapse number. *Neuron* **56**, 58-65 (2007).

304. Belichenko, P.V. et al. Widespread changes in dendritic and axonal morphology in Mecp2-mutant mouse models of Rett syndrome: evidence for disruption of neuronal networks. *J Comp Neurol* **514**, 240-58 (2009).

305. Chen, R.Z., Akbarian, S., Tudor, M. & Jaenisch, R. Deficiency of methyl-CpG binding protein-2 in CNS neurons results in a Rett-like phenotype in mice. *Nat Genet* **27**, 327-31 (2001).

306. Calfa, G., Hablitz, J.J. & Pozzo-Miller, L. Network hyperexcitability in hippocampal slices from Mecp2 mutant mice revealed by voltage-sensitive dye imaging. *J Neurophysiol* **105**, 1768-84 (2011).

307. Moretti, P. et al. Learning and memory and synaptic plasticity are impaired in a mouse model of Rett syndrome. *J Neurosci* **26**, 319-27 (2006).

308. Hao, S. et al. Forniceal deep brain stimulation rescues hippocampal memory in Rett syndrome mice. *Nature* **526**, 430-4 (2015).

309. Lu, H. et al. Loss and Gain of MeCP2 Cause Similar Hippocampal Circuit Dysfunction that Is Rescued by Deep Brain Stimulation in a Rett Syndrome Mouse Model. *Neuron* **91**, 739-747 (2016).

310. Blackman, M.P., Djukic, B., Nelson, S.B. & Turrigiano, G.G. A critical and cell-autonomous role for MeCP2 in synaptic scaling up. *J Neurosci* **32**, 13529-36 (2012).

311. Cull-Candy, S., Brickley, S. & Farrant, M. NMDA receptor subunits: diversity, development and disease. *Curr Opin Neurobiol* **11**, 327-35 (2001).

312. Watanabe, M., Inoue, Y., Sakimura, K. & Mishina, M. Developmental changes in distribution of NMDA receptor channel subunit mRNAs. *Neuroreport* **3**, 1138-40 (1992).

313. Liu, N., He, S. & Yu, X. Early natural stimulation through environmental enrichment accelerates neuronal development in the mouse dentate gyrus. *PLoS One* **7**, e30803 (2012).

314. Martinowich, K. et al. DNA methylation-related chromatin remodeling in activity-dependent BDNF gene regulation. *Science* **302**, 890-3 (2003).

315. Monteggia, L.M. et al. Essential role of brain-derived neurotrophic factor in adult hippocampal function. *Proc Natl Acad Sci U S A* **101**, 10827-32 (2004).

316. Larimore, J.L. et al. Bdnf overexpression in hippocampal neurons prevents dendritic atrophy caused by Rett-associated MECP2 mutations. *Neurobiol Dis* **34**, 199-211 (2009).

317. Chang, Q., Khare, G., Dani, V., Nelson, S. & Jaenisch, R. The disease progression of Mecp2 mutant mice is affected by the level of BDNF expression. *Neuron* **49**, 341-8 (2006).

318. Chen, W.G. et al. Derepression of BDNF transcription involves calcium-dependent phosphorylation of MeCP2. *Science* **302**, 885-9 (2003).

319. Zhou, Z. et al. Brain-specific phosphorylation of MeCP2 regulates activity-dependent Bdnf transcription, dendritic growth, and spine maturation. *Neuron* **52**, 255-69 (2006).

320. Dani, V.S. et al. Reduced cortical activity due to a shift in the balance between excitation and inhibition in a mouse model of Rett syndrome. *Proc Natl Acad Sci U S A* **102**, 12560-5 (2005).

321. Nelson, E.D., Kavalali, E.T. & Monteggia, L.M. MeCP2-dependent transcriptional repression regulates excitatory neurotransmission. *Curr Biol* **16**, 710-6 (2006).

322. Samaco, R.C. et al. Loss of MeCP2 in aminergic neurons causes cell-autonomous defects in neurotransmitter synthesis and specific behavioral abnormalities. *Proc Natl Acad Sci U S A* **106**, 21966-71 (2009).

323. Lioy, D.T. et al. A role for glia in the progression of Rett's syndrome. *Nature* **475**, 497-500 (2011).

324. Derecki, N.C. et al. Wild-type microglia arrest pathology in a mouse model of Rett syndrome. *Nature* **484**, 105-9 (2012).

325. Alvarez-Saavedra, M., Saez, M.A., Kang, D., Zoghbi, H.Y. & Young, J.I. Cell-specific expression of wild-type MeCP2 in mouse models of Rett syndrome yields insight about pathogenesis. *Hum Mol Genet* **16**, 2315-25 (2007).

326. He, L.J. et al. Conditional deletion of Mecp2 in parvalbumin-expressing GABAergic cells results in the absence of critical period plasticity. *Nat Commun* **5**, 5036 (2014).

327. Leontovich, T.A., Mukhina, J.K., Fedorov, A.A. & Belichenko, P.V. Morphological study of the entorhinal cortex, hippocampal formation, and basal ganglia in Rett syndrome patients. *Neurobiol Dis* **6**, 77-91 (1999).

328. Giacometti, E., Luikenhuis, S., Beard, C. & Jaenisch, R. Partial rescue of MeCP2 deficiency by postnatal activation of MeCP2. *Proc Natl Acad Sci U S A* **104**, 1931-6 (2007).

329. Gong, S., Yang, X.W., Li, C. & Heintz, N. Highly efficient modification of bacterial artificial chromosomes (BACs) using novel shuttle vectors containing the R6Kgamma origin of replication. *Genome Res* **12**, 1992-8 (2002).

330. Gustafsson, B., Wigstrom, H., Abraham, W.C. & Huang, Y.Y. Long-term potentiation in the hippocampus using depolarizing current pulses as the conditioning stimulus to single volley synaptic potentials. *J Neurosci* **7**, 774-80 (1987).

331. Malenka, R.C. & Nicoll, R.A. NMDA-receptor-dependent synaptic plasticity: multiple forms and mechanisms. *Trends Neurosci* **16**, 521-7 (1993).

332. Chapleau, C.A. et al. Hippocampal CA1 pyramidal neurons of Mecp2 mutant mice show a dendritic spine phenotype only in the presymptomatic stage. *Neural Plast* **2012**, 976164 (2012).

333. Ethell, I.M. & Ethell, D.W. Matrix metalloproteinases in brain development and remodeling: synaptic functions and targets. *J Neurosci Res* **85**, 2813-23 (2007).

334. Reinhard, S.M., Razak, K. & Ethell, I.M. A delicate balance: role of MMP-9 in brain development and pathophysiology of neurodevelopmental disorders. *Front Cell Neurosci* **9**, 280 (2015).

335. Wen, T.H. et al. Genetic Reduction of Matrix Metalloproteinase-9 Promotes Formation of Perineuronal Nets Around Parvalbumin-Expressing Interneurons and Normalizes Auditory Cortex Responses in Developing Fmr1 Knock-Out Mice. *Cereb Cortex*, 1-14 (2017).

336. Kaufmann, W.E., Naidu, S. & Budden, S. Abnormal expression of microtubule-associated protein 2 (MAP-2) in neocortex in Rett syndrome. *Neuropediatrics* **26**, 109-13 (1995).

337. Kaufmann, W.E., Taylor, C.V., Hohmann, C.F., Sanwal, I.B. & Naidu, S. Abnormalities in neuronal maturation in Rett syndrome neocortex: preliminary molecular correlates. *Eur Child Adolesc Psychiatry* **6 Suppl 1**, 75-7 (1997).

338. Dani, V.S. & Nelson, S.B. Intact long-term potentiation but reduced connectivity between neocortical layer 5 pyramidal neurons in a mouse model of Rett syndrome. *J Neurosci* **29**, 11263-70 (2009).

339. Zhang, L., He, J., Jugloff, D.G. & Eubanks, J.H. The MeCP2-null mouse hippocampus displays altered basal inhibitory rhythms and is prone to hyperexcitability. *Hippocampus* **18**, 294-309 (2008).

340. van Zundert, B., Yoshii, A. & Constantine-Paton, M. Receptor compartmentalization and trafficking at glutamate synapses: a developmental proposal. *Trends Neurosci* **27**, 428-37 (2004).

341. Blue, M.E., Naidu, S. & Johnston, M.V. Altered development of glutamate and GABA receptors in the basal ganglia of girls with Rett syndrome. *Exp Neurol* **156**, 345-52 (1999).

342. Blue, M.E., Naidu, S. & Johnston, M.V. Development of amino acid receptors in frontal cortex from girls with Rett syndrome. *Ann Neurol* **45**, 541-5 (1999).

343. Liu, L. et al. Role of NMDA receptor subtypes in governing the direction of hippocampal synaptic plasticity. *Science* **304**, 1021-4 (2004).

344. Kirson, E.D. & Yaari, Y. Synaptic NMDA receptors in developing mouse hippocampal neurones: functional properties and sensitivity to ifenprodil. *J Physiol* **497 (Pt 2)**, 437-55 (1996).

345. Lu, H.C., Gonzalez, E. & Crair, M.C. Barrel cortex critical period plasticity is independent of changes in NMDA receptor subunit composition. *Neuron* **32**, 619-34 (2001).

346. Huang, Z.J. et al. BDNF regulates the maturation of inhibition and the critical period of plasticity in mouse visual cortex. *Cell* **98**, 739-55 (1999).

347. Chattopadhyaya, B. et al. Experience and activity-dependent maturation of perisomatic GABAergic innervation in primary visual cortex during a postnatal critical period. *J Neurosci* **24**, 9598-611 (2004).

348. Chattopadhyaya, B. et al. GAD67-mediated GABA synthesis and signaling regulate inhibitory synaptic innervation in the visual cortex. *Neuron* **54**, 889-903 (2007).

349. Kwan, P. & Sander, J.W. The natural history of epilepsy: an epidemiological view. *J Neurol Neurosurg Psychiatry* **75**, 1376-81 (2004).

350. Riban, V. et al. Evolution of hippocampal epileptic activity during the development of hippocampal sclerosis in a mouse model of temporal lobe epilepsy. *Neuroscience* **112**, 101-11 (2002).

351. Lukasiuk, K., Wilczynski, G.M. & Kaczmarek, L. Extracellular proteases in epilepsy. *Epilepsy Res* **96**, 191-206 (2011).

352. Schubert, M., Siegmund, H., Pape, H.C. & Albrecht, D. Kindling-induced changes in plasticity of the rat amygdala and hippocampus. *Learn Mem* **12**, 520-6 (2005).

353. Beck, H., Goussakov, I.V., Lie, A., Helmstaedter, C. & Elger, C.E. Synaptic plasticity in the human dentate gyrus. *J Neurosci* **20**, 7080-6 (2000).

354. Dityatev, A. Remodeling of extracellular matrix and epileptogenesis. *Epilepsia* **51 Suppl 3**, 61-5 (2010).

355. Perosa, S.R. et al. Extracellular matrix components are altered in the hippocampus, cortex, and cerebrospinal fluid of patients with mesial temporal lobe epilepsy. *Epilepsia* **43 Suppl 5**, 159-61 (2002).

356. Rankin-Gee, E.K. et al. Perineuronal net degradation in epilepsy. *Epilepsia* **56**, 1124-33 (2015).

357. Suzuki, F., Makiura, Y., Guilhem, D., Sorensen, J.C. & Onteniente, B. Correlated axonal sprouting and dendritic spine formation during kainate-induced neuronal morphogenesis in the dentate gyrus of adult mice. *Exp Neurol* **145**, 203-13 (1997).

358. Ben-Ari, Y. & Represa, A. Brief seizure episodes induce long-term potentiation and mossy fibre sprouting in the hippocampus. *Trends Neurosci* **13**, 312-8 (1990).

359. Anwyl, R., Walshe, J. & Rowan, M. Electroconvulsive treatment reduces long-term potentiation in rat hippocampus. *Brain Res* **435**, 377-9 (1987).

360. Barr, D.S., Hoyt, K.L., Moore, S.D. & Wilson, W.A. Post-ictal depression transiently inhibits induction of LTP in area CA1 of the rat hippocampal slice. *Epilepsy Res* **27**, 111-8 (1997).

361. Wilczynski, G.M. et al. Important role of matrix metalloproteinase 9 in epileptogenesis. *J Cell Biol* **180**, 1021-35 (2008).

362. Wu, Y.P. et al. The tissue plasminogen activator (tPA)/plasmin extracellular proteolytic system regulates seizure-induced hippocampal mossy fiber outgrowth through a proteoglycan substrate. *J Cell Biol* **148**, 1295-304 (2000).

363. Sloviter, R.S. "Epileptic" brain damage in rats induced by sustained electrical stimulation of the perforant path. I. Acute electrophysiological and light microscopic studies. *Brain Res Bull* **10**, 675-97 (1983).

364. Sloviter, R.S. & Damiano, B.P. Sustained electrical stimulation of the perforant path duplicates kainate-induced electrophysiological effects and hippocampal damage in rats. *Neurosci Lett* **24**, 279-84 (1981).

365. Hatanpaa, K.J. et al. Hippocampal sclerosis in dementia, epilepsy, and ischemic injury: differential vulnerability of hippocampal subfields. *J Neuropathol Exp Neurol* **73**, 136-42 (2014).

366. Cavazos, J.E., Das, I. & Sutula, T.P. Neuronal loss induced in limbic pathways by kindling: evidence for induction of hippocampal sclerosis by repeated brief seizures. *J Neurosci* **14**, 3106-21 (1994).

367. Haussler, U., Rinas, K., Kilias, A., Egert, U. & Haas, C.A. Mossy fiber sprouting and pyramidal cell dispersion in the hippocampal CA2 region in a mouse model of temporal lobe epilepsy. *Hippocampus* (2015).

368. Smart, S.L. et al. Deletion of the K(V)1.1 potassium channel causes epilepsy in mice. *Neuron* **20**, 809-19 (1998).

369. Bidmon, H.J. et al. Structural alterations and changes in cytoskeletal proteins and proteoglycans after focal cortical ischemia. *Neuroscience* **82**, 397-420 (1998).

370. Smith, C.C. et al. Differential regulation of perineuronal nets in the brain and spinal cord with exercise training. *Brain Res Bull* **111**, 20-6 (2015).

371. Hartig, W. et al. Damaged Neocortical Perineuronal Nets Due to Experimental Focal Cerebral Ischemia in Mice, Rats and Sheep. *Front Integr Neurosci* **11**, 15 (2017).

372. Roth, B.L. DREADDs for Neuroscientists. *Neuron* **89**, 683-94 (2016).

373. Armbruster, B.N., Li, X., Pausch, M.H., Herlitze, S. & Roth, B.L. Evolving the lock to fit the key to create a family of G protein-coupled receptors potently activated by an inert ligand. *Proc Natl Acad Sci U S A* **104**, 5163-8 (2007).

374. Alexander, G.M. et al. Remote control of neuronal activity in transgenic mice expressing evolved G protein-coupled receptors. *Neuron* **63**, 27-39 (2009).

375. Giamanco, K.A., Morawski, M. & Matthews, R.T. Perineuronal net formation and structure in aggrecan knockout mice. *Neuroscience* **170**, 1314-27 (2010).

376. Saghatelyan, A.K. et al. Reduced perisomatic inhibition, increased excitatory transmission, and impaired long-term potentiation in mice deficient for the extracellular matrix glycoprotein tenascin-R. *Mol Cell Neurosci* **17**, 226-40 (2001).

377. Carulli, D. et al. Animals lacking link protein have attenuated perineuronal nets and persistent plasticity. *Brain* **133**, 2331-47 (2010).

378. Bradbury, E.J. et al. Chondroitinase ABC promotes functional recovery after spinal cord injury. *Nature* **416**, 636-40 (2002).

379. Cafferty, W.B. et al. Chondroitinase ABC-mediated plasticity of spinal sensory function. *J Neurosci* **28**, 11998-2009 (2008).

380. Berretta, S. Extracellular matrix abnormalities in schizophrenia. *Neuropharmacology* **62**, 1584-97 (2012).

381. Babb, T.L., Kupfer, W.R., Pretorius, J.K., Crandall, P.H. & Levesque, M.F. Synaptic reorganization by mossy fibers in human epileptic fascia dentata. *Neuroscience* **42**, 351-63 (1991).

382. Farris, S., Lewandowski, G., Cox, C.D. & Steward, O. Selective localization of arc mRNA in dendrites involves activity- and translation-dependent mRNA degradation. *J Neurosci* **34**, 4481-93 (2014).

383. Madisen, L. et al. A robust and high-throughput Cre reporting and characterization system for the whole mouse brain. *Nat Neurosci* **13**, 133-40 (2010).

384. Alves, J.N. et al. AAV vector-mediated secretion of chondroitinase provides a sensitive tracer for axonal arborisations. *J Neurosci Methods* **227**, 107-20 (2014).

385. Zhao, R.R. et al. Lentiviral vectors express chondroitinase ABC in cortical projections and promote sprouting of injured corticospinal axons. *J Neurosci Methods* **201**, 228-38 (2011).

386. Muir, E.M. et al. Modification of N-glycosylation sites allows secretion of bacterial chondroitinase ABC from mammalian cells. *J Biotechnol* **145**, 103-10 (2010).

387. Pollock, E., Everest, M., Brown, A. & Poulter, M.O. Metalloproteinase inhibition prevents inhibitory synapse reorganization and seizure genesis. *Neurobiol Dis* **70**, 21-31 (2014).

388. Konopka, A. et al. Matrix metalloproteinase-9 (MMP-9) in human intractable epilepsy caused by focal cortical dysplasia. *Epilepsy Res* **104**, 45-58 (2013).

389. Bouilleret, V. et al. Recurrent seizures and hippocampal sclerosis following intrahippocampal kainate injection in adult mice: electroencephalography, histopathology and synaptic reorganization similar to mesial temporal lobe epilepsy. *Neuroscience* **89**, 717-29 (1999).

390. Shepherd, J.D. & Bear, M.F. New views of Arc, a master regulator of synaptic plasticity. *Nat Neurosci* **14**, 279-84 (2011).

391. Shibley, H. & Smith, B.N. Pilocarpine-induced status epilepticus results in mossy fiber sprouting and spontaneous seizures in C57BL/6 and CD-1 mice. *Epilepsy Res* **49**, 109-20 (2002).

392. Sutula, T., Cascino, G., Cavazos, J., Parada, I. & Ramirez, L. Mossy fiber synaptic reorganization in the epileptic human temporal lobe. *Ann Neurol* **26**, 321-30 (1989).

393. Bell, B., Lin, J.J., Seidenberg, M. & Hermann, B. The neurobiology of cognitive disorders in temporal lobe epilepsy. *Nat Rev Neurol* **7**, 154-64 (2011).

394. Heck, N., Garwood, J., Loeffler, J.P., Larmet, Y. & Faissner, A. Differential upregulation of extracellular matrix molecules associated with the appearance of granule cell dispersion and mossy fiber sprouting during epileptogenesis in a murine model of temporal lobe epilepsy. *Neuroscience* **129**, 309-24 (2004).

395. Pitkanen, A. & Lukasiuk, K. Molecular and cellular basis of epileptogenesis in symptomatic epilepsy. *Epilepsy Behav* **14 Suppl 1**, 16-25 (2009).

396. de Lanerolle, N.C. et al. A retrospective analysis of hippocampal pathology in human temporal lobe epilepsy: evidence for distinctive patient subcategories. *Epilepsia* **44**, 677-87 (2003).

397. Suttkus, A. et al. Aggrecan, link protein and tenascin-R are essential components of the perineuronal net to protect neurons against iron-induced oxidative stress. *Cell Death Dis* **5**, e1119 (2014).

398. Bozdagi, O., Nagy, V., Kwei, K.T. & Huntley, G.W. In vivo roles for matrix metalloproteinase-9 in mature hippocampal synaptic physiology and plasticity. *J Neurophysiol* **98**, 334-44 (2007).

399. Arranz, A.M. et al. Hyaluronan deficiency due to Has3 knock-out causes altered neuronal activity and seizures via reduction in brain extracellular space. *J Neurosci* **34**, 6164-76 (2014).

400. Retchkiman, I., Fischer, B., Platt, D. & Wagner, A.P. Seizure induced C-Fos mRNA in the rat brain: comparison between young and aging animals. *Neurobiol Aging* **17**, 41-4 (1996).

401. Bragin, A., Wilson, C.L., Almajano, J., Mody, I. & Engel, J., Jr. High-frequency oscillations after status epilepticus: epileptogenesis and seizure genesis. *Epilepsia* **45**, 1017-23 (2004).

402. Le Van Quyen, M. et al. Cell type-specific firing during ripple oscillations in the hippocampal formation of humans. *J Neurosci* **28**, 6104-10 (2008).

403. Wittner, L. & Miles, R. Factors defining a pacemaker region for synchrony in the hippocampus. *J Physiol* **584**, 867-83 (2007).

404. Jones, P.L. & Jones, F.S. Tenascin-C in development and disease: gene regulation and cell function. *Matrix Biol* **19**, 581-96 (2000).

405. Miyata, S., Komatsu, Y., Yoshimura, Y., Taya, C. & Kitagawa, H. Persistent cortical plasticity by upregulation of chondroitin 6-sulfation. *Nat Neurosci* **15**, 414-22, s1-2 (2012).

406. Hartig, W. et al. Cortical neurons immunoreactive for the potassium channel Kv3.1b subunit are predominantly surrounded by perineuronal nets presumed as a buffering system for cations. *Brain Res* **842**, 15-29 (1999).

407. Moleres, F.J. & Velayos, J.L. Expression of PrP(C) in the rat brain and characterization of a subset of cortical neurons. *Brain Res* **1056**, 10-21 (2005).

408. Kaufmann, W.E. et al. Social impairments in Rett syndrome: characteristics and relationship with clinical severity. *J Intellect Disabil Res* **56**, 233-47 (2012).

409. Veeraragavan, S. et al. Loss of MeCP2 in the rat models regression, impaired sociability and transcriptional deficits of Rett syndrome. *Hum Mol Genet* **25**, 3284-3302 (2016).